ABSTRACT

COMPLETE STRESS-STRAIN CHARACTERISTICS OF HIGH PERFORMANCE CONCRETE

by
Insang Lee

High performance concrete (HPC) has recently become a widely used concrete construction material for modern buildings, bridges, and pavements, etc. To produce such a better quality of concrete, chemical and mineral admixtures such as fly ash, slag cement, and silica fume, ground granulated blast furnace slag, as well as air-entraining agents are commonly used in the field construction. It has been found that high performance concrete can improve the workability, ultimate strength and durability of the concrete. However, the enhancement of ductility in concrete, and concrete structures as a whole is still inconclusive and needs more research. The ductility can be found from the behavior of stress-strain curve, therefore, a well-defined stress-strain curve can be used to understand its ductility and other mechanical behavior. In this research, a series of compression tests are conducted.

Silica fume has been used to get high performance silica fume high strength concrete. The shape of the ascending part of the stress-strain curve for high performance silica fume high strength concrete behaves a more linear and steeper curve. The slope of the descending part also exhibits a steeper curve for the high strength concrete as compared to that of the normal concrete. Fly ash also has been used to improve concrete characteristics. The use of fly ash in concrete increases the ductility of concrete by 9.8%, but the improvement is not significant and thus more research work is needed in this

field. Steel fibers and confinements increase the ductility of high performance concrete, thus concrete does not fail even after reaching high strain value.

This research presents a complete stress-strain behavior and its empirical equation of high performance concrete under compression. Once the ultimate strength and concrete strain are known, only one or two parameters are needed to study the ascending and descending behavior of concrete. The proposed empirical equations also study the effects of steel fibers and/or steel hoops, and can be found useful in designing modern high performance concrete structures. The comparison between the experimental and analytical results shows a good agreement.

COMPLETE STRESS-STRAIN CHARACTERISTICS OF HIGH PERFORMANCE CONCRETE

by
Insang Lee

A Dissertation
Submitted to the Faculty of
New Jersey Institute of Technology
in Partial Fulfillment of the Requirements for the Degree of
Doctor of Philosophy in Civil Engineering

Department of Civil and Environmental Engineering

May 2002

APPROVAL PAGE

COMPLETE STRESS-STRAIN CHARACTERISTICS OF HIGH PERFORMANCE CONCRETE

Insang Lee

Dr. C. T. Thomas Hsu, Dissertation Advisor — Date
Professor of Civil and Environmental Engineering, NJIT

Dr. Perumalsamy N. Balaguru, Committee Member — Date
Professor of Civil and Environmental Engineering, Rutgers University, NJ

Dr. John R. Schuring, Committee Member — Date
Professor and Chairman of Civil and Environmental Engineering, NJIT

Dr. Jay N. Meegoda, Committee Member — Date
Professor of Civil and Environmental Engineering, NJIT

Dr. Pedro Muñoz, Committee Member — Date
Senior Structural Engineer, DMJM+HARRIS, Boston, MA

BIOGRAPHICAL SKETCH

Author: Insang Lee

Degree: Doctor of Philosophy in Civil Engineering

Date: May 2002

Undergraduate and Graduate Education:

- Doctor of Philosophy in Civil Engineering
  New Jersey Institute of Technology, New Jersey, 2002
- Master of Science in Civil Engineering
  New Jersey Institute of Technology, New Jersey, 1996
- Bachelor of Science in Civil Engineering
  Korea University, Seoul, Korea, 1992

Major: Civil Engineering

Presentations and Publications:

Insang Lee, Wonsiri Punurai, Cheng-Tzu Thomas Hsu, "Complete Stress-Strain Behavior of High Performance Fly Ash concrete." 15th ASCE Engineering Mechanics Conference June 2-5, 2002 (Accepted).

Insang Lee, Yuan Libo, Farhad Ansari and Hong Ding, "Fiber-optic Crack-tip Opening Displacement Sensor for Concrete." *Cement & Concrete Composites.* Vol. 19, No. 1 1997, pp.59-68.

Farhad Ansari, Yuan Libo and Insang Lee, "A High Resolution Optical Fiber Polarimetric Strain and Displacement Transducer for Structural Elements." Proceedings of Intelligent Civil Engineering Materials and Structures, ASCE, 1997, pp. 106-121.

This dissertation is dedicated to
my parents and wife

ACKNOWLEDGMENT

I would like to express my sincere gratitude to my Advisor, Dr. C. T. Thomas Hsu for his faith, encouragement and guidance throughout this research.

I would also like to thank Dr. Perumalsamy N. Balaguru, Dr. John R. Schuring, Dr. Jay N. Meegoda, and Dr. Pedro Muñoz for serving as members of my dissertation committee.

The financial assistance received from the Department of civil and Environmental Engineering is gratefully appreciated.

Special thanks to Mr. Allyn Luke for his help and assistance with my experiments.

I would like to thank to Mr. Zhichao Zhang and Mr. Jian Chen for their help and guidance during this research.

Finally, I do express my sincere appreciation to my parents and wife for their endless patience, support, and constant encouragement.

TABLE OF CONTENTS

TABLE OF CONTENTS
(Continued)

Chapter **Page**

TABLE OF CONTENTS
(Continued)

Chapter **Page**

TABLE OF CONTENTS
(Continued)

Chapter **Page**

LIST OF TABLES

LIST OF TABLES
(Continued)

Table **Page**

LIST OF FIGURES

LIST OF FIGURES
(Continued)

Figure **Page**

LIST OF FIGURES
(Continued)

Figure **Page**

LIST OF FIGURES
(Continued)

Figure **Page**

LIST OF FIGURES
(Continued)

Figure **Page**

LIST OF FIGURES
(Continued)

Figure **Page**

CHAPTER 1

INTRODUCTION

1.1 General

During the past decade, high performance concrete has become popular. High performance concrete (HPC) is not synonym of high strength concrete. It has other properties in addition to strength. These include ductility, density, durability, or resistance of the concrete against some forms of attack. Increasing constructions in a hostile environment make HPC widely use.

A complete stress-strain curve is needed for rational design and analysis of a concrete structure. Especially, concrete structures built in severe environments need good maintenance because of huge amount of construction expenses and difficulty in repairing. Thus, a well-defined stress-strain curve is needed for proper design and rehabilitation.

The Brittleness of concrete and machine-specimen interaction makes it difficult to get a complete stress-strain curve of concrete. The Experimental difficulty obtaining a complete stress-strain curve has resulted in developing several different testing techniques for the tests. Although numerous stress-strain curves have been proposed, most of them do not give acceptable concrete strains either in the ascending or in the descending branch of stress-strain curve. This is due to the fact that different gage lengths to determine the strains have been used in most concrete compression tests.

In this research, attempts will be made to get acceptable concrete strains for the entire stress-strain curve. The effect of gage length over the specimen length will be investigated. The concrete behavior under compression for unconfined, confined and

steel fibers will be included in this investigation. Also, concrete with fly ash and steel fiber will be studied. Various parameters and their relationships will also be investigated.

1.2 Objectives of Present Research

The objectives of present research are as follows:

(A) Experimental Investigation:

1. To study the size effect on the maximum compressive strengths of 3 x 6-in., 4 x 8-in. and 6 x 12-in. concrete cylinders.
2. To determine the strains using 4-in. long gage length on 3 x6-in. and 4 x 8-in. concrete cylinders, respectively. The resulting compressive stress-strain curves of these two concrete cylinders will be compared and studied.
3. To test and study the compressive stress-strain behavior of high strength and high performance concrete cylinders. The variables which affect the stress-strain characteristics are maximum concrete compressive strength (f′c), steel fiber volume ratio (0.5%, 1%, 2%), spacing of hoops (1", 2", 4"), and etc. A 4-in. gage length will be used to measure the strain on both surfaces of 4 x 8-in. cylinders.
4. To test and study the compressive stress-strain behavior of high performance fly ash concrete cylinders. The variables include steel fiber volume ratio (0.5%, 1%, 2%), spacing of hoops (1", 2", 4"), and etc. A 4-in. gage length will be used to measure the strain on both surfaces of 4 x 8-in. cylinders.

(B) Analytical Investigation

1. To develop an empirical stress-strain equation for high strength and high performance concrete under compression. The proposed equation will include the

effects of f′c, steel fiber volume ratio, spacing of hoops, and etc. The combined effect of steel fiber volume ratio and spacing of hoop will also be included in this study.

2. To develop an empirical stress-strain equation for high performance fly ash concrete under compression. The proposed equation will include the effects of different fly ash replacement, steel fiber volume ratio, spacing of steel hoop, and the combined effect of steel fiber volume ratio and spacing of hoop.

1.3 Originality of Present Research

High-performance concrete has been increasingly used recently. High performance concrete is a concrete that has enhanced properties beyond regular concrete. To make a higher and/or high performance concrete, some admixtures such as silica fume, fly ash, and ground granulated blast furnace slag can be used. By using the admixtures, concrete properties become more durable in service. Because brittleness of higher strength concrete may cause an unexpected total collapse of structure, ductility of structure is needed for higher strength concrete structures. It is well known that the stress-strain curve plays an important role on structural design and analysis; however, no reliable high-performance concrete stress-strain curves are currently available in the literature.

In this research, the author will try to obtain information regarding the effect of gage length on the stress-strain characteristics. There are many stress-strain curves available, but no research has been conducted on gage length effect over the cylinder height. A 4-in. extensometer will be used for all testings. Some previous developed stress-strain curves are based on the deformations measured from the machine platens (Hsu 1992).

Deformations from this kind of testing setup are come from not only concrete deformation but also extra deformations due to the machine flexibility and end zone effect. Empirical stress-strain equations for high strength and high performance concrete with and without steel fiber will be studied. The behavior of concrete confined with steel hoop will also be investigated. Fly ash concrete with and without steel fiber using overweight replacement method will be studied. Comparison of various existing empirical stress-strain equations will be conducted. Stress-strain equations to account for fly ash concrete with and without steel fiber or steel hoop are the original ones.

1.4 Literature Review

In recent years, high performance concrete has been widely used. This is due to the increasing demand for durable concrete subject to severe exposure. To be a high performance concrete, it should have higher strength and also have improved microstructure. It includes ductility, durability, and density (Papworth and Ratcliffe 1994). After the term, high performance concrete (HPC), becomes popularly used, there have been several attempts to define HPC. But until now, no specific criteria is used to describe high performance concrete.

Foster defined that HPC is a concrete made with appropriate materials combined according to a selected mix design and properly mixed, transported, placed, consolidated, and cured so that the resulting concrete will give excellent performance in the structure in which it will be exposed, and with the loads to which it will be subjected for its design life (Foster 1994). The Strategic Highway Research Program (SHRP) defined HPC as three-parameters (Goodspeed 1996).

1) A maximum water-cement ratio(w/c) of 0.35
2) A minimum durability factor of 80 percent as determined by ASTM C666 procedure
3) A minimum strength criteria of either
    (a) 21MPa (3000psi) within 4 hours after placement (very early strength)
    (b) 34MPa (5000psi) within 24 hours(high early strength)
    (c) 69MPa (10,000psi) within 28 days(very high strength)

According to Breitenbücher, HPC is defined as high strength concrete with an improved durability or an increased resistance of the concrete against chemical or physical attack (Breitenbücher 1998). Russel defined HPC as concrete meeting special combinations of performance and uniformity requirements that cannot always be achieved routinely using conventional constituents and normal mixing, placing, and curing practices (Russel 1999).

1.4.1 An Overview of Concrete Properties

Portland cement concrete is a composite material consisting of cementitious matrix and aggregate. The properties of composite material depend on not only the properties of constituent materials but also the transition zone. Transition zone is the interfacial region between coarse aggregate and cement matrix (Mehta 1993).

This transition zone is the weakest portion in the concrete. This is because there is no significant chemical reaction between aggregate and cement paste and poor packing of the cement paste around aggregate (wall effect) and bleeding of water make water pockets below coarse aggregate (Young 1998). So to get a high performance concrete,

modification of microstructure is needed. One way to solve this problem is adding appropriate pozzolanic materials in the mixing of concrete.

1.4.2 Pozzolanic Material

According to ACI 116R, pozzolan is "a siliceous or siliceous and aluminous material, which in itself possesses little or no cementitious value but will, in finely divided form and in the presence of moisture, chemically react with calcium hydroxide at ordinary temperatures to form compounds possessing cementitious properties." Mineral admixtures that are, or both cementitious and pozzolanic can be used as a partial replacement for portland cement. Some of the most used materials are condensed silica fume and low and high calcium fly ash. When properly used as a portion of the cementitious material, these pozzolanic admixtures can improve the properties of the fresh and hardened concrete.

1.4.3 Application of Mineral Admixtures

Mineral admixtures are finely divided siliceous materials, which are added to concrete. Their function is to modify the properties of the concrete so as to make it more suitable for the work. The commonly used admixtures can be summarized as follows:

(a) Fly ash

Fly ash is the finely divided residue that results from the combustion of ground or powered coal. Fly ash was available from 1930s. In early years, it was used for a massive structure such as dam because it could reduce construction cost by replacing cement with

fly ash. But with extensive research, they recognized that fly ash could improve concrete properties. Some advantages of using fly ash are as follows (ACI 1999).

a. low temperature rise during initial hydration preventing crack, especially in massive structures
b. improve durability to aggressive chemical attack
c. improve workability in fresh concrete
d. reduce cost of construction
e. reduce expansion by alkali-silica reaction

Fly ash can be divided into two categories, depending on calcium content of fly ash. The category is termed as low-calcium fly ash (class F), and the second category is called as high-calcium fly ash (class C). Generally these two fly ashes have different characteristics (Chen 1985).

In this research, overweight replacement method using class F fly ash will be used to design mix proportion. The method was developed in China (Chen 1985). The method needs an overweight coefficient of cementitious materials to calculate the weight of fly ash and cement in fly ash concrete. Because the component of fly ash is unlike that of the portland cement, the amount of fly ash put into the mix is greater than the cement removed. The main requirements of the overweight replacement method is to select to the proportions of the constituent materials so as to produce a concrete with all the desired properties at a minimum cost. The performance of fly ash concrete designed by the overweight replacement method can be similar to that of normal concrete with the following characteristics:

a. adequate workability

b. same 28 day strength

c. satisfactory durability

d. cost saving

(b) Silica Fume

Silica Fume is a byproduct of electric arc furnace used for the production of silicon metal or alloy. Because the silica fume is of highly reactive pozzolans and pozzolanic additives, it can be used to improve early strength and durability of concrete. It is noticeable that the silica fume is commercially available in considerable amounts worldwide, and the use of the material has advantages to environmental protection. Some effects of silica fume on properties of hardened concrete are as follows (ACI 1999):

a. Reduce permeability

b. Increase the strength of concrete

c. Improve chemical attack resistance

d. Durability to thermal cracking

(c) Ground Granulate Blast Furnace Slag (GGBF Slag)

Ground Granulate Blast Furnace Slag is the glassy granular material formed when molten blast-furnace slag is rapidly chilled, as by immersion in water (ACI 1999). The workability and placeability of concrete containing GGBF slag yields improved characteristics when compared with concrete not containing GGBF slag. As fineness of slag is increased, higher concrete strengths are achieved.

1.4.4 General Stress-Strain Equations for Normal and High Strength Concretes under Compression

For rigorous analysis of concrete structure, a complete stress-strain equation is needed. Low and medium strength concrete is ratherly easier than high strength concrete to get a full stress-strain curve. Due to the brittleness of high strength concrete, it needs special technique to get a full curve. The axial deformation has been used for test control. But for high strength concrete, the large energy release during failure causes unstable descending branch (Mier et al. 1997).

To overcome this problem, one might use the circumferential deformation (Jansen et al.1995) or the combination of axial deformation and axial load proposed by Okubo and Nishimatsu (1985). Until now, Numerous stress-strain curve equations have been developed. Some equations are shown as follows.

(1) Smith and Young (1956)

$$f = f_c' (\frac{\varepsilon}{\varepsilon_0}) \exp(1 - \frac{\varepsilon}{\varepsilon_0}) \tag{1.1}$$

where

f = stress at any strain

f_c' = maximum stress

ε = strain

ε_0 = strain at the maximum stress

(2) Desayi and Krishman (1964)

$$f = \frac{E\varepsilon}{1 + (\frac{\varepsilon}{\varepsilon_0})^2} \tag{1.2}$$

where

E = a constant (same as initial tangent modulus)

(3) Sargin (1971)

$$\eta = \left[\frac{Ax + (D-1)x^2}{1 + (A-2)x + Dx^2} \right] \tag{1.3}$$

Where

$$\eta = \frac{f}{f_c'}$$

$$x = \frac{\varepsilon}{\varepsilon_0}$$

A = Parameter mainly affecting the slope of the ascending branch

D = Parameter mainly affecting the slope of the descending branch

(4) Popovics (1973)

$$f = f_c' \frac{\varepsilon}{\varepsilon_0} \frac{n}{n - 1 + (\varepsilon/\varepsilon_0)^n} \tag{1.4}$$

where the n power can be expressed as an approximate function of the compressive strength of normal weight concrete as follows:

$$n_{\text{concrte}} = 0.4\text{x}10^{-3} f_c' + 1.0$$

$$n_{\text{mortar}} = 0.15\text{x}10^{-3} f_c' + 1.0$$

$$n_{\text{paste}} = 12$$

(5) Wang, shah, and Naaman (1978)

$$Y = \frac{AX + BY}{1 + CX + DX^2} \tag{1.5}$$

where

$$Y = \frac{f}{f_c'},\ X = \frac{\varepsilon}{\varepsilon_0}$$

A, B, C, D are constants representing strain hardening portion

(6) Desayi et al. (1978)

$$f = \frac{A}{1 + B\varepsilon + C\varepsilon^2 + D\varepsilon^3} \tag{1.6}$$

A, B, C, and D are parameters to be obtained from the boundary condition and test results.

(7) Carreira and Chu (1985), Ezeldin et al.(1992), Nataraja et al. (1999)

$$\frac{f}{f_c'} = \frac{\beta(\frac{\varepsilon}{\varepsilon_0})}{\beta - 1 + (\frac{\varepsilon}{\varepsilon_0})^{\beta}} \tag{1.7}$$

Where

$$\beta = \frac{1}{1 - \frac{f_c'}{\varepsilon_0 E_{it}}} \text{ for } \beta \geq 1.0 \text{ and } \varepsilon \leq \varepsilon_u$$

β is a material parameter that depends on the shape of the stress-strain curve

E_{it} is the initial tangent modulus.

ε_u is the ultimate strain or strain at which failure is defined.

(8) Hsu and Hsu (1994)

$$\eta = \frac{n\beta x}{n\beta - 1 + x^{n\beta}} \text{ for } 0 \leq x < x_d \tag{1.8}$$

where

$$\eta = \frac{f_c}{f_c'}$$

$$x = \frac{\varepsilon}{\varepsilon_0}$$

$$\beta = \frac{1}{1 - \frac{f_c'}{\varepsilon_0 E_{it}}} \quad \text{for } \beta \geq 1.0$$

β and n are the material parameters. β depends on the shape of the stress-strain diagram, and n depends on the strength of material. x_d is the strain at $0.3f'_c$ in the descending portion of the stress-strain curve.

Note: This equation was also used for confined and steel fiber concrete.

(9) Wee, Chin and Mansur (1996)

$$f = f_c' \left[\frac{k_1 \beta (\frac{\varepsilon}{\varepsilon_0})}{k_1 \beta - 1 + (\frac{\varepsilon}{\varepsilon_0})^{k_2 \beta}} \right] \tag{1.9}$$

where

$$\beta = \frac{1}{1 - \frac{f_c'}{\varepsilon_0 E_{it}}}$$

for $f_c' \leq 50\text{MPa}$, $k_1 = k_2 = 1$

for $50 \leq f_c' < 120\text{MPa}$, $k_1 = (\frac{50}{f_c'})^3$ and $k_2 = (\frac{50}{f_c'})^{1.3}$

1. 5 Test Setup for Obtaining Concrete Stress-Strain Curve of Plain Concrete

For a design of reinforced concrete structure, the concrete compressive stress block is needed. The stress-strain curve obtained from monotonic compressive testing has been used to represent the stress-strain curve under eccentric compression or for the

compressive zone of a beam because both curve shapes are similar. Since ultimate concrete strain is a required parameter and this is likely to be in the descending branch of the stress-strain curve, the complete stress-strain curve becomes necessary to design and analyze concrete structures.

Even though lots of stress-strain curves are proposed, there is insufficient information on the shape of curve, especially in high strength concrete. One of the reasons why there are insufficient experimental results on the complete stress-strain curve is that it is very difficult to get descending part of the curve. The problem is that the interaction between the testing machine and the specimen is unclear. After the specimen reaches peak strength, the load is decreased. However the strain energy stored in the machine needs path to release. This causes an impulsive failure.

In the case of high strength concrete, the problem is worse because the strain energy is high. If the compression-testing machine is stiffer than the specimen, this can prevent the specimen from a sudden failure. Still many testing machines used in normal laboratory have a limited stiffness to apply high strength concrete. Wang and co-workers introduced a simple method (Wang 1978). They used a hardened steel tube in parallel with concrete cylinder. This testing setup ensures that the sum of the loading carried by the steel tube and the concrete is always increasing up to the strain of 0.006. Thus, there is no energy release from the testing machine. Although the method is simple, it has certain limitation. The maximum strain of 0.006 may not be sufficient for steel fiber and confined cylinder. Because the load is shared by concrete and steel tube, high capacity of testing machine is needed.

Another way is using servo-controlled closed-looped testing machine. A properly chosen feed back signal is critical in this testing method. The present experimental tests will use the MTS servo-controlled closed-loop-testing machine to study compressive stress-strain behavior of concrete cylinder.

1.6 Concrete Stress-Strain Curve with Fiber

High strength concrete is brittle and has very steep descending branch of the stress-strain curve. These cause explosive failure after peak and make it difficult to get descending part because the strain change is small. To overcome brittle characteristic of high strength concrete, fiber has been used to improve high strength concrete. Fiber has been used to reinforce the brittle materials since ancient times, such as straw in sunbaked bricks and horsehair in reinforced plaster.

Nowadays, fibers have been produced from steel, plastic, and glass in various shapes and sizes. Currently, steel fiber is used widely including highway, airport pavement, and hydraulic structures. The capacity of a structure to absorb energy, with acceptable deformation and without failure is essential in seismic design. So sufficient ductility is essential for seismic analysis. The addition of steel fiber has little effect on its pre-crack behavior but significantly improve post-crack response (Ezeldin and Balaguru 1992).

1.7 Concrete Stress-Strain Curve with Steel Hoop Confinement

Closely spaced steel hoop confinements improve ductility of concrete structures. So properly used transverse confinements increase the capacity of concrete to sustain large

deformation without a substantial strength loss (Ahmad and Shah 1982). Thus, steel hoop confinement can be found useful in design of concrete structures subjected to seismic or impact loading. Confinement is effective when stress approaches ultimate strength because confining reaction of transverse reinforcement resists progressive internal cracking. Thus, confinement can also improve the stress-strain characteristics at high strain. It has shown that confinement effectiveness depends on properties of confinement, configuration and degree of confinement (Issa and Tobaa 1994, Nicolo and et al. 1997).

1.8 Gage Length Effect on the Stress-Strain Curve

The shape of stress-strain curve in compression is affected by many variables. An extensive research was carried by RILEM (1996). They conducted special test program about strain softening of concrete in uniaxial compression. The main parameters affecting descending branch of the stress-strain curve are stiffness of testing machine, type of feedback signal, loading rate, size and shape of the specimen, gage length and concrete composition. Although intensive experimental parameters are investigated, no sufficient information is available about gage length effect on stress-strain curve. Deformations measured from specimen surface give strain values of stress-strain curve. After peak load, concrete begins to spall and disturb strain measuring in specimen. However deformations from platen to platen give stable behavior. This makes platen to platen strain measurements popular. Many stress-strain equations or curves proposed are derived and based on platen to platen deformation measurements, they include deformations due to machine flexibility and end zone effect except true concrete strain. To overcome this problem, a more refined stress-strain curve is needed.

CHAPTER 2

STRESS-STRAIN BEHAVIOR OF HIGH PERFORMANCE SILICA FUME HIGH STRENGTH CONCRETE WITH STEEL FIBERS AND HOOPS

2.1 Introduction

Over the last decade, high performance-high strength (HP/HS) concrete has been used in severe environments, such as seafloor tunnels, offshore piers and structures for hazard wastes (Mehta 1990). Some advantages of using high performance-high strength concrete are achieving longer spans, shallow members, enhanced mechanical properties, durability and ductility. Besides these, economical long-term maintenance becomes key roles using high performance-high strength concrete. High strength concrete was popular in 80s. After 90s, high performance became passionate terminology in concrete research. Note that high performance concrete is not equivalent to high strength concrete.

High Performance means to achieve an improved microstructure in concrete. As mentioned before, appropriate pozzolanic materials in the concrete mixing is useful to get desirable performance and strength. In recent years, silica fume has been used as concrete property-enhancing material, as a partial replacement for portland cement. The size of silica fume is about 100 times finer than that of cement. This fineness can make dense microstructure and thus high strength is possible. Adding silica fume increases water demand, so water-reducing admixtures are needed to obtain workability.

The Scandinavian countries started to study the performance of silica fume. Bernhardt (1952) published the first paper in 1952. Norcem(1978) did the first major replacements of silica fume concrete for chemical attack resistance in 1978 (ACI Manual

of Concrete Practice 1999). There are differences between high performance-high strength and normal concrete. One of key difference is material behavior, which can be explained by its stress-strain curve. This chapter will present stress-strain behavior of high performance silica fume high strength with and without steel fiber.

2.2 Experimental Program

2.2.1 Materials

The materials used in present research are fin the ollowings:

- Cement: ASTM type I Portland cement was used except marked batches.
- Fine aggregate: Air dried sand from a local source was used.
- Coarse aggregate: 3/8-inch basalt was used. Before mixing, the aggregates were washed and air-dried to get saturated surface dry (SSD).
- Water: Tap water with ambient temperature was used.
- Silica fume: Commercially available micro-silica was used to get high strength.
- Superplasticizer: High range water reducer was used to maintain good workability.
- Steel fiber: Steel fibers hooked at both ends were used. The length (l) is 30mm and diameter (d) is 0.5mm. The aspect ratio l/d of steel fiber is 60.
- Steel hoop: The tie confinement with circular hoops was used. Regular tie wires are used to make the steel hoops.

Table 2.1 lists the mixing proportions of present study. The mix proportions are based on 1 cubic yard mix.

Table 2.1 Mixing Proportions for High Performance Silica Fume High Strength Concrete

	HP/HSC†	Weight Ratio
Water (lb)	265	0.30
Cement (lb)	870	1
Silica Fume (lb)	44	0.05
Sand (lb)	1218	1.4
Coarse Aggregate* (lb)	1877	2.15
Superplasticizer (fl oz)	348	
W/C	0.30	
W/(C+SF)	0.29	

† Mix proportion per yd^3
* 3/8 in. Maximum Size Basalt

2.2.2 Mixing and Curing

Concrete was mixed in the concrete laboratory using an electric mixer. The sand and cement were mixed first for a while without water. About 70% of water was added to the mixer and the coarse aggregate was added with the rest of water and superplasticizer. Main specimen size was 4-x 8-in. cylinder. Reusable plastic molds were used for whole casting. The polyethylene covering was also used to prevent surface dry. The mixing was cast and externally vibrated for about 15seconds. After 24 hours, the specimens were demolded and cured in moisture curing room with 100 percent relative humidity until a day before testing. All steps of casting were done according to ASTM C192.

2.2.3 Experimental Set-up

Before testing, specimens were sawed at both ends to get flat and strong surface and then capped with a sulfur compound at both ends. The final height was about 8.2in. The

concrete cylinders were tested in a closed-loop servo hydraulic MTS 815 concrete testing machine, which has 1 million pounds loading capacity. Figure A.1 shows the testing machine setup. Two extensometers at the middle half of the height were used to get strain and two strains were averaged. To obtain a full stress-strain curve, a slow rate of $1.0x10^{-5}$ strain/sec was adopted for a whole compression test. Figure A.2 shows an extensometer setup. An electric data acquisition system was used to record loads and corresponding strains.

2.3 Test Results of Plain Concrete

To study the material behavior of High Performance Silica Fume High Strength Concrete, the size of 4 x 8-in. cylinder has been mainly used except for gage length study and size effect study. Due to the inherent brittle characteristic of HSC, most tests can not complete their entire descending branch of stress-strain curve. Many tests were unsuccessful because the crack occured outside of gage length. This explains that why top to bottom strain measurement is popular. More detailed research may be needed to establish better testing methods for high strength concrete. Total 20 cylinders were tested to get full stress-strain curves. Due to their brittle characteristics, only five specimens showed the complete ascending and descending branches of stress-strain curve. Table 2.2 depicts HP/HSC test results showing full curves. Other failed test results can be found in Table A.1. To find material properties, analysis was based on the tests showing both ascending and descending branches. Figure A.3 shows the typical cylinders after compression test. In general, the normal strength concrete gradually fails after reaching

its peak load, but the high strength concrete suddenly explodes at peak load. Typical splitting rupture failure has been shown.

Table 2.2 Test Results for High Performance Silica fume High Strength Concrete

Specimen	f_c' (psi)	ε_0	E_{it} (ksi)	E_c (ksi)
P1	10810	0.002468	6903	5985
P2	11060	0.002590	6166	5579
P3	11190	0.002654	6630	5707
P4	11220	0.002607	6962	5677
P5	11290	0.002646	6851	5763
Ave.	11110	0.002593	6702	5742

Note: f_c' : Maximum Compressive Stress (psi)
ε_0 : Strain at Peak Stress
E_{it} : Initial tangent Modulus (ksi)
E_c : Modulus of Elasticity of Concrete at $0.4f_c'$ (ksi)

2.3.1 Modulus of Elasticity

Modulus of elasticity is a necessary parameter to determine the stresses in materials and structures. Even though concrete has nonlinear stress-strain behavior, modulus of elasticity is important material property to design and analyze concrete structures. The cementitious material has already microcracks between the paste and fillers before loading (Mehta and Monteiro 1993). As the load is increased, the crack in transition zone and the matrix is going to be bigger and finally reaches failure. However, until about 50 to 60 percent of ultimate load, microcrack is considered stable and matrix cracking is minimal. Since the concrete is nonlinear material, four methods are used to determine modulus of elasticity. (ASTM E6)

1. Tangent modulus: the slope of the stress-strain curve at any specified stress or strain
2. Initial tangent modulus (E_{it}): the slope of the stress-strain curve at the origin
3. Chord modulus (E_c): the slope of a line drawn between two specified points on the stress-strain curve, with the initial point corresponding to a strain of 50 microstrains.
4. Secant modulus: the slope of a line drawn from origin to any specified on the stress-strain curve.

Table 2.2 shows initial tangent modulus and chord modulus (modulus of elasticity) of concrete of present study. The initial tangent modulus of elasticity represents the initial behavior of concrete. The chord modulus of elasticity used in present research is derived from points between 50 micro-strain and 40 percents of ultimate loading. Here, the initial tangent modulus shows around 16% larger than that of chord modulus. Figure A.7 shows comparisons of chord modulus of elasticity with three available equations. The test results are in the range between ACI 363R-92 and CEB-FIP 90 models. To avoid the laboratory tests, modulus of elasticity can be found from the compressive strength in normal strength concrete. The best-fit equations between modulus of elasticity and ultimate strength in this study are

$$E_c = 541400(f_c')^{1/4} \tag{2.1}$$

$$E_{it} = 628000(f_c')^{1/4} \tag{2.2}$$

The compressive strength (f_c') is expressed in psi.

Figure A.8 shows E_{it} relationship equation with other test data, in which the ultimate stress (f_c') is expressed in psi. The above equations are based on basalt coarse aggregate.

The modulus of elasticity of HP/HSC is strongly influenced by the coarse aggregate (Aïtcin and Metha 1990).

2.3.2 Strain at Peak Stress

The strain at ultimate stress is needed in design to specify failure allowed in concrete structure (Carreira and Chu 1985). The strain at ultimate stress is one of important parameters to get analytical stress and strain curve. But strain at ultimate stress depends on several testing condition such as loading rate, type of aggregate, size and shape of specimen, and capping material (Popovics 1973).

Several empirical equations are available to relate compressive strength to strain at ultimate stress (Taewe 1992, Attard and Setuge 1996). The strain at ultimate stress also depends on test condition. Present study was measured by an extensometer. To get a reliable relationship between compressive strength and ultimate strain, test results done by Jansen and et al (1995) were compared with present study. Their strain values were obtained using both extensometer and platen-to-platen measurements. The test results show obvious difference between two experimental techniques. As can be seen in Figure A.9, the strain at ultimate stress increases as compressive strength increases. The following equation is obtained from best curve fitting.

$$\varepsilon_0 = 1\text{E-}07\, f_c' + 0.0013 \qquad (2.3)$$

2.3.3 Specimen Size Effect on Ultimate Stress

The 6 x 12-in cylinders are standard size to measure the compressive strength. For normal strength concrete, standard testing machine has enough capacity to apply the

required load. But for high strength concrete, high capacity loading frame is needed. This makes 4 x 8-in cylinders popular in high strength concrete.

Table 2.3 Ultimate Strength of Different Specimen Sizes

Batch	6 x 12-in.	4 x 8-in.	3 x 6-in.
Mix I	10.0	10.33	10.19
	10.23	10.05	10.66
	10.59	11.12	10.71
	10.93	11.11	10.99
	10.45	10.53	9.95
	9.94	10.02	10.79
Mix II	11.12	11.58	11.23
	10.55	10.44	12.11
	10.99	11.53	11.55
	10.12	11.23	10.85
	10.55	10.89	11.32
	10.33	10.84	11.53
Average	10.48	10.81	10.99
Standard Deviation	0.385	0.533	0.602

Note: All units are ksi

Comparison of different sizes of cylinder test results is shown in Table 2.3. The observation is that three different cylinder sizes give almost the same strength. As shown in Table 2.3, 4 x 8-in. cylinders have a slight higher strength than 6 x 12-in. cylinder. But 3 x 6-in. cylinders have the same compressive strength as 4 x 8-in. cylinders. This comparison shows that there is no size effect on compressive strength among 3 x 6-in., 4 x 8-in., and 6 x 12-in. concrete cylinders. The test results are different from previous

reported results (Lessard and et al. 1993). They found that 4 x 8-in. cylinders have a strength which is 105 percent that of the 6 x 12-in. specimens.

2.3.4 Effect of Gage Length Ratio

The strain values used in stress-strain curve are obtained from different devices (extensometer, compressometer, mechanical, or strain gage). Different researchers use different gage lengths. It is necessary to study the effect of gage length ratio. The gage length ratio means the ratio of gage length to total specimen height. To study this effect on stress-strain behavior, two sizes (3 x 6-in., 4 x 8-in.) of cylinder specimens with the same gage length (4-in.) were tested. The gage length ratio for 3 x 6-in. specimen is 0.67 and 0.5 for 4 x 8-in. specimen.

Figure 2.1 shows several normalized stress-strain curves for each case. From this graph, one can conclude that specimen with smaller gage length ratio show more ductility than that of larger ratio. This is because the measurement using larger gage ratio can detect more cracks processed within the gage length region during loading stage. The platen-to-platen axial measurements are widely used, especially in high strength concrete because the test technique is able to capture all cracks within the specimen tested. In high strength concrete, sudden spalling of concrete cylinder surface makes it difficult to get a post peak behavior. Thus, the platen-to-platen measurements include extra deformation from the weak contact between loading plate and specimen, consequently the stress-strain curves become more brittle. It is concluded that strain values measured in the stress-strain curve are strongly dependent on the gage length ratio used in compression test. In current ASTM standard, a gage length ratio equal to 0.5 is being used for 6x12-in. cylinder test.

Indeed, a gage length ratio equal to 1.0(platen to platen measurement) would make the worst descending behavior(most brittle case) upon the stress-strain behavior of concrete cylinder under compression.

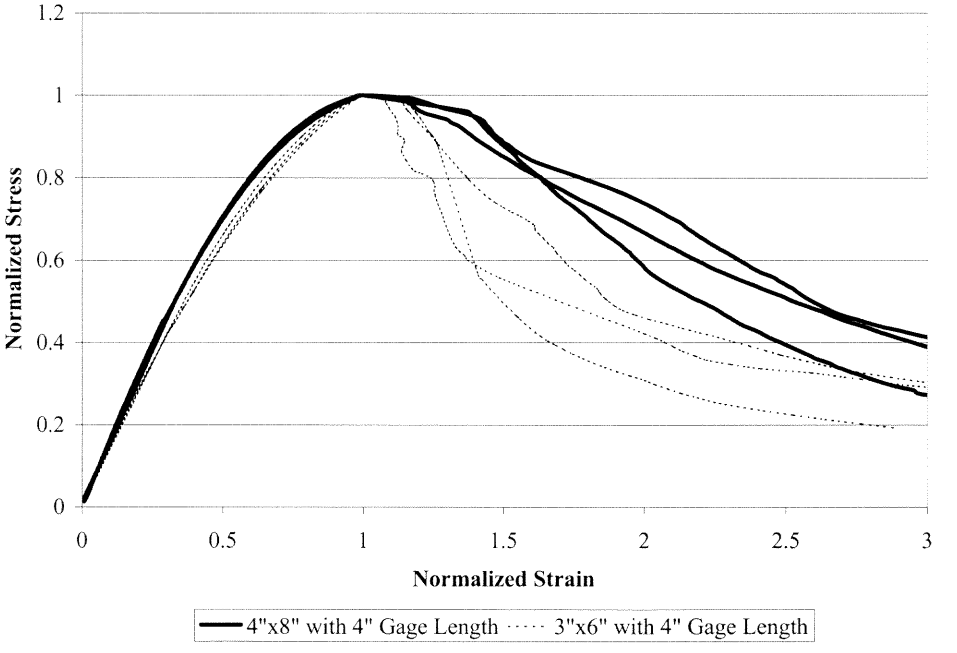

Figure 2.1 Comparison of Various Gage Length Ratios

2.3.5 Analytical Stress-Strain Curve for HP/HSC

To develop an analytical equation for HP/HSC, the following conditions must be considered.

1. The equation should show both ascending and descending branches of stress-strain curve
2. The stress-strain curve should be only one equation and simple so that it can be easily used in design and analysis

3. The stress-strain curve should be applied for both unconfined and confined concretes.
4. The parameters used in stress-strain curve should be simple and can be easily determined from experiments.

Various empirical stress-strain curves have been investigated and the original stress-strain equation proposed by Popovics (1973) is modified here to investigate both ascending and descending branches of stress-strain curve. The following expression for a complete stress-strain relationship under uniaxial compression is proposed at present study to analyze the behavior of cementitious materials, such as HPC and HSC

$$y = \frac{ax}{a - 1 + x^b} \tag{2.4}$$

Where, $y = \frac{f_c}{f_c'}$, $x = \frac{\varepsilon_c}{\varepsilon_0}$, f_c = concrete stress, f_c' = maximum compressive strength of concrete, ε_c = concrete strain, ε_0 = concrete strain at f_c'. a and b are material constants that can be determined by experiments.

In the Popovics (1973) and Carreira and Chu's (1985) equation, a and b are not included. Instead of using two parameters, they used n or β parameter, which can be determined from the ultimate strength, ultimate strain, and initial tangent modulus. But in HP/HSC, the descending branch is different from that of normal strength concrete. Also, using steel fiber and steel hoop confinement in concrete can change the post peak behavior. Hence, Equation (2.4) represents a modified formula from which the original equations are the work of Hsu and Hsu (1994), and Chin, Mansur and Wee (1997).

2.3.6 Proposed Parameters for Plain Concrete

a and b are material parameters that depend on the shape of stress-strain curve. For plain concrete, a and b factors are in the followings:

$$a = b = 0.91 f_c' - 5.69 \tag{2.5}$$

Here, the ultimate strength is expressed in ksi.

Note that above equation is valid when the strength is more than 9000psi. For the strength below 9000psi, the equation developed by Carreira and Chu (1985) can be used to predict the behavior of concrete.

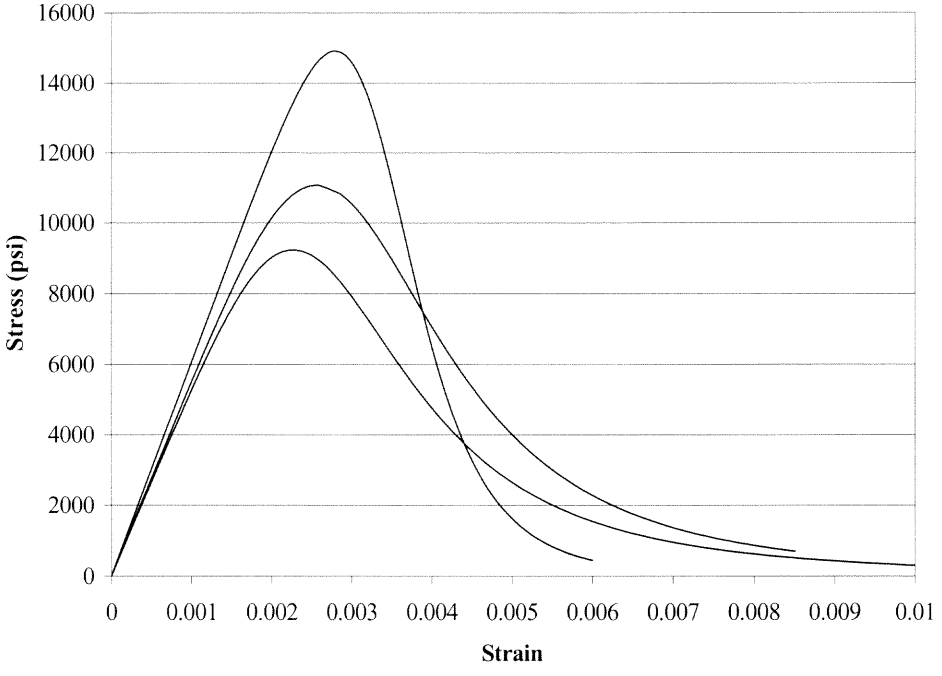

Figure 2.2 Proposed Stress-Strain Curves of Plain Concrete of Different Strength

Figure A.10 shows empirical stress-strain curves for plain concrete. Figure A.11 and Figure A.8 show comparisons between the present test result and proposed equation. The figures show that the proposed equation reveals good agreement with test results. Figure

A.13 shows the validity of proposed equation as compared to other test results (Wee et al. 1996). The ultimate strength was 14909ksi. All the material properties needed in analytical model are derived from their results. Figure 2.2 depicts stress-strain curves at different strength using the proposed equation. In design stage, only ultimate strength is given, and the parameters *a* and *b* can be determined from Equation (2.5) of which the ultimate strength is a function.

2.4 HP/HS Fibrous Concrete

2.4.1 Introduction

In recent years, fibrous concrete has gained broad acceptance to overcome brittleness of HP/HS concrete. The current field application includes highway and airport pavement, and hydraulic structure (Shah and Batson 1987). By using steel fiber, one can improve ductility of structures. This improvement is necessary for structures subjected to seismic loading, impact, or fatigue loading (Fanella and Namman 1985). Under these loading conditions, the structures may be subjected to large deformations (Nataraja 1999).

Adding steel fiber to concrete mix does not change much the ascending behavior, but it enhances the post peak behavior. Adding steel fiber in concrete also enhances material behavior such as flexural strength, fatigue strength and tensile strength. A number of empirical stress-strain equations have been proposed recently (Ezeldin and Balaguru 1992, Hsu and Hsu 1994, Mansur and et al. 1999). All of them modified the equation proposed by Carreira and Chu (1985) to predict its fibrous concrete behavior.

2.4.2 Stress-Strain Behavior of Fibrous Concrete

Adding steel fiber to concrete definitely increases its ultimate strain and toughness. Toughness is defined as an ability of absorbing energy during loading. The toughness can be defined as the area under the stress-strain curve. In the steel fiber-reinforced concrete, the curve after strain value 0.015 becomes flat. So most researchers use 0.015 as a limiting value for calculating the toughness. In present research, this value is also used for analysis.

To evaluate the effect of steel fiber on toughness of concrete, Toughness Ratio (TR) was proposed by Ezeldin and Balaguru (1992). They compared toughness value of cementitious material to that of rigid plastic material. Fanella and Naaman (1985) proposed another approach, Toughness Index (TI). Toughness Index is defined as the ratio of the toughness of the fiber-reinforced concrete to that of the unreinforced control concrete.

In present study, Toughness Ratio is used to quantify the effect of steel fiber on stress-strain curve. Though higher amount of steel fiber increases ductility of concrete, excessive amount usage of steel fiber in concrete (3%) decreases ductility eventually (Fanella and Naaman 1985). This is due to harsh mix causing nonuniform of steel fiber. Table 2.4 shows the test results of fiber-reinforced concrete. The addition of steel fiber definitely increases the ultimate strain and strength of concrete. Most of all, post peak behavior has been improved a lot. This proves steel fiber addition is good for ductility improvement.

To study the effect of steel fiber on stress-strain curve, toughness ratio is used. Toughness can be calculated from the area under the stress-strain curve. Toughness ratio

is defined as a ratio of steel fiber concrete to that of rigid plastic material. The steel fiber volume fraction and its aspect ratio play an important role in behavior of steel fiber-reinforced concrete. The Reinforcing Index (RI) includes two effects, and can be given by:

$$RI = V_f \times (l/d) \tag{2.6}$$

where

V_f = Volume Fraction of steel fiber

l = length of steel fiber (= 30mm)

d = Diameter of steel fiber (=0.5mm)

Table 2.4 Compression Test Results of Fiber-Reinforced High Performance Silica Fume High Strength Concrete

Specimen	f'_c (ksi)	ε_0	E_c (ksi)	Toughness (psi)	Toughness Radio
HP05S1	11.45	2968	5399	81	0.470
HP05S2	11.30	2900	6001	100	0.590
HP05S3	11.93	2808	6361	97	0.541
HP05S4	12.09	2901	6009	84	0.465
Ave.	11.69	2811	5943	90	0.516
HP1S1	12.11	2904	6083	101	0.556
HP1S2	12.41	3078	6293	95	0.510
HP1S3	13.13	3304	5806	119	0.604
HP1S4	12.57	3219	6098	100	0.532
Ave.	12.56	3126	6070	104	0.551
HP2S1	12.95	3430	5864	126	0.649
HP2S2	13.60	3732	6327	138	0.676
HP2S3	14.08	3364	6183	135	0.639
HP2S4	14.08	3280	6213	141	0.667
Ave.	13.68	3469	6146	135	0.658

Note: The value after HP shows fiber volume fraction and the number after S means cylinder number.
HP05S1 means 0.5% volume ratio steel fiber specimen number1.

2.4.3 Compressive Strength

The ultimate strength has been found to increase as steel fiber is added to concrete mixing. The 2% adding to mix increases 23% of ultimate strength in plain concrete. The effect is clear and a correlation equation between steel fiber contents and ultimate strength can be found from best curve fitting, i.e.

$$f_{cf}^{'} = f_{c}^{'} + 2.15(RI) \tag{2.7}$$

Where

$f_{c}^{'}$ = Ultimate Strength of Plain Concrete (ksi)

$f_{cf}^{'}$ = Ultimate Strength of Steel Fiber-Reinforced Concrete (ksi)

RI = Reinforcing Index

2.4.4 Strain at Peak Stress

The ultimate strain value also increases with higher Reinforcing Index. This means adding steel fiber to concrete mixing helps high strength concrete to sustain more deformation during loading. The relationship is in the following (See Table 2.4):

$$\varepsilon_{f0} = \varepsilon_{0} + 0.0007(RI) \tag{2.8}$$

Where

ε_{f0} = Ultimate Strain of Steel-Fiber Reinforced Concrete

ε_{0} = Ultimate Strain of Plain Concrete

2.4.5 Proposed Parameters for Fiber-Reinforced Concrete

From regression analysis, the following relationship equation can be found. The parameters *a* and b have the same relationship as the reinforcing index. Figure A.14 and

Figure A.15 show comparisons of proposed equation and experimental data for 0.5% steel fiber content. From Figure A.16 through Figure A.19 are comparisons of proposed equation and test data for 1-% fiber and 2-% fiber. The proposed equation shows good agreement with test result. Figure A.20 shows relationship between reinforcing index and toughness ratio. This proves that steel fiber addition can improve post peak behavior substantially.

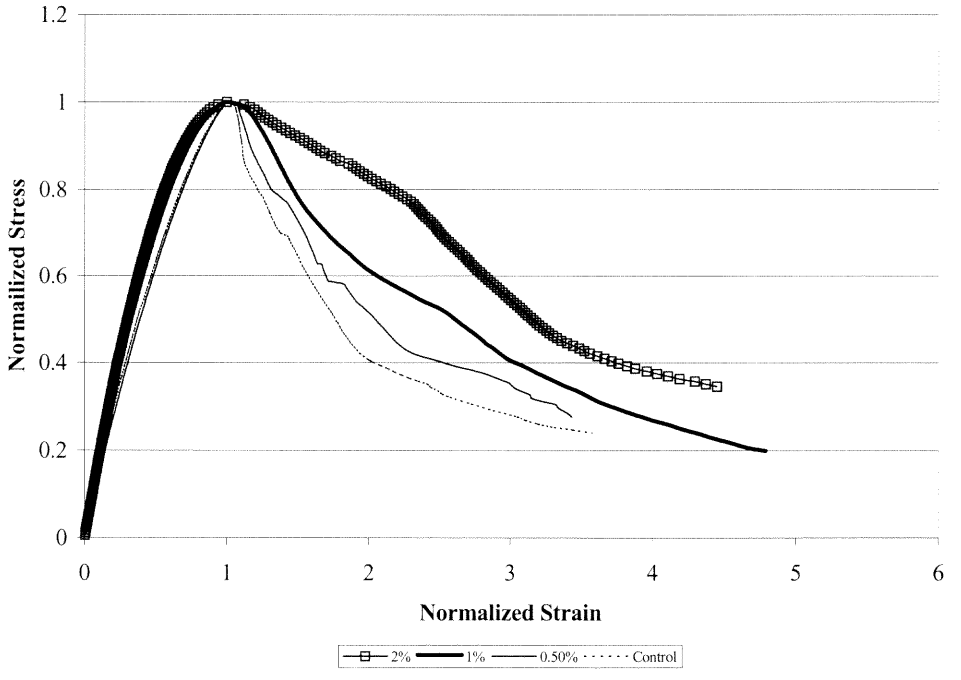

Figure 2.3 Experimental Stress-Strain Curve of Different Steel Fiber Contents

The relationship between fiber volume fraction and parameters is as follows (See Table 2.4):

$$a = b = 4.35 - 1.786(RI) \tag{2.9}$$

2.5 Confined HP/HS Concrete

High strength concrete (HSC) has been widely used recently for newer high-rise buildings. Using high performance/high strength concrete usually reduces the size of columns and beams in buildings, so one can get more space to use and rent. However high strength concrete has some unwelcome characteristics, in which it exhibits more brittle behavior. To compensate for this disadvantage, more confining reinforcements have been used. Confinement is achieved through the use of spirals or ties to enclose the longitudinal reinforcement. The main advantages of using more confinement are to increase the concrete ductility and strength. Use of confinement has been found to be effective in enhancement of ductility, especially in earthquake regions. As a result, it helps the structure to sustain larger deformations. Also, the confinements increase compressive strength so that it compensates strength loss from spalling of concrete cover (Ahmad and shah 1982).

The confinement effect depends on confining reinforcement, specimen size and shape (round, square, and rectangular), concrete properties such as strength and type of aggregate (Issa and Tobaa 1994, Nicole and etc. 1997). One of important parameter affecting confinement effect is spacing of reinforcement. Desayi and et al. (1978) found that the confinement is effective only when the pitch of confining reinforcement is less than least lateral dimension of the specimen. Ahmad also reported that when spacing of spirals exceeds the value of about 1.25 times the diameter of confined concrete, the effect of confinement is negligible (Ahmad and shah 1982). The influence of confinement is insignificant at low concrete stress, as evidenced by the almost identical values of initial

tangent modulus and Poisson's ratio for both the confined and unconfined concretes (Mansur and et al 1997).

2.5.1 Stress-Strain Behavior of Confined Concrete

The test data needed for developing analytical stress-strain equation come from Mansur and et al.'s (1997) test data. Their specimen size was prism with 100 x 100 x 200-mm. The ties have a yield strength, f_y of 71.5 ksi. To prevent premature failure by splitting ties, all steel ties were welded at the ends. The Different tie spacings were investigated and also steel fiber effect was studied. Figure A.21 through Figure A.28 show comparisons of test data and present proposed equation.

2.5.2 Proposed Parameters for Confined Plain Concrete

The equation2.4 can be used for confined plain concrete. *a* and *b* are material parameters that depend on the shape of stress-strain curve. For confined plain concrete, *a* and *b* factors are in the followings:

$$a = b = 2.336 - 5.3945\left(\frac{\rho_s f_y}{f_c'}\right) \tag{2.10}$$

Where

$$\rho_s = \frac{A_{sp}}{A_c} = \frac{\text{Volume of hoop in one hoop}}{\text{Volume of core for length s}}$$

f_y = yielding strength of steel (ksi)

f_c' = Ultimate strength of unconfined concrete (ksi)

2.5.3 Proposed Parameters for Confined Fibrous Concrete

Two material properties for confined fibrous concrete are obtained.

$$a = 3.6892 - 3.2405\left(\frac{\rho_s f_y}{f_c'}\right) \tag{2.11}$$

$$b = 2.1738 - 0.9848\left(\frac{\rho_s f_y}{f_c'}\right) \tag{2.12}$$

Where

f_y = yielding strength of steel (ksi)

f_c' = Ultimate strength of unconfined concrete (ksi)

2.6 Summary of Proposed Equation

From the present investigation, the proposed equations may be adequate to express stress-strain behavior for various cases. The two parameters (a, b) are equal for plain, steel fiber, and hoop case. But they are different in hoop with steel fiber case. With help of b factor, one can adjust the descending part efficiently. This characteristic is useful when the descending part has a large ductility. The original equation developed by Carreira and Chu (1985) is the best curve available. However, their approaches include an initial tangent modulus, that is not an appropriate material property of whole stress-strain curve.

There is a need to improve the test technique and method for HSC under compression. It has been found to be difficult to obtain a complete stress-strain curve using a 4-in. gage length in 4 x 8-in. concrete cylinder.

CHAPTER 3

STRESS-STRAIN BEHAVIOR OF HIGH PERFORMANCE FLY ASH CONCRETE WITH STEEL FIBERS AND HOOPS

3.1 Introduction

Fly ash is the finely divided residue that results from the combustion of ground or powered coal. The most influential factor of the ash produced is the coal source (Cook 1983). Fly ash is widely used nowadays as a replacement of portland cement because of its pozzolanic and cementitious properties (ACI 232.2R 1996). For the effective use of fly ash, it is important to understand the difference between fly ash and portland cement. The use of fly ash in concrete mix changes concrete properties. It changes both freshly mixed concrete and hardened concrete.

3.1.1 Property of Fresh Fly Ash Concrete

Workability is significant because a concrete mixture that does not have ease of placing, compacting, and finishing yields unsatisfactory strength and durability. The fly ash particles are typically small, ranging in diameter from 1 to 150 μm and spherical (Berry and Malhotra 1980). These characteristics cause a reduction water amount for a given degree of workability (Ravina 1984). Bleeding is the results from the inability of the constituent materials to hold all the mixing water (Metha 1993). Bleeding causes strength loss, usually larger in upper part of concrete structure. The use of fly ash provides larger surface area and can reduce bleeding (Idorn and Henriksen 1984). Setting of concrete is

the start of solidification. The use of fly ash may extend setting time of concrete if the portland cement content is reduced.

3.1.2 Property of Hardened Fly Ash Concrete

Both the strength development rate and ultimate strength, which are important in construction project, are controlled by the characteristics of the particular fly ash, the cement, and the mix proportion. The strength development is a function of the pore-filling process, which takes place with the formation of hydration products.

For a low-calcium fly ash, the laboratory research showed that compared with concrete without fly ash proportioned for equivalent 28 days compressive strength, a typical fly ash might develop lower strength at seven days of age or before when tested at room temperature (Abdun-Nur 1961). Comparing to low-calcium fly ash, a significant contribution to the strength of concrete found at early ages when the high-calcium fly ash was used. However the concrete mix with the high-calcium fly ash did not show dramatic strength gain like low-calcium fly ash mixture.

The modulus of elasticity of class F fly ash concrete, as well as its compressive strength, is somewhat lower at early ages and a little higher at later ages than similar concrete without fly ash (Lane and Best 1982). However the effect of fly ash is small. So cement and aggregate characteristics will have a greater effect on modulus of elasticity (Cain 1979).

Volume change, or drying shrinkage is basically a function of the volume of cement paste, the water cement ratio, the type of aggregate, the curing temperature, and relative humidity. If fly ash increases the water requirements of concrete, an increase in

drying shrinkage can be anticipated. Thus, ASTM C618 limits the increase in drying shrinkage to 0.03%.

3.1.3 Design Methods of Mix Proportioning

Fly ash may be used in concrete either as a blended cement or additional cementitious material. Because different fly ashes have different chemical composition, well-defined trial batch and testing program is needed. Due to flexibility of proportioning, fly ash as separate use is used widely. For the use of fly ash, several mix proportioning design methods have been developed (Cannon 1968, Gopalan and Hague 1989).

(1) Simple replacement method

With this method, portland cement and fly ash mixes are produced by simple equal mass or equal volume replacement of cement in concrete mix. This is simple to use, but fly ash concrete with this mix proportion shows lower early age strength than the corresponding plain portland cement concrete but equal strength can be achieved at later ages, usually after 90 days (Lovewell and Washa 1958). This method is suitable for mass concrete application such as dam or foundation. In these structures, the early strength of the concrete is not prime concern and the later age strength is important.

(2) Fly ash addition method

This method needs an addition of fly ash to cement. The cementitious content of the mix is increased by this method. It has found that addition of fly ash generally produced increased strength in concrete at all ages.

(3) Rational Method

In 1980, Owens (1980) developed a new method, in that the mix proportions of a portland cement concrete are modified to incorporate fly ash to produce an equivalent fly ash concrete. The appropriate adjustment factors for the cement and water contents are needed to get mix proportion.

(4) Overweight replacement method

The overweight replacement is similar to Owens's rational method. The method was developed in China. The method needs an overweight coefficient of cementitious materials to calculate the weight of fly ash and cement in fly ash concrete. Because the component of fly ash is unlike that of the portland cement, the amount of fly ash put into the mix is greater than the amount of cement removed, the difference being accommodated by simultaneous change in the aggregate proportions. The main requirement of overweight replacement method is to select the proportions of the constituent materials so as to produce concrete with all the desired properties in both the plastic and hardened states at a minimum cost. The performance of fly ash concrete designed by the overweight replacement method can be similar to that of normal concrete with the following characteristics (Chen 1986):

a. adequate workability
b. same 28 day strength
c. satisfactory durability
d. cost savingIf a suitable mix proportioning of normal concrete without fly ash is known, the following steps of the mix design procedure can be used to achieve an equivalent strength using fly ash concrete.

Step 1: Determination of the Overweight Coefficient of Cementitious Materials

$a = (C+F)/C_0$

Where a: overweight coefficient of cementitious materials

C_0: weight of cement in normal concrete (known)

C: weight of cement in fly ash concrete (unknown)

F: weight of fly ash in fly ash concrete (unknown)

Table 3.1 Fly Ash Overweight Coefficient

F/(F+C) (f % by weight)	Overweight coefficient of cementitious materials
0	1
10	1.02-1.035
15	1.035-1.055
20	1.055-1.085
30	1.085-1.10

The overweight coefficient of cementitious materials will depend on the fly ash characteristics related to the ordinary portland cement, particularly water demand, pozzolanic activity and cement replacement level selected by the designer. Normally, the values of fly ash overweight coefficient vary between 1.02 and 1.10, and will be selected by the table, which is based on tests or site experiences. The table about the overweight coefficient of cementitious materials is shown below. Of course, the cement replacement level (f % by weight) will be determined at the same time. The general trends are that the greater is the value of F/(F+C), the greater is the value of the overweight coefficient of cementitious materials. If the cement replacement level is constant, the greater is the

activity of cement, the greater is the value of overweight coefficient of cementitious materials.

Step 2: Determination of the Specific Gravity of Cement, Fly Ash and Sand

Obtain the specific gravity of cement (γ_c), the specific gravity of fly ash (γ_f) and the specific gravity of sand (γ_s) by tests or experience.

Step 3: Determination of Cement, fly ash and Sand Weight

The weight of cement in fly ash concrete (C), the weight of fly ash concrete (F) and the weight of sand in fly ash concrete (S) are determined as:

$$C = (C_0)(1\text{-}f\,\%)(a)$$

$$F = (C_0)(f\,\%)(a)$$

$$S = S_0 - (C/\gamma_c + F/\gamma_f - C_0/\gamma_c)(\gamma s)$$

Where S_0: weight of sand in normal concrete (known)

Note that the weight of water and coarse aggregate in fly ash concrete are the same as normal concrete. Now, all unknown values become known.

Step 4: trial mix

If the workability and the strength differ in the design values respectively, modify the overweight coefficient of cementitious materials. The mix design method has the flexibility and can be readily programmed for computer use.

3.2 Experimental Program

3.2.1 Materials

The materials used in present research are in the followings:

- Cement: ASTM type I Portland cement

- Fine aggregate: Air dried sand
- Coarse aggregate: 3/8-inch basalt was used. Before mixing, the aggregates were washed and air-dried to get saturated surface dry (SSD).
- Water: Tap water with ambient temperature
- Fly Ash: Type F Fly Ash
- Steel fiber: Steel fibers hooked at both ends were used. The length (l) is 30mm and diameter (d) is 0.5mm. The aspect ratio l/d of steel fiber is 60. The density is 7.8g/cm^3 and Young Modulus is 200GPa.
- Steel hoop: The tie confinement with circular hoops was used. Tie wires with 3/16-in. diameter were used to make the steel hoops. The circular hoops at different pitches of 1, 2, and 4 in, were used. To fix the tie wire confinements in the position, 28 gauge soft wires were used.

3.2.2 Mixing and Testing

Concrete was mixed in the concrete laboratory using an electric mixer. The sand, cement and fly ash were mixed first for a while without water. About 70% of water were added to the mixer and the coarse aggregate was added with the rest of water. Main specimen size was 4-x 8-in. cylinder. Reusable plastic molds were used for whole casting. The polyethylene covering was also used to prevent surface dry.

After 24 hours, the specimens were demolded and cured in moisture curing room with 100 percent relative humidity until a day before testing. All steps of casting were done according to ASTM C192. The mix proportions for 1 cubic yard are shown in Table 3.2. The overweight coefficients used for 10%, 20% and 30% are 1.03, 1.06 and 1.9

respectively. Compression test was proceeded under Strain Control (0.0002 in/sec) on 28 days from the mixing date. Splitting tension test (ASTM C 496) was performed to have tensile strength of each mixture.

Table 3.2 Mix Proportion of High Performance Fly Ash Concrete (lb/yd^3)

	Fly ash(F)	Cement(C)	Sand	Gravel	Water	W/(C+F)
Control Mix	0	700	1184	1728	340	0.485
10% fly ash	73	656	1136	1728	340	0.466
20% fly ash	150	600	1087	1728	340	0.453
30% fly ash	231	540	1036	1728	340	0.441

3.3 Plain Fly Ash Concrete

3.3.1 Test Results of Plain Fly Ash Concrete

To investigate the effect of fly ash replacement on material properties, three different mix proportions were selected. Control cylinders without fly ash were also prepared and tested. Table B.1 lists test results of plain concrete without fly ash. The table summaries the compressive strength, strain at peak stress, and modulus of elasticity. Ten specimens were prepared and tested at 28 days. Typical fly ash specimens after failure are shown in Figure B.1. The failure mode is not different from that of normal strength concrete without fly ash. Table B.2, Table B.3 and Table B.4 demonstrate test results of 10%, 20% and 30% replacement, respectively.

3.3.2 Compressive Strength

The test data of compressive strength in fly ash concrete with different fly ash replacement are shown in Figure 3.1. It is known that compressive strength of fly ash concrete depends on quality of fly ash, materials, curing condition. Fly ash concrete proportioned on one-for-one replacement method (either by volume or by weight) results in lower strength at early age (Berry and Malhotra 1980). With overweight replacement method, however, lower fly ash replacements do not change their compressive strength. The present tests indicate that 10% and 20% fly ash replacements do not improve ultimate strength of concrete. Meanwhile 30% fly ash replacement results in a slightly lower strength than that of the control mixing without fly ash. This shows that concrete mix with higher fly ash replacement may need higher overweight coefficient as indicated in Table 3.1.

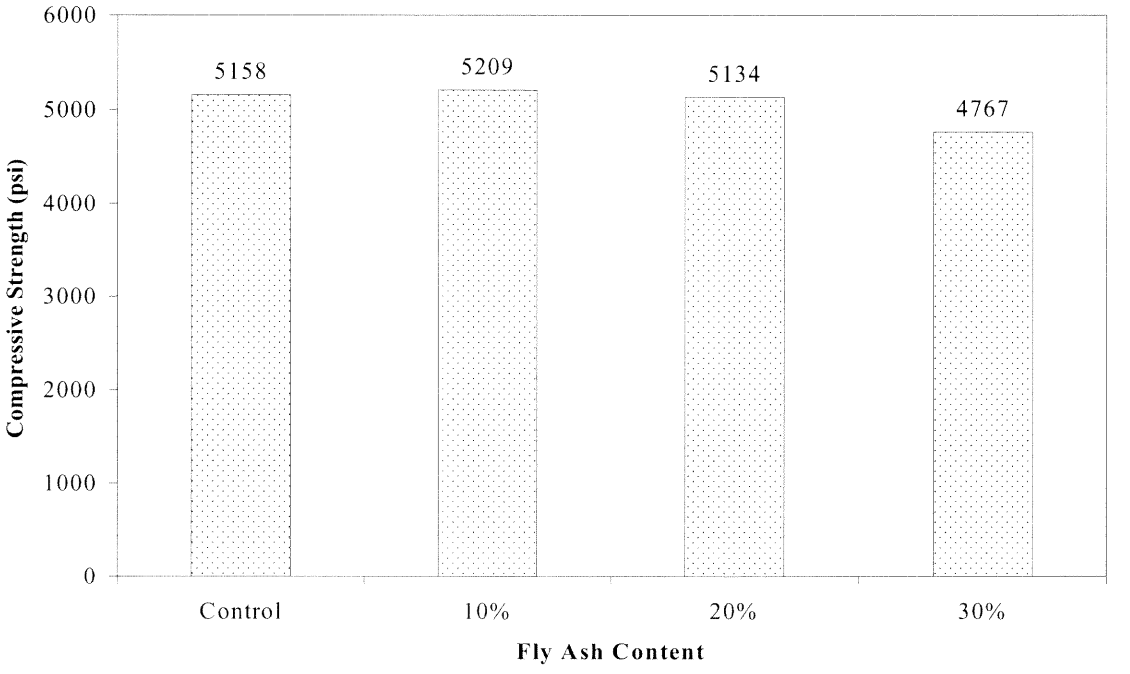

Figure 3.1 Effect of Fly Ash Overweight Replacement on 28 Days Compressive Strength

3.3.3 Modulus of Elasticity

Table 3.3 summaries the compressive strength, strain at peak stress, and modulus of elasticity from present study. The modulus of elasticity shown in Table 3.3 is the chord modulus according to ASTM C469-94. For normal weight concrete, ACI suggests

$$Ec = 57{,}000\sqrt{fc'} \tag{3.1}$$

Because of non-homogeneous characteristic the modulus of elasticity of concrete depends on materials used and transition zone. The modulus of elasticity at present study is slightly larger than that by the ACI equation. The control mix without fly ash also gives higher value. Thus the difference may be derived from aggregate characteristics of the mix.

Table 3.3 Compression Test Results of Different Fly Ash Replacement

Mix	Compressive Strength (psi)	Strain at Peak Stress	Modulus of Elasticity (ksi)	ACI Modulus of Elasticity (ksi)
Control	5158	0.001694	4513	4093
10% Replacement	5209	0.001657	4536	4113
20% Replacement	5134	0.001676	4648	4084
30% Replacement	4767	0.001606	4645	3884

3.3.4 Tensile Strength

There are two kinds of tension test. One is direct tension test and the other is splitting tension test. Direct tension test of concrete is seldom used, because the specimen holding devices introduce secondary stresses that cannot be ignored (Metha 1993). Splitting tension, according to ASTM C 496, can be carried out using 4 x 8-in cylinders. The splitting tension strength is computed from the following formula:

$$T = \frac{2P}{\pi l d} \tag{3.2}$$

Where T is the tensile strength, P the failure load, l the length and d is the diameter of the specimen. Test results are shown in Table 3.4. As indicated in Table 3.4, the tensile strength of fly ash concrete is approximately 12% of the compressive strength. In portland cement concrete, the direct tensile/compressive strength ratio is 10 to 8 percent for normal strength concrete. Therefore, fly ash concrete does not change significantly the tensile strength.

Table 3.4 Splitting Tension Test Results of High Performance Fly Ash Concrete

Mix	Failure Load (lb)	Tension Strength(lb/in^2)	T/f_c'
10% Fly Ash	33355	663	0.12
20% Fly Ash	33170	659	0.12
30% Fly Ash	28270	562	0.11

3.3.5 Stress-Strain Behavior

Figure 3.2 shows the complete stress-strain curves of concrete mixed with different percentage fly ash replacement. The replacement of cement by fly ash does not change the ascending branch but slightly changes the descending branch of stress-strain curve. Thus the use of fly ash in concrete slightly increases the ductility of concrete. The higher fly ash replacement shows higher durability rather than ductility as reported herein and by others (Lam et al. 1998). They found that the total area under the curve of the fly ash concrete is about 12% larger than that of the portland cement concrete. Their fly ash replacement was 25% and test age was 56 days. In the present study, 30% fly ash

replacement concrete has increased about 9.8% in ductility than that of normal concrete. This shows that the proper use of fly ash may slightly improve the ductility of concrete structure.

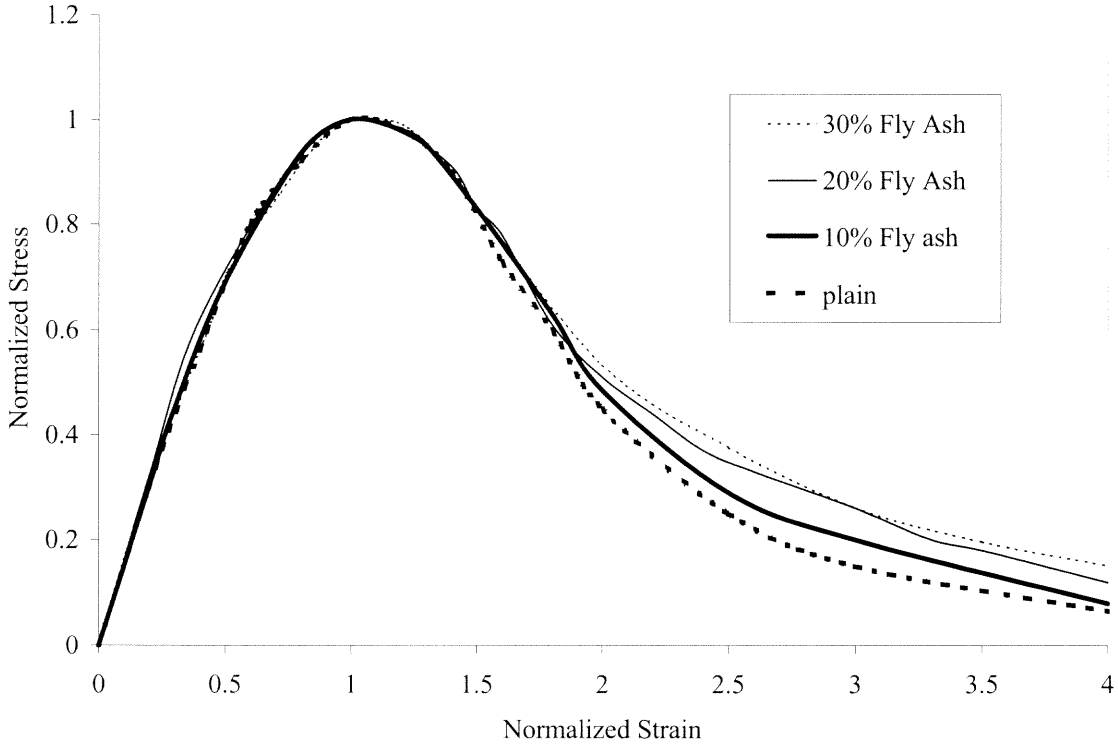

Figure 3.2 Normalized Stress-Strain Curve with Different Fly Ash Replacement Percentage

3.4. Fly Ash Fiber-Reinforced Concrete

3.4.1 Fly Ash Fiber-Reinforced Concrete Test Results

Fly ash concrete with different steel fiber content was tested. The general test results are similar to those using portland cement concrete with steel fiber. The ultimate strength and strain at peak stress are different from those in normal concrete. While the ascending branch of stress-strain curve remains the same as that in normal concrete, the descending branch of the curve behaves differently. The typical 0.5% volume fraction specimens after testing are shown in Figure B.2. Also Figure B.3 and Figure B.4 depict failure mode

of 1% and 2% volume fraction, respectively. It is noted that fly ash specimens never completely collapse even after reaching a high strain value. Table 3.5 shows the present test results. Detailed results of present compression tests are shown in Table B.5 through Table B.7.

Table 3.5 Compression Test Results of Fiber-Reinforced Concrete

Mix	Compressive Strength (psi)	Strain at Peak Stress	Modulus of Elasticity (ksi)	Toughness (psi)	Toughness Ratio
Control	5134	0.001676	4648		
0.5%	5286	0.001924	4290	28.1	0.354
1%	5737	0.002108	4648	44.1	0.519
2%	5978	0.002612	4397	72.6	0.779

Note: 20% Fly Ash Replacement

3.4.2 Compressive Strength

The addition of steel fibers to concrete mix definitely improves its ultimate compressive strength. In the present study, the 20% overweight replacement mix proportion was used to study the effect of fiber-reinforcement on its stress-strain behavior. Figure 3.3 shows comparisons of different fiber contents mixing. It is noted that the steel fiber volume fraction and its aspect ratio play an important role in stress-strain behavior of steel fiber-reinforced concrete. With 2% steel fiber volume fraction, the ultimate strength increases 16% more than that of normal concrete. Fanella and Naaman (1985) found that the addition of steel fiber improves compression strength up to 15percent. As both the volume fraction of fibers and their aspect ratio lead to improvements, their combined

effects can give better understanding of steel fiber. The following correlation equation between steel fiber contents and ultimate strength was obtained from regression analysis.

$$f'_{cf} = f'_c + 716(RI) \tag{3.3}$$

where

f'_c = Ultimate Strength of Plain concrete (psi)

f'_{cf} = Ultimate Strength of Steel Fiber Reinforced Concrete (psi)

RI = Reinforcing Index

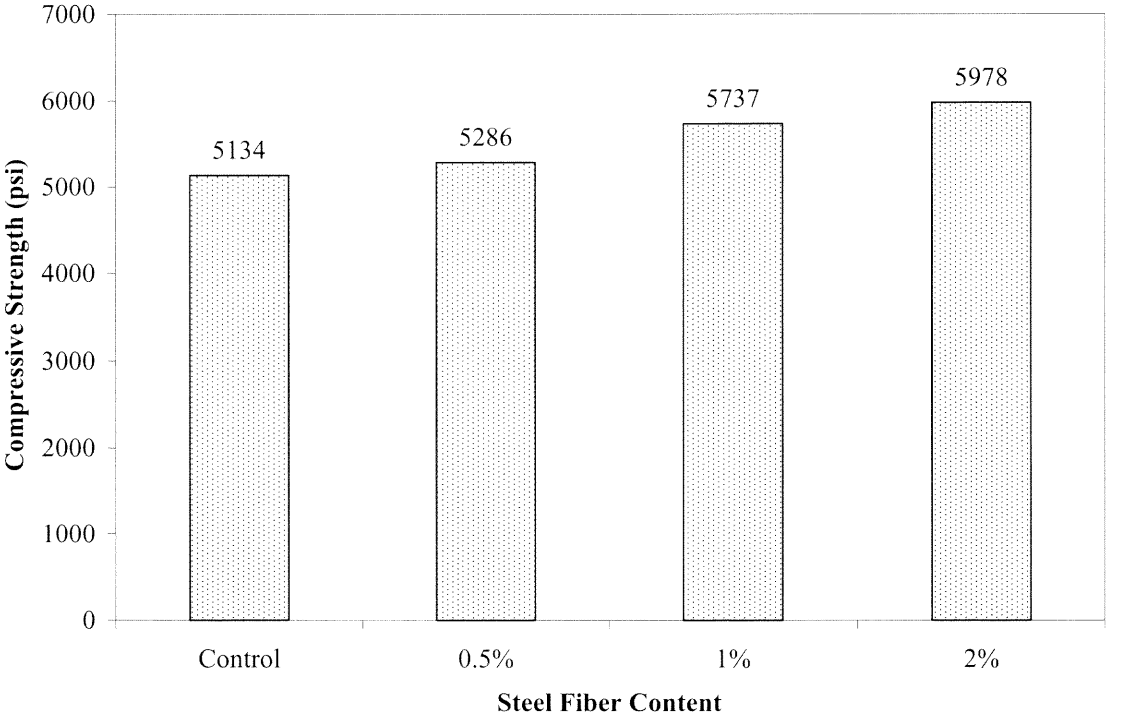

Figure 3.3 Influence of Volume Fraction of Fiber on Compressive Strength

3.4.3 Strain at Peak Stress

Figure 3.4 shows the strain at peak stress as a function of fiber volume fraction. The strain at peak stress increases from 0.001676 to 0.002612. It is clear that the addition of

steel fiber is found to increase the strain corresponding to the peak stress. The following relationship between the reinforcing index and strain at peak stress is given by:

$$\varepsilon_{f0} = \varepsilon_0 + 0.0008(RI) \tag{3.4}$$

where

ε_{f0} = Ultimate Strain of Steel Fiber Reinforced Concrete

ε_0 = Ultimate Strain of Plain Concrete

RI = Reinforcing Index

The above equation is almost the same as that found in a high performance high strength concrete with silica fume.

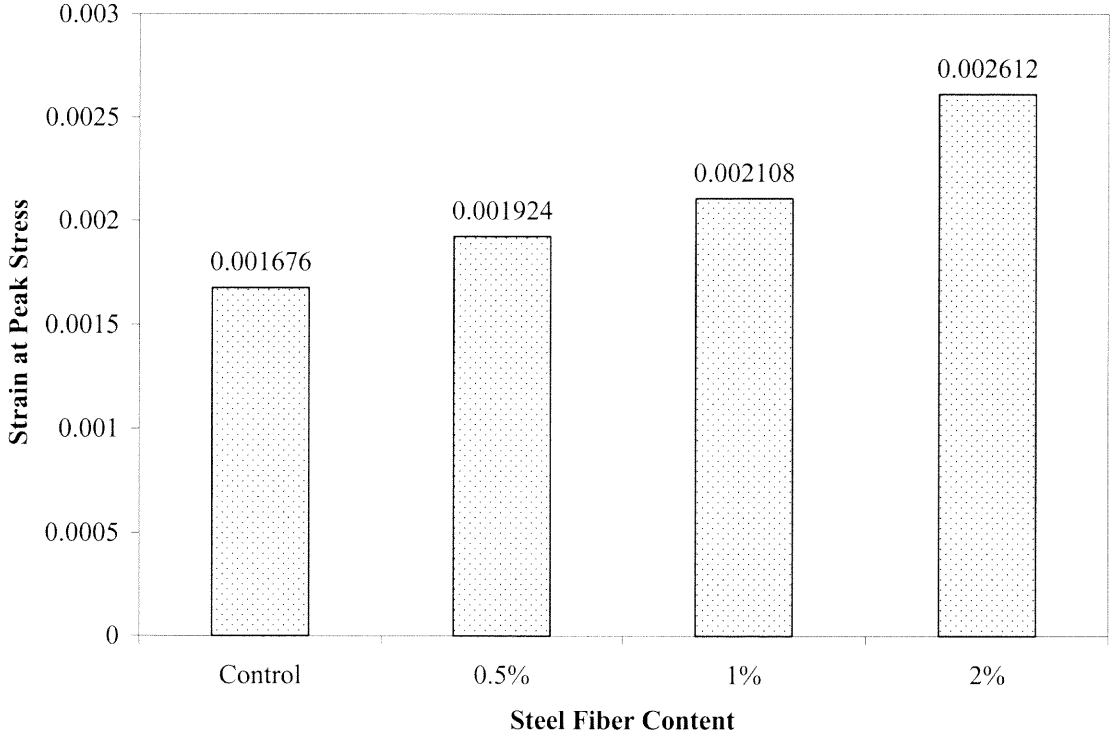

Figure 3.4 Influence of Volume Fraction of Fiber on Strain at Peak Stress

3.4.4 Toughness

To evaluate the effect of steel fiber on toughness of concrete, toughness ratio was used. Ezeldin and Balaguru (1992) proposed this rigid plastic approach. Nataraja and et al. (1999) also used this method to study effect of steel fiber on its strain-stress curve. With adding steel fiber to concrete mixing, toughness ratio is increased substantially. The 2% steel fiber mixing shows its 120% increased toughness ratio than that by 0.5% steel fiber mixing.

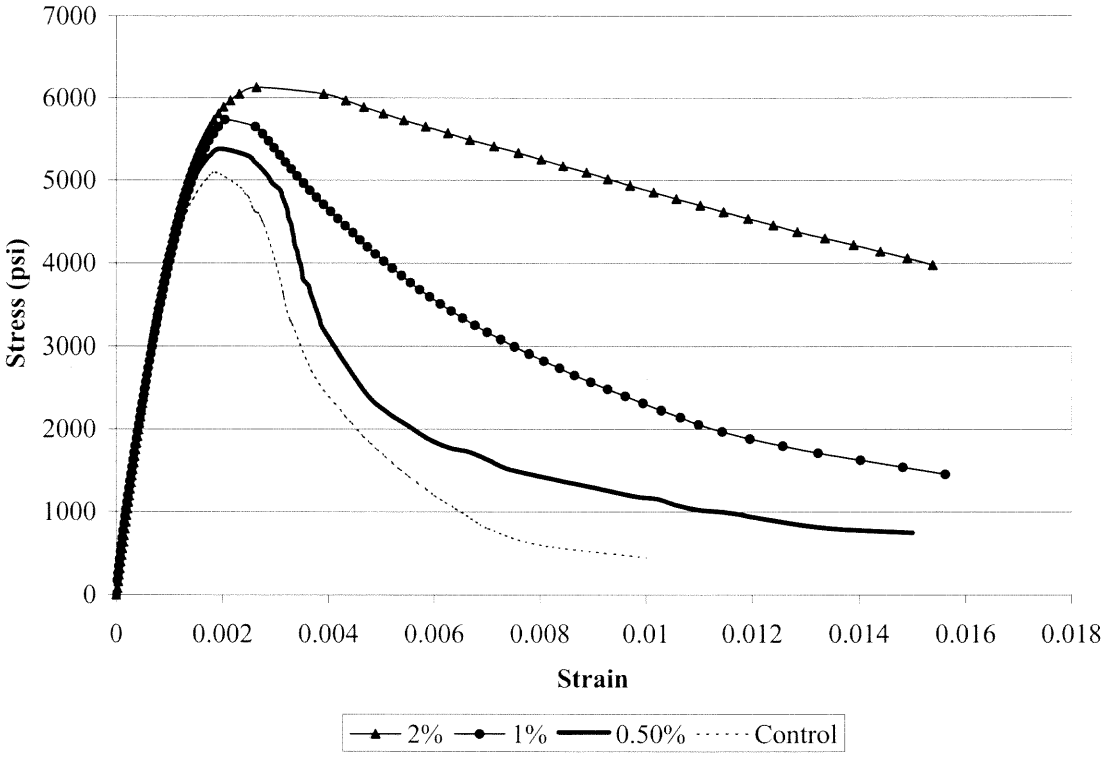

Figure 3.5 Stress-Strain Curve of Different Steel Fiber Content

3.4.5 Stress-Strain Behavior

Figure 3.5 shows the test results of fiber-reinforced concrete. The addition of steel fiber does not change its ascending branch of stress-strain curve, but significantly changes its

descending branch. This proves that steel fiber addition is good for ductility improvement. The toughness of concrete is related to its ability to absorb energy. Under impact or seismic loading, the structures should have enough ductility to withstand their complete collapse, and hence save the human lives.

3.5 Fly Ash Concrete with Tie Confinement

Table 3.6 shows the present compression test results of fly ash concrete with tie confinement. The circular hoops at different pitches of 1, 2, and 4 in, were used. To fix the tie wire confinements in the position, 28 gauge soft wires were used. Figure 3.6 shows some setup of circular hoops.

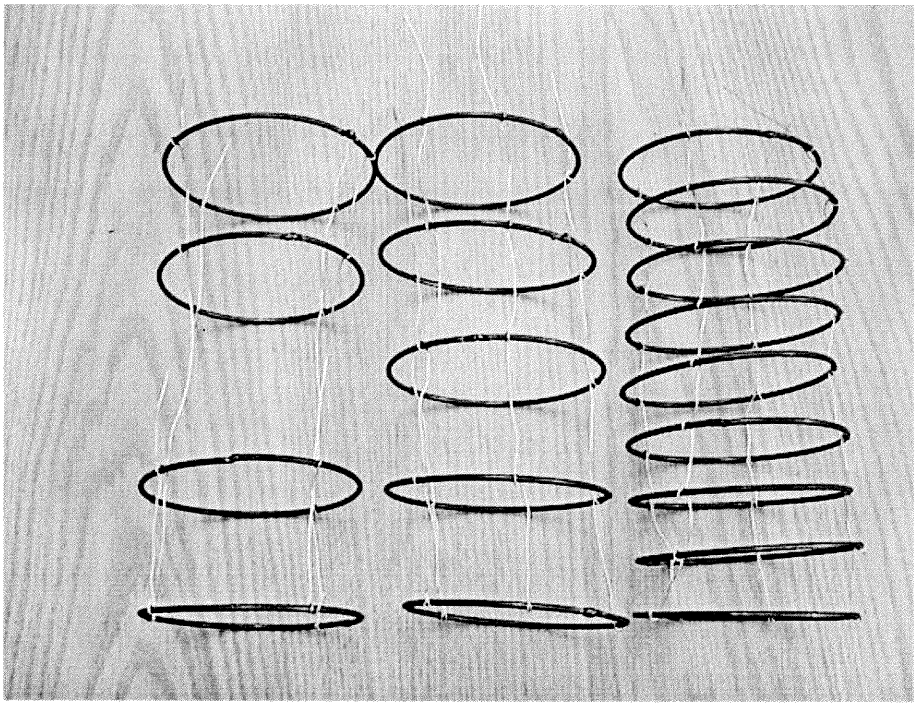

Figure 3.6 Setup of Circular Hoop

Figure 3.7 illustrates the typical stress-strain curves at different tie spacing for plain concrete. Observing the curves from the figure, the compressive strength and its corresponding strain increase with increasing tie confinements.

Table 3.6 Compression Test Results of High Performance Fly Ash Concrete with Confinements

Mix	Compressive Strength (psi)	Strain at Peak Stress	Modulus of Elasticity (ksi)
S=4"	5173	0.002276	4614
S=2"	5253	0.002553	4826
S=1"	5424	0.003072	5127

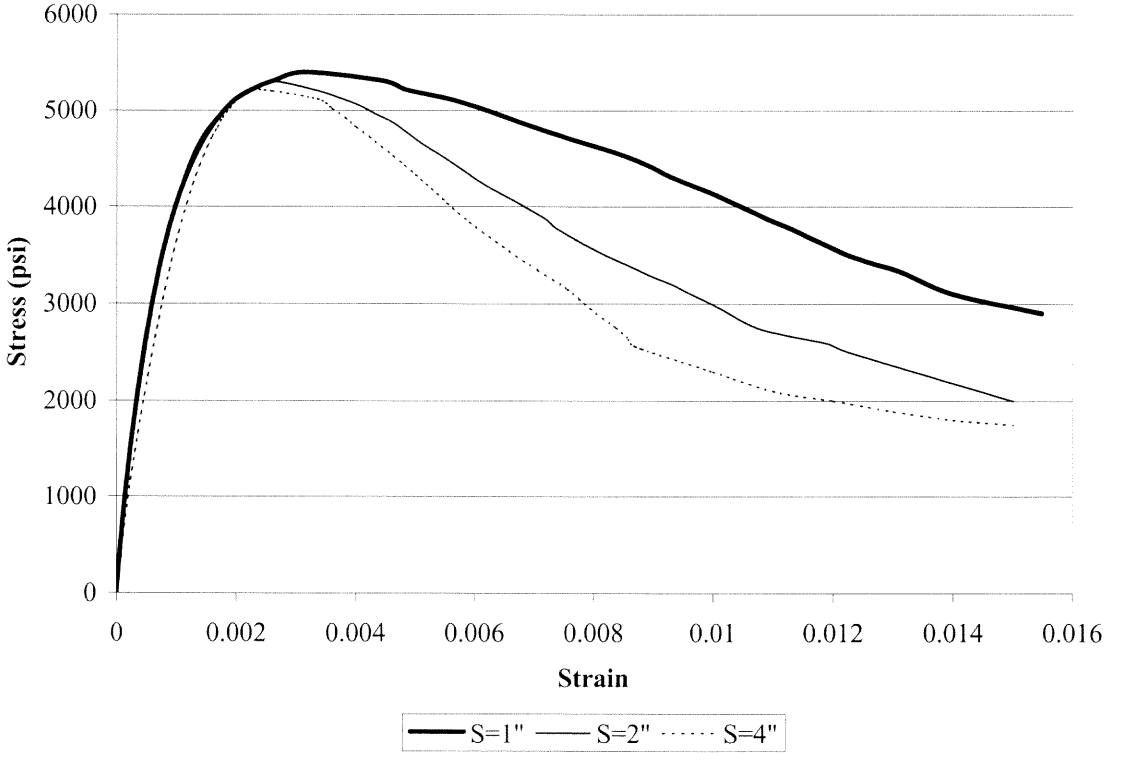

Figure 3.7 Stress-Strain Curve of Fly Ash Concrete with Confinements

The detailed test results are shown in Table B.8 through Table B.10. There is significant change in the descending part of stress-strain curve. Since the confinement by circular hoops provides passive confinement, lateral reinforcement becomes effective only after considerable deformations have taken place in axial direction (Sargin 1971, Deyasi 1978). Figure B.5, Figure B.6, and Figure B.7 show specimens after failure.

3.6 Fly Ash Concrete with Tie Confinement and Steel Fiber

To study the effect of combined action, the fiber-reinforced concrete was mixed with circular hoop. The fiber volume fraction was fixed to 0.5% The test results are shown in Table 3.7. Also the typical stress-strain curves are depicted in Figure 3.8. The compressive strength and strain at peak stress increase with increasing tie confinement. The detailed test results are shown in Table B.11 through Table B.13. Figure B.8 depicts the typical cylinders after failure.

Table 3.7 Compression Test Results of Fiber-Reinforced High Performance Fly Ash Concrete with Confinements

Mix	Compressive Strength (psi)	Strain at Peak Stress	Modulus of Elasticity (ksi)
S=4"	5298	0.002537	4545
S=2"	5547	0.002719	4735
S=1"	5857	0.003307	3875

3.7 Analytical Stress-Strain Curve

A number of empirical equations have been developed to represent uniaxial stress-strain behavior of concrete (Popovics, 1973). However most of them can be used for only

ascending portion of a complete stress-strain curve. In 1985, Carreira and Chu extended the empirical equation proposed by Popovics (1973) to include both ascending and descending branches of the curve (Carreira and Chu, 1985). Recently, Hsu and Hsu (1994a, 1994b) proposed a complete stress-strain equation under axial compression.

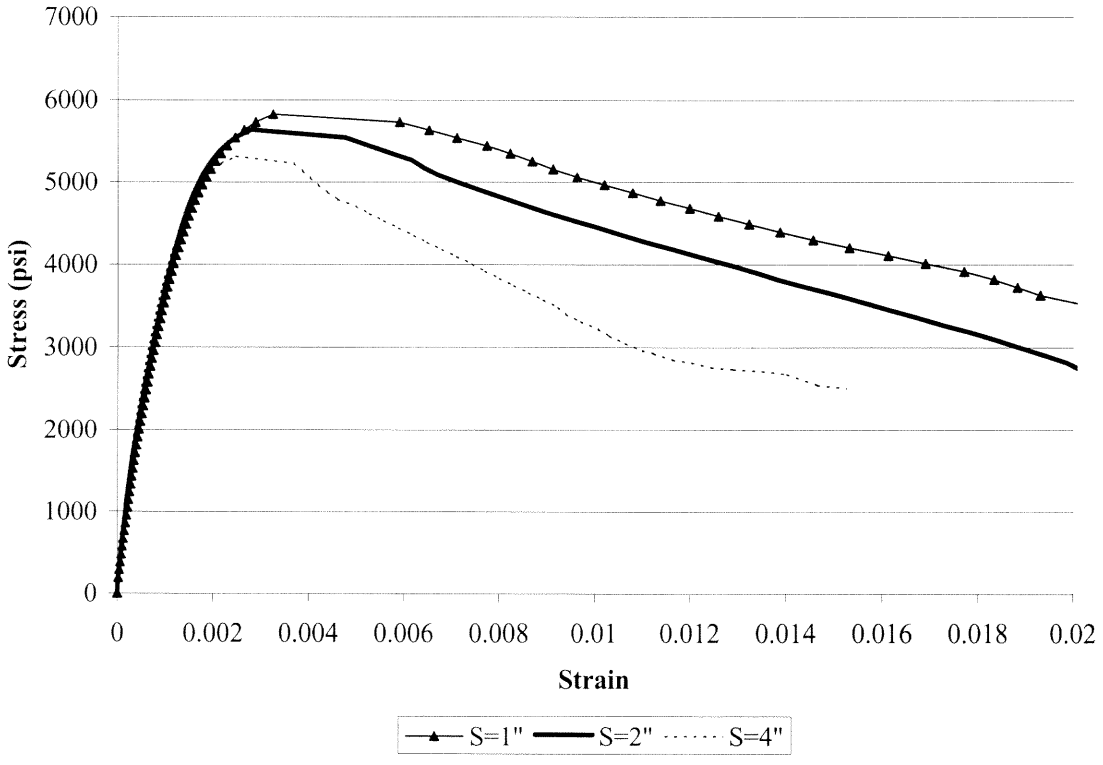

Figure 3.8 Stress-Strain Curve of Fiber Reinforced Fly Ash Concrete with Confinements

Their empirical formula includes the effect of steel fibers and/or hoops in plain concrete. But no well-documented paper is available for fly ash concrete. In this research, the constants a and b in Equation 3.5 represent the effect of steel fibers and/or hoops in fly ash concrete.

$$y = \frac{ax}{a - 1 + x^b} \tag{3.5}$$

where

$$y = \frac{f_c}{f_c'}, \quad x = \frac{\varepsilon_c}{\varepsilon_0}$$

f_c = concrete stress

f_c' = maximum compressive strength of concrete

ε_c = concrete strain, ε_0 = concrete strain at f_c'

a and *b* are material constants that can be determined by experiments. The following relationships are found based on present tests and curve fittings. Figure B.8 through Figure B.48 illustrate the comparative results of complete stress-strain curves between the experimental results and the proposed equations.

3.7.1 Parameters for Plain Fly Ash Concrete with/without Confinements

Fly ash changes the characteristics of hardened concrete. From the stress-strain curves found in present study, fly ash concrete has different stress-strain curve than that of normal concrete. Thus, the effect of fly ash has to be included in the analytical stress-strain model. Based on present tests, the following *a* and *b* can be used for different fly ash replacement without confinements

$$a, b = 3.7 - 0.02\text{Rp} \tag{3.6}$$

Where Rp = % fly ash replacement

The expression of stress-strain curve is the same as the one for a unconfined concrete except using different *a* and *b*. *a* and *b* parameters are depend on the volumetric ratio of confinements. The expression of *a* and *b* with steel confinement are:

$$a, b = 2 - 28.937\ \rho_s \tag{3.7}$$

where ρ_s = volumetric ratio

3.7.2 Parameters for Fly Ash Fibrous Concrete with and without Confinement

The addition of steel fiber to concrete mix shows its ductility improvement. The following relationships are found from the present compression tests.

For Fly Ash with Steel Fiber

$$a = 2.775 - 0.5929Sv \tag{3.8}$$

$$b = 2.85 - 0.7Sv \tag{3.9}$$

Where Sv = steel fiber volume fraction

For Fly Ash with Steel Hoop plus Steel Fiber (0.5%)

$$a = 1.9 - 22.765\rho_s, \tag{3.10}$$

$$b = 1.8 - 22.765\rho s \tag{3.11}$$

Where ρ_s = volumetric ratio

3.8 Summary

A simple empirical equation is proposed herein to depict the complete stress-strain behavior of high performance fly ash concrete under compression. The equation is valid for a normal strength concrete. Once the ultimate strength and concrete strain are known, only two parameters are needed to study the ascending and descending behavior of

concrete. The proposed equation fits well in various concrete mixtures including steel fibers and/or hoops, and can be found useful in studying the behavior of fly ash concrete structures reinforced with steel fibers in addition to the standard steel reinforcing bars and stirrups.

CHAPTER 4

DESIGN IMPLICATION OF PROPOSED STRESS-STRAIN EQUATION

4.1 Definitions of Ductility

In design it is significant to ensure ductile behavior in case of failure of structure. Ductility is the ability to sustain inelastic deformations without substantial decreases in the load carrying capacity (Shin and et al. 1989). Ductility is an essential property in structures that have to respond to inelastic in severe earthquake. It is measured in term of strain, displacement, and rotation (Nawy 2001). Three measures of ductility are identified:

1. Strain ductility

$$\mu_e = \frac{\varepsilon}{\varepsilon_y} \tag{4.1}$$

Where ε is the maximum sustainable strain and ε_y is the yield strain ductility.

2. Curvature ductility

$$\mu_\phi = \frac{\phi_m}{\phi_y} \tag{4.2}$$

Where ϕ_m is the maximum sustainable curvature and ϕ_y is the yield curvature.

3. Displacement ductility

$$\mu_\Delta = \frac{\Delta}{\Delta_y} \tag{4.3}$$

Where Δ is the maximum sustainable displacement and Δ_y is the yield displacement.

The values of all these ductility factors have to be considerably greater than 1.0 for inelastic behavior to be sustainable.

From the previous three definitions, strain ductility has been chosen to study ductility in the concrete specimen. With this concept ductility can be easily calculated from stress-strain curve under compression. The concrete, especially high strength concrete, is a brittle material, and hence plain concrete cannot sustain large deformation. To overcome this problem, fibers and confinements have been used. They have proven their ability to improve the mechanical properties of the concrete, both as a structure and a material (Nawy 2001).

4.2 Steel Fiber Effect on Ductility

Different types of fiber are available. It can be made from steel, glass, or polypropylene (Fanella and Naaman 1985). Present study is concentrated on steel fiber. The steel fiber can be added from 0.25 to 2% by volume. High values of steel fiber content cause harsh mix and make difficult to apply to normal structures. Thus, the present research uses 1% and 2% steel fiber by volume to study the effect of steel fiber on concrete.

As shown in Figure 4.1, adding steel fiber to a concrete mix significantly changes the concrete post-peak stress-strain behavior. The figures show that the strain value can reach up to 0.015, which is considered as lower bound of toughness. Plain fly ash concrete shows the strain value at 0.01 and then the specimen has no capacity to resist any more loading. However in case of fiber-reinforced concrete, the specimen can sustain

larger strain value and still can support certain amount of load. The 2% fiber-reinforced specimen did not fail at 0.015 strain and it also showed a stable descending behavior. The strength drop was only 34%. This is much different phenomenon from that of plain concrete specimen from which a large strain value can not obtain.

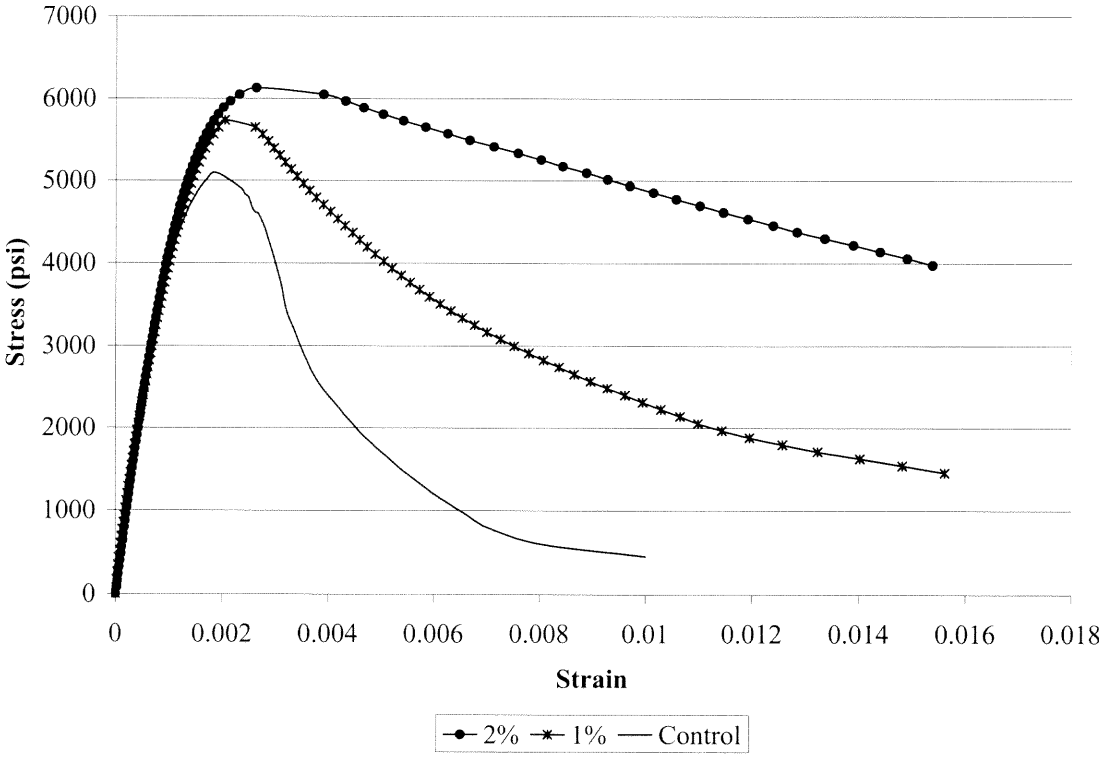

Figure 4.1 Stress-Strain Curve of Fly Ash Concrete with Different Steel Fiber Content

4.3 Confinement Effect on Ductility

Concrete may be confined by transverse reinforcement, in the form of closely spaced steel spirals or hoops. The confinement is not stressed when the stress is low. However at high stress stage the confinement starts to apply confining reaction to concrete. Thus, the transverse reinforcement provides passive confinement. The effectiveness of confinement

depends on details of the confining reinforcement. Earlier investigations have shown that confinement of concrete by circular spirals is more effective than other types (Desayi and et al. 1978). The effect of confinement on ductility is significant but effect on strength is marginal. To study effectiveness of confinement, three different hoop spacings were used. The typical high performance fly ash concrete stress-strain curves obtained from the present study are given in Figure 4.2. From these curves it can be noted that the descending branches is flatter for a smaller spacing. However the increase in strength is minimal with confinement.

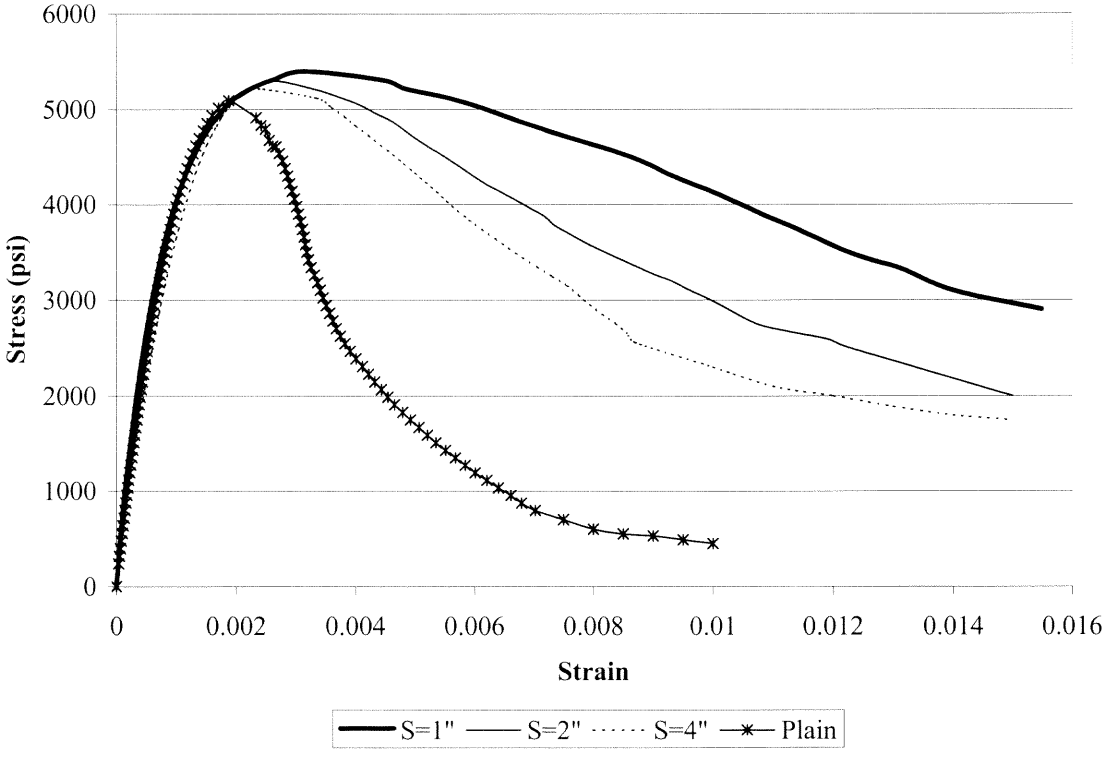

Figure 4.2 Stress-Strain Curve of Fly Ash Concrete with Different Hoop Spacing

Observing the curves from the figures, there is not much difference in the initial portion of the stress-strain curves for confined and unconfined plain concretes. The confining reinforcement prevents spalling of the concrete cover so that concrete can keep its loading capacity. With confinement, the ductility improvement is substantial. Comparing load from 4000psi to 3000psi in descending branch, the concrete with 2-in spacing confinement can deform more than 10 times than that of plain concrete.

4.4 Design Recommendations

Steel fiber-reinforced concretes are designed to contain a maximum of 2% by volume of fibers, using the same mixture procedures and placement as nonfibrous concretes. Concrete is weak in tension. Microcracks start to generate in the matrix of structural element at about 10-15% of the ultimate load, propagating into macrocracks at 25-30% of the ultimate. Consequently, plain concrete members cannot be expected to sustain large transverse loading without the addition of continuous bar-reinforcing elements in the tensile zone of supported members such as beams or slabs. But the developing microcracking and macrocracking still cannot be arrested or slowed down by the sole use of main continuous reinforcement. The function of such reinforcement is to replace the function of the tensile zone of a section and assume the tension equilibrium force in the section. Consequently, the addition of randomly spaced discontinuous fiber elements should aid in arresting the development or propagation of the microcracks, which are known to generate at such an early stage of loading history. Fibers are able to add to the stiffness and crack control performance through preventing the microcracks from propagating and widening and also increase ductility due to their energy absorption

capacity. Common applications of fiber-reinforced concrete include overlays in bridge decks, industrial floors, highway and airport pavements, thin shell structures, and seismic- and explosion-resisting structures (Nawy 2001).

It is distinctly advantageous to use high strength concrete in columns of tall structures, resulting in significantly smaller column sizes, and additional floor space and reduced cost. Confining the concrete not only can arrest the increase in brittleness but increases the ductility of concrete to very high levels. Seismic codes are continuously being modified, so designers are required to provide the energy-absorbing and energy-dissipating capabilities necessary for a structural system to survive strong earthquake motions; they do this through ductility increase (Nawy 2001). Thus the present research results of experimental stress-strain curves under compression and proposed empirical equations of steel fibers and/or steel hoops can be used for designing modern high-rise buildings and structures.

CHAPTER 5

CONCLUSION

5.1 On Behavior of High performance Silica Fume High Strength Concrete with Steel Fiber and Hoops

1. The strain corresponding to the peak stress for the high performance silica fume high strength concrete is greater than that for the normal concrete. Therefore, the constant values of 0.002 and 0.003 for the strain corresponding to peak stress and ultimate strain, as specified by ACI committee 318, are conservative.
2. The shape of the ascending part of the stress-strain curve for high performance silica fume high strength concrete behaves a more linear and steeper curve. The slope of the descending part also exhibits a steeper curve for the high strength concrete as compared to that of the normal concrete.
3. Test results shows that there is no significant size effect on the compressive strength among 3 x 6-in, 4 x 8-in, and 6 x 12-in concrete cylinders.
4. The specimens with smaller gage length ratio show more ductility than one with larger ratio. This is because larger gage ratio measuring can detect more cracks processed during its loading stage.
5. The addition of steel fiber to concrete mix increases ultimate strength and strain at peak stress. The 2% steel fiber adding by volume increases 23% ultimate strength of plain concrete.
6. The strain corresponding to the peak stress increases with increasing lateral tie confinements.

7. Both steel fiber addition and confinements increase the ductility of concrete.
8. Analytical equation has been proposed herein to generate a complete stress-strain curve for the high performance silica fume high strength concrete.
9. A good agreement is achieved for the stress-strain curves between various experimental results and the proposed analytical equations.
10. The proposed stress-strain equation also gives good results compared to the experimental data from Wee et al. (1997).

5.2 On Behavior of High performance Fly Ash Concrete with Steel Fiber and Hoops

1. Low replacement fly ash concrete designed by the overweight replacement method can reach the same strength as that of normal concrete at 28 days. However in high replacement fly ash concrete, it shows slightly lower strength than that of normal concrete.
2. The modulus of elasticity of fly ash concrete is slightly larger than that in normal concrete.
3. The use of fly ash in concrete increases the ductility of concrete, but the improvement is not significant and thus more research work is needed in this field.
4. The use of steel fiber in fly ash concrete changes the ultimate strength and strain at peak. Adding 2% steel fiber in concrete increases 16% strength than that of normal concrete. With help of steel fiber, fly ash concrete does not fail even after reaching a high strain value.
5. Both the maximum compressive strength and strain corresponding to peak stress increase with increasing number of tie confinements.

6. A simple empirical equation is proposed herein to depict the complete stress-strain behavior of high performance fly ash concrete under compression. The equation is valid for a normal strength concrete. Once the ultimate strength and concrete strain are known, only one or two parameters are needed to study the ascending and descending behavior of concrete.
7. The proposed equation fits well in various concrete mixtures including steel fibers and/or hoops, and can be found useful in studying the behavior of fly ash concrete structures reinforced with steel fibers in addition to the standard steel reinforcing bars and stirrups.
8. A good agreement is also achieved for the stress-strain curves between the present experimental results and the proposed analytical equation for various cases.

APPENDIX A

EXPERIMENTAL DATA OF HIGH PERFORMANCE SILICA FUME HIGH STRENGTH CONCRETE

In this appendix, experimental results of high performance silica fume high strength concrete are shown.

Table A.1 Test Results of Ultimate Strength for High Performance Silica Fume High Strength concrete

Specimen	$f_c^{'}$ (ksi)	ε_0	Test Age (days)
HP1	12.3	0.002709	28
HP2	12.29	0.002769	28
HP3	12.6	0.002878	28
HP4	11.77	0.002548	28
HP5	11.51	0.002469	28
HP6	10.85	0.002434	28
HP7	10.98	0.002419	28
HP8	11.40	0.002633	28
HP9	11.22	0.002554	28
HP10	11.48	0.002678	29
HP11	11.4	0.002778	29
HP12	11.28	0.002734	29
HP13	11.48	0.002738	29
HP14	11.28	0.002607	29
HP15	11.54	0.002680	29
HP16	10.41	0.002653	30
HP17	9.98	0.002788	30
HP18	10.39	0.002699	30
HP19	11.71	0.002864	30
HP20	10.43	0.002756	30

Note: The above specimens were not able to obtain a complete stress-strain curve because the cracks occurred outside the gage length region.

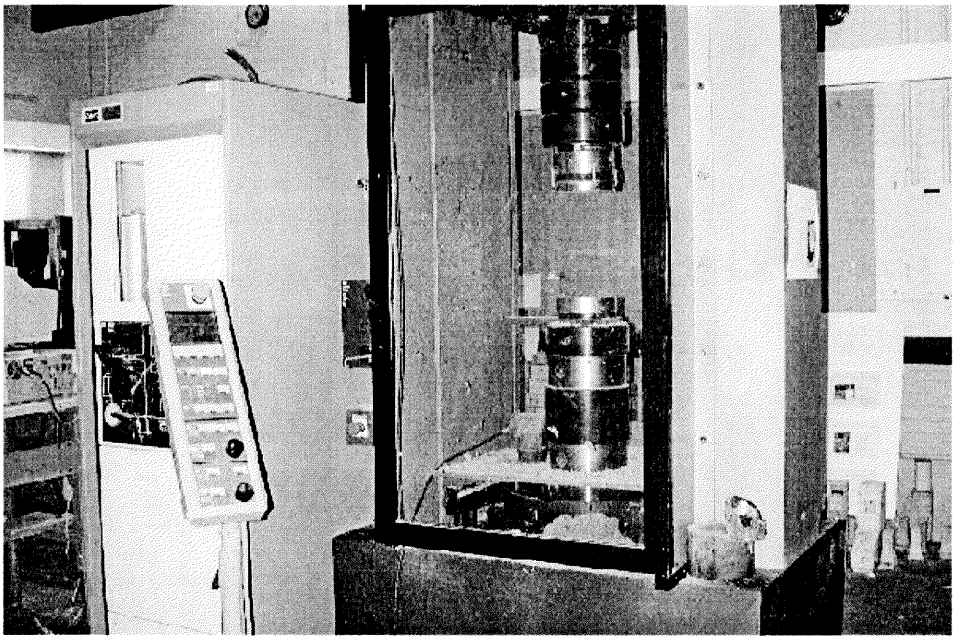

Figure A.1 Testing Machine Setup for Compression Test

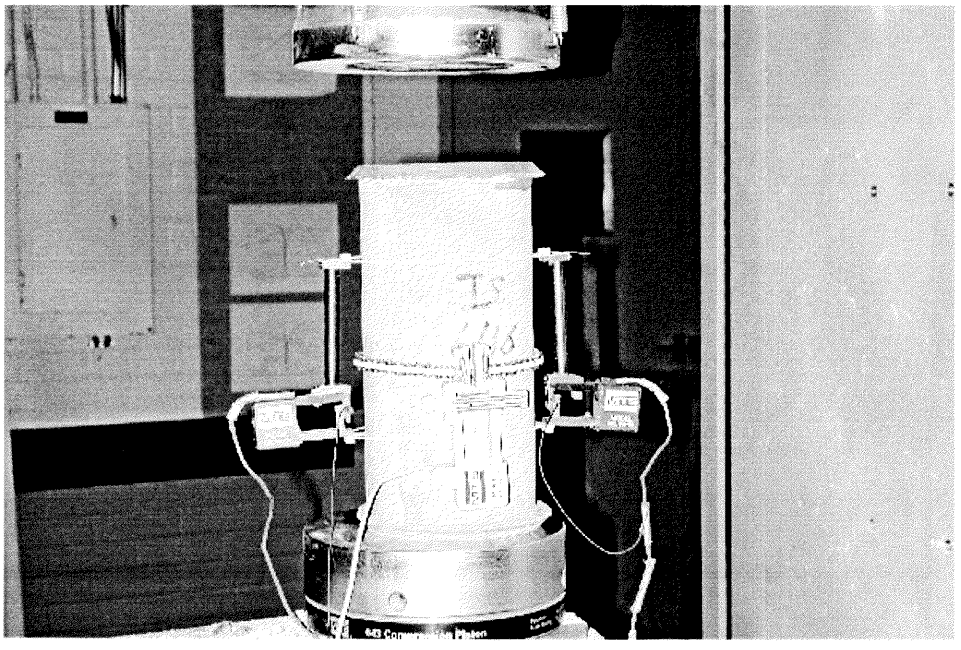

Figure A.2 Gage Setup for Measuring Strain Values

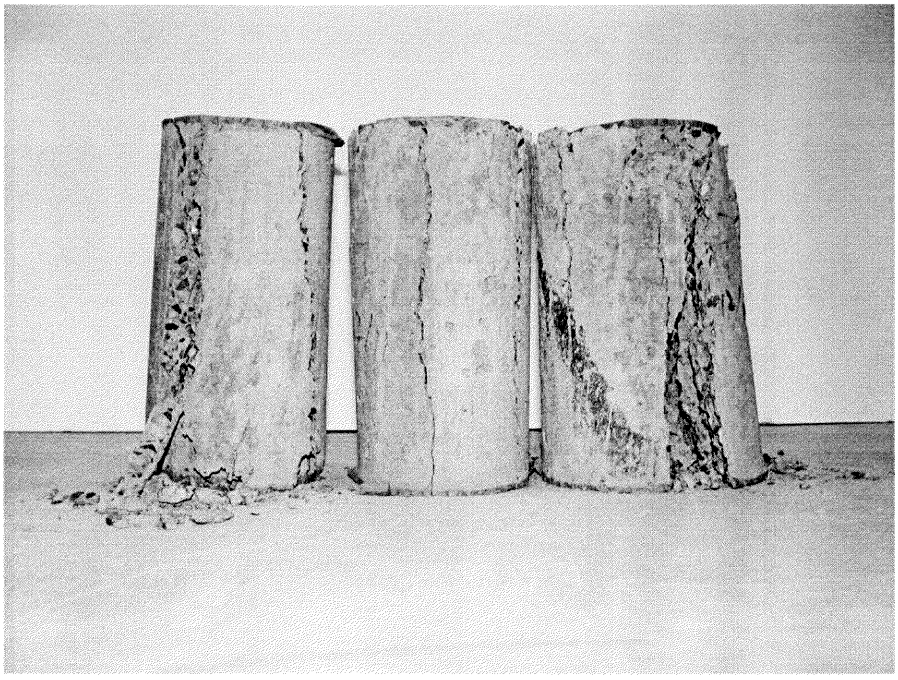

Figure A.3 Cylinder after Compression Test (Plain Concrete)

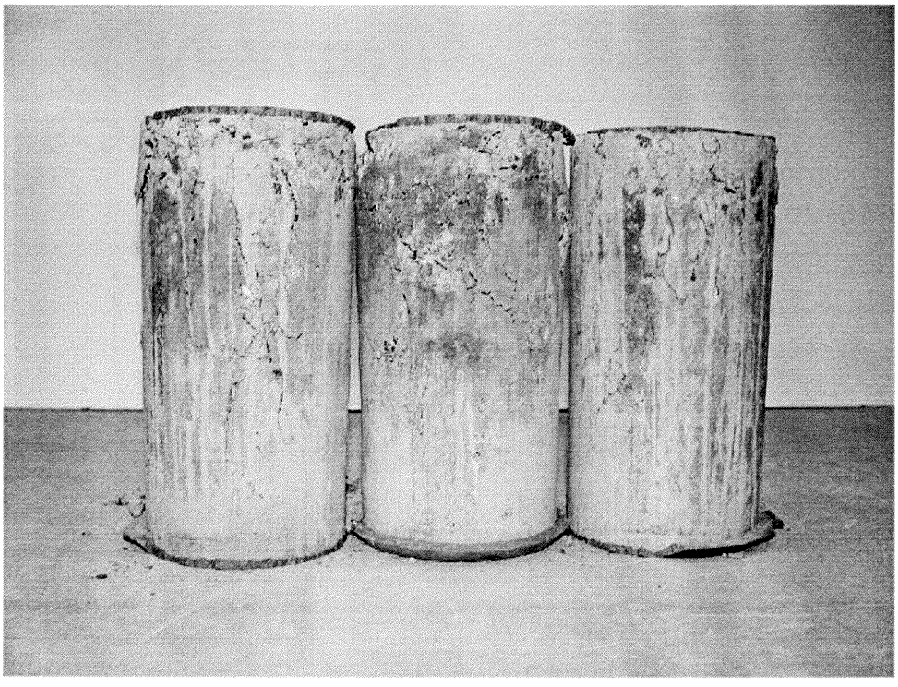

Figure A.4 Cylinder after Compression Test (Steel 0.5%)

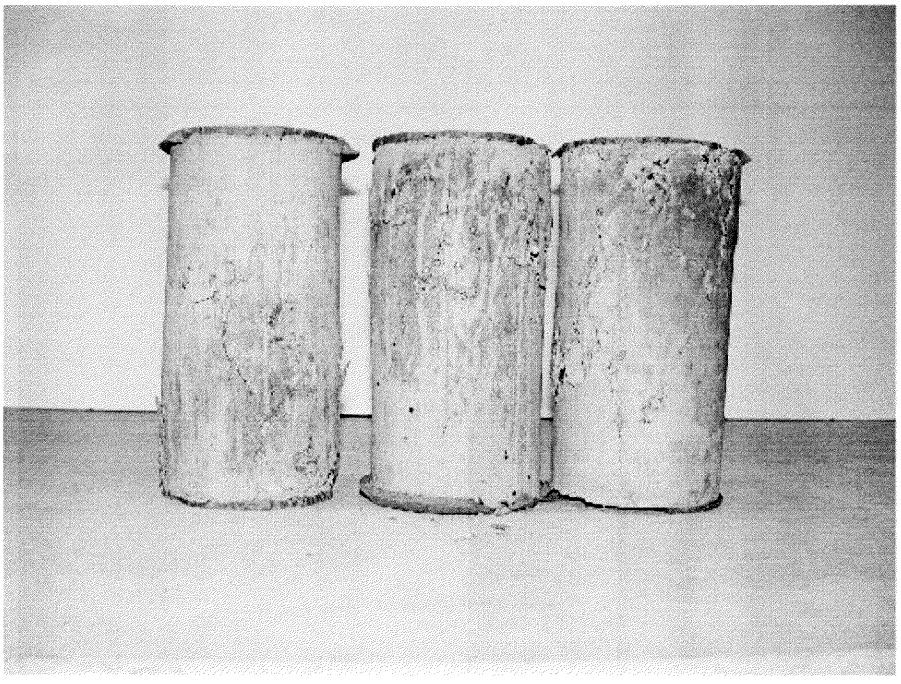

Figure A.5 Cylinder after Compression Test (Steel Fiber1%)

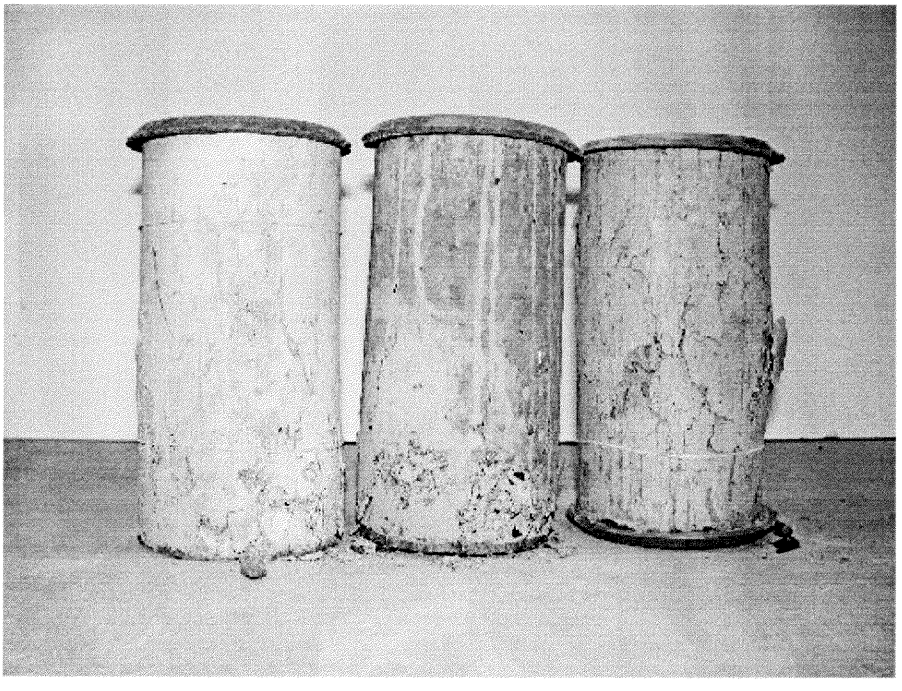

Figure A.6 Cylinder after Compression Test (Steel Fiber2%)

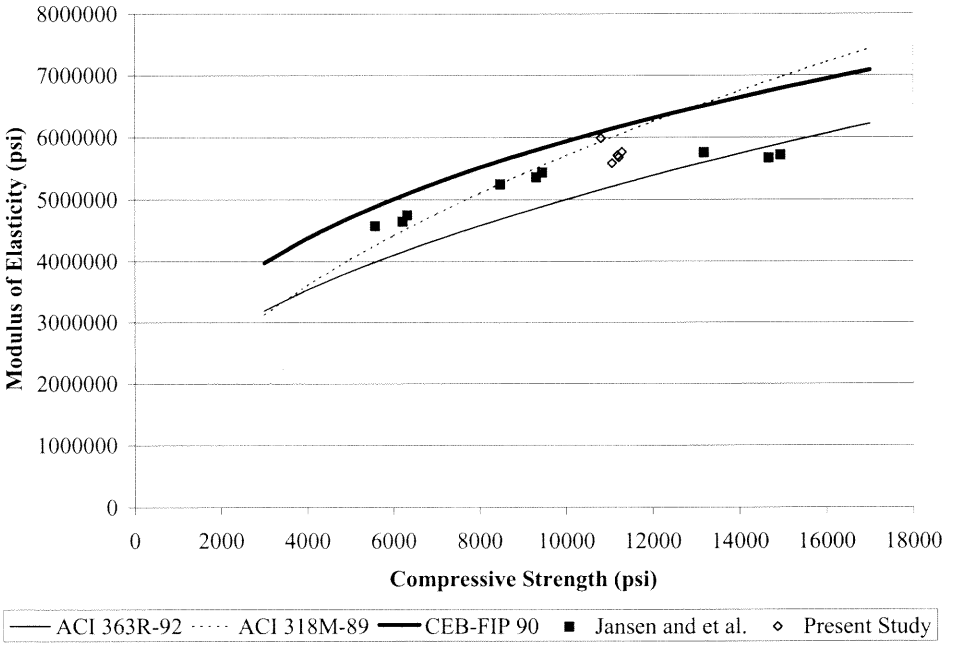

Figure A.7 Modulus of Elasticity as a function of Compressive Strength

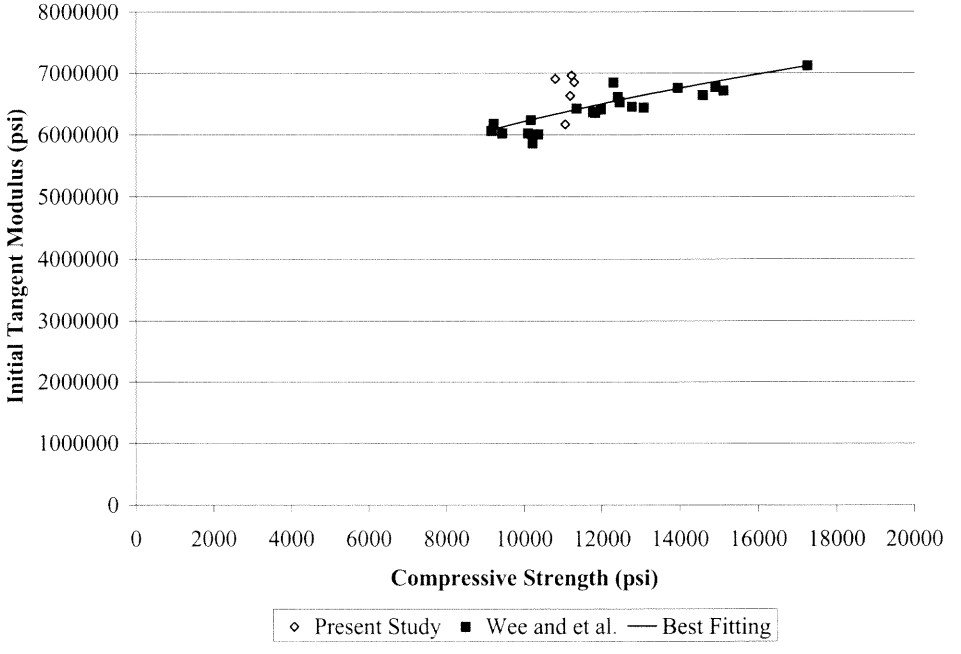

Figure A.8 Initial Tangent Modulus of Elasticity as a function of Compressive Strength

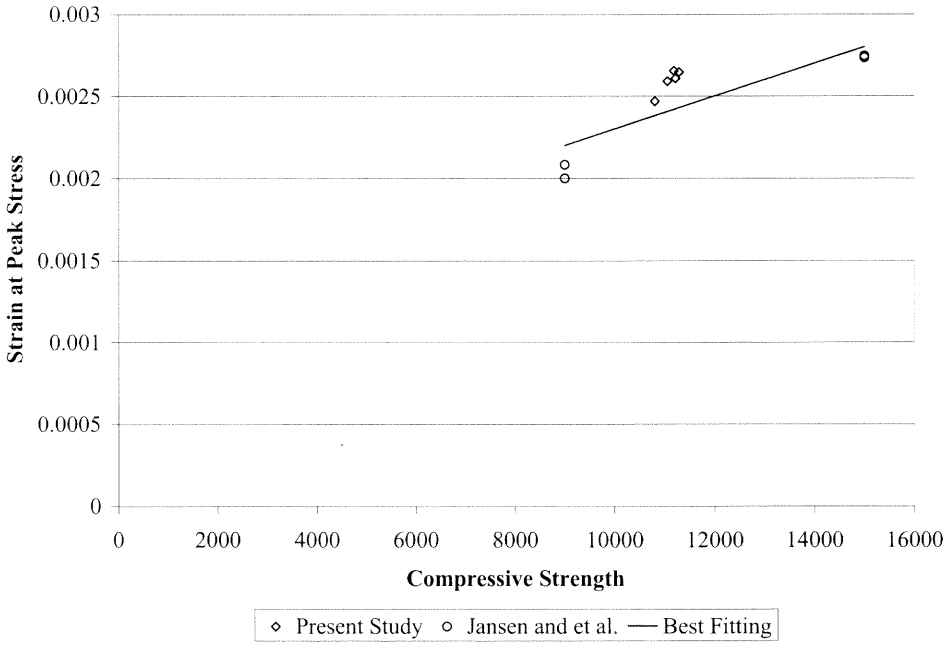

Figure A.9 Strain at Peak Stress as a function of Compressive Strength

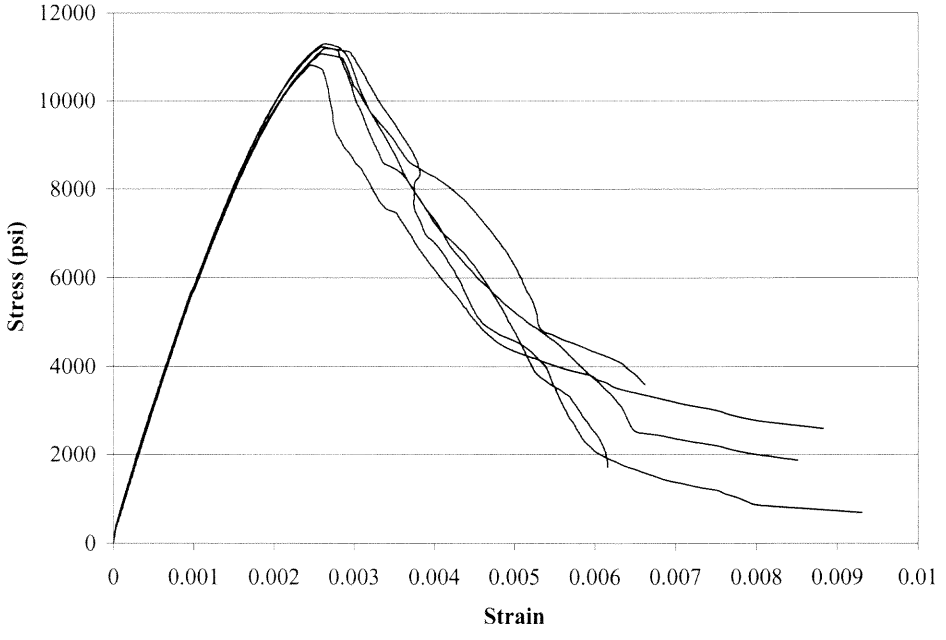

Figure A.10 Empirical Stress-Strain Curve of Plain Concrete

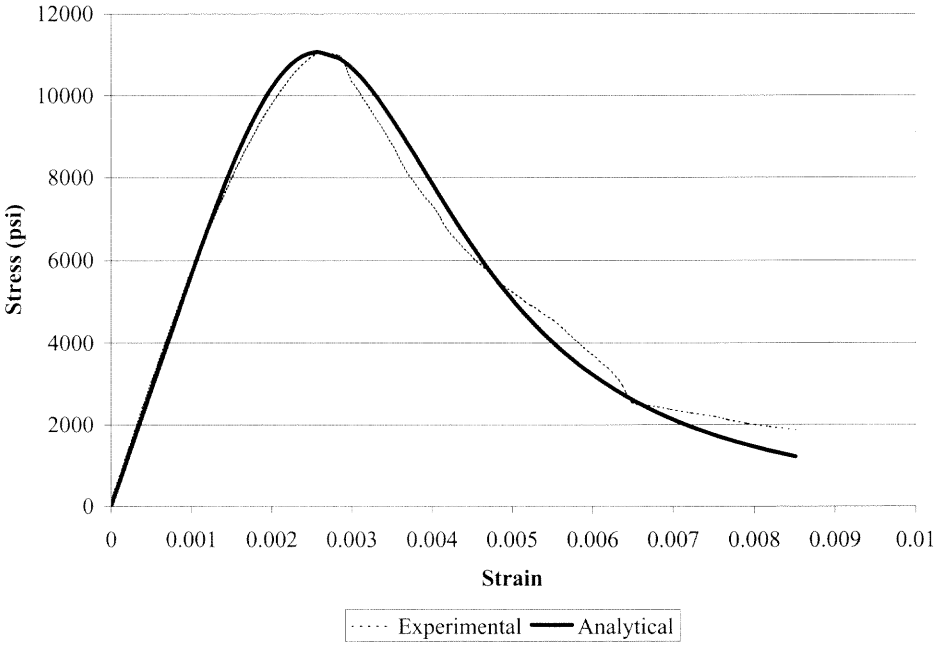

Figure A.11 Comparison of Proposed Equation and Experimental Data for Plain Concrete (P2)

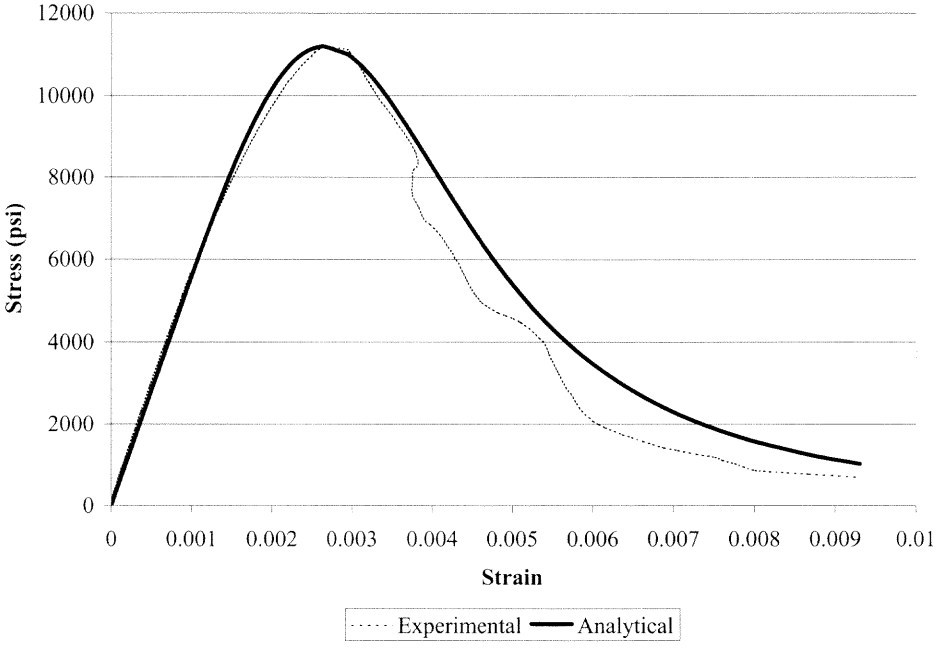

Figure A.12 Comparison of Proposed Equation and Experimental Data for Plain Concrete (P3)

Figure A.13 Comparison of proposed Equation and Wee et al.'s Test Data

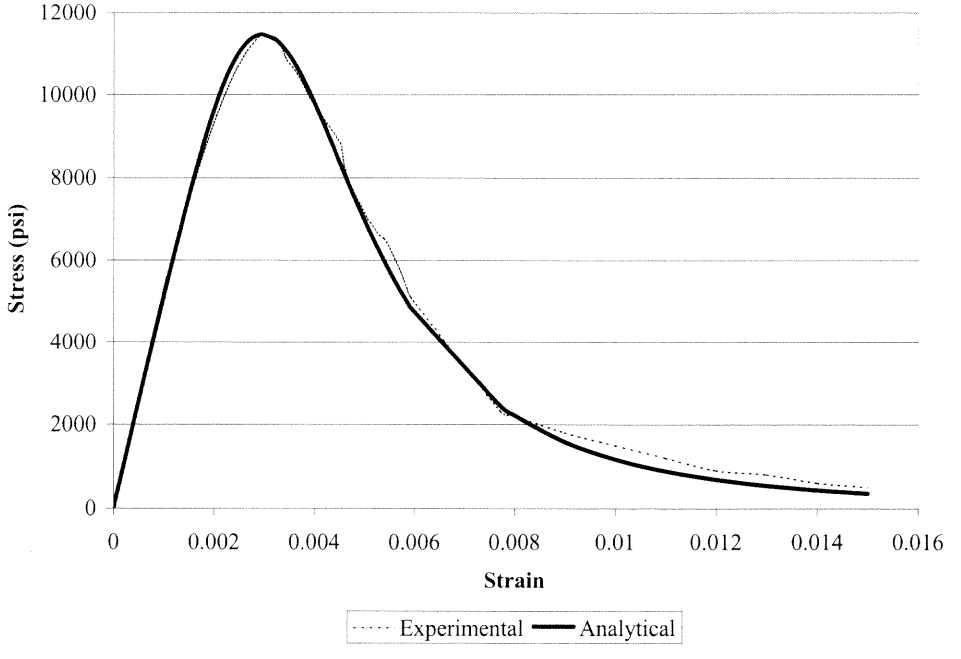

Figure A.14 Comparison of Proposed Equation and Experimental Data (Steel Fiber 0.5%, HP05S1)

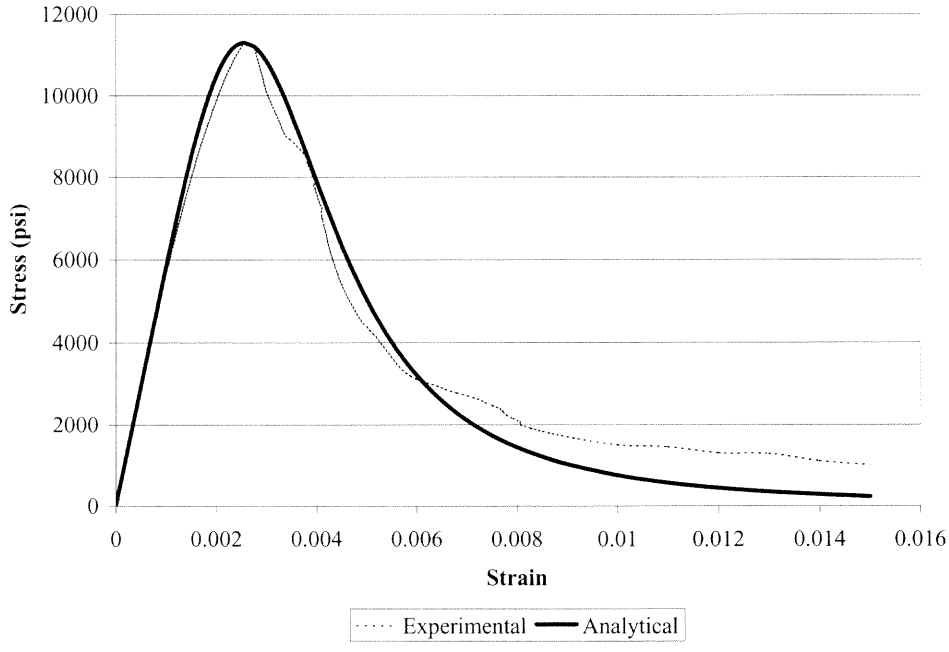

Figure A.15 Comparison of Proposed Equation and Experimental Data (Steel Fiber 0.5%, HP05S2)

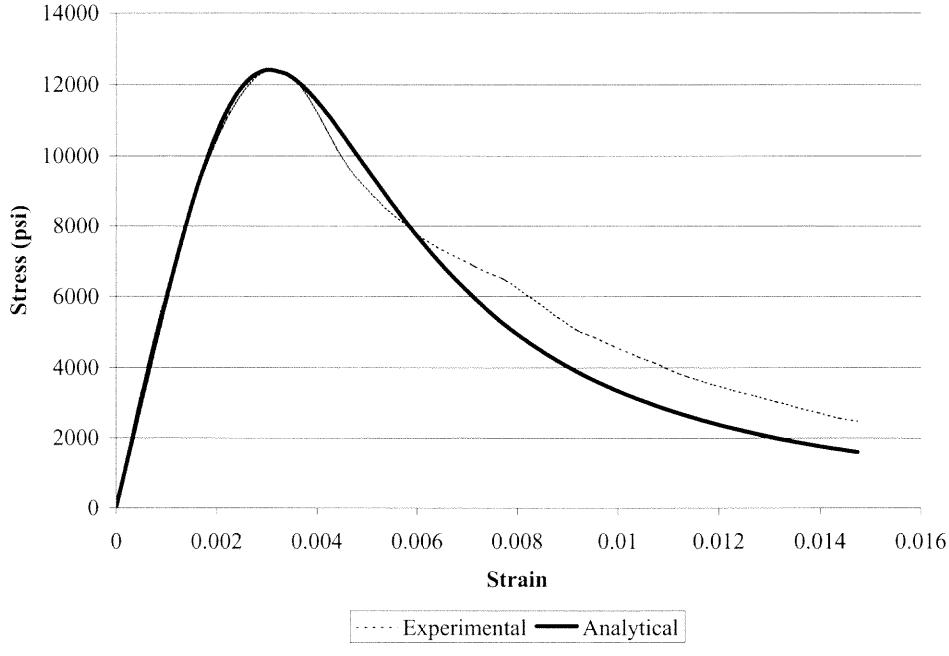

Figure A.16 Comparison of Proposed Equation and Experimental Data (Steel Fiber 1%, HP1S2)

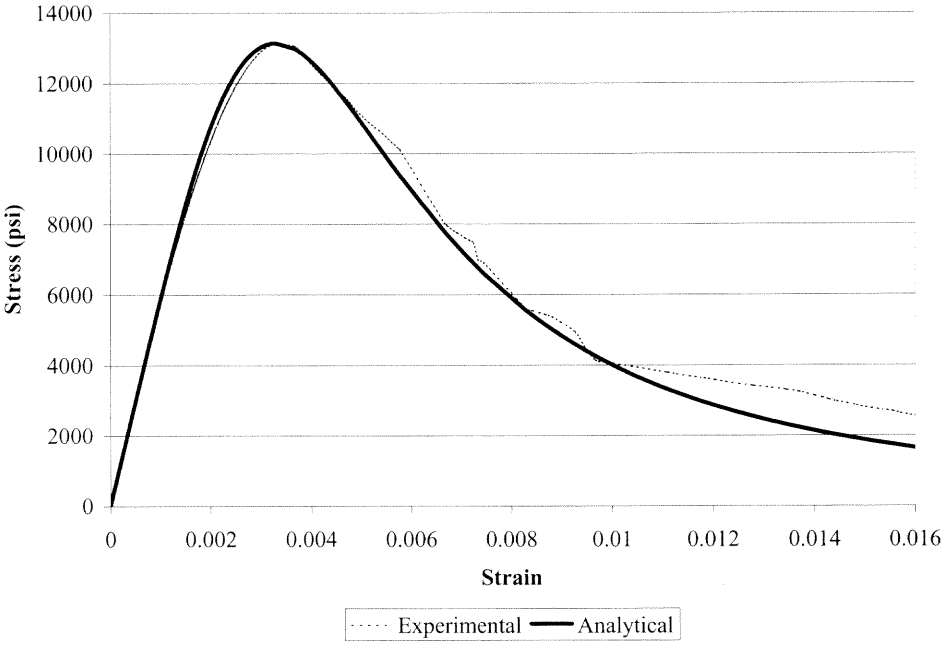

Figure A.17 Comparison of Proposed Equation and Experimental Data (Steel Fiber 1%, HP1S3)

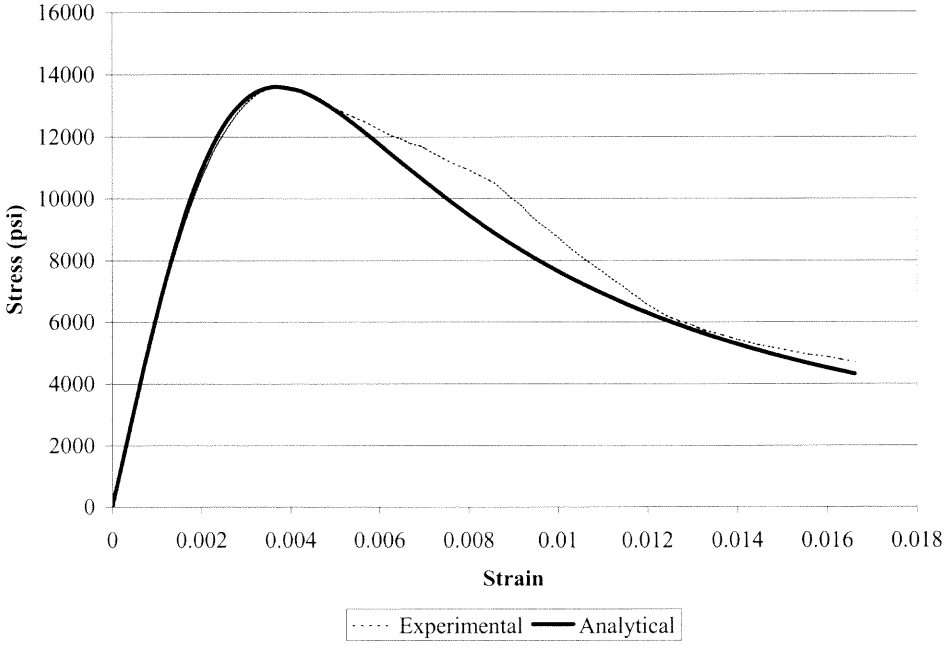

Figure A.18 Comparison of Proposed Equation and Experimental Data (Steel Fiber 2%, HP2S2)

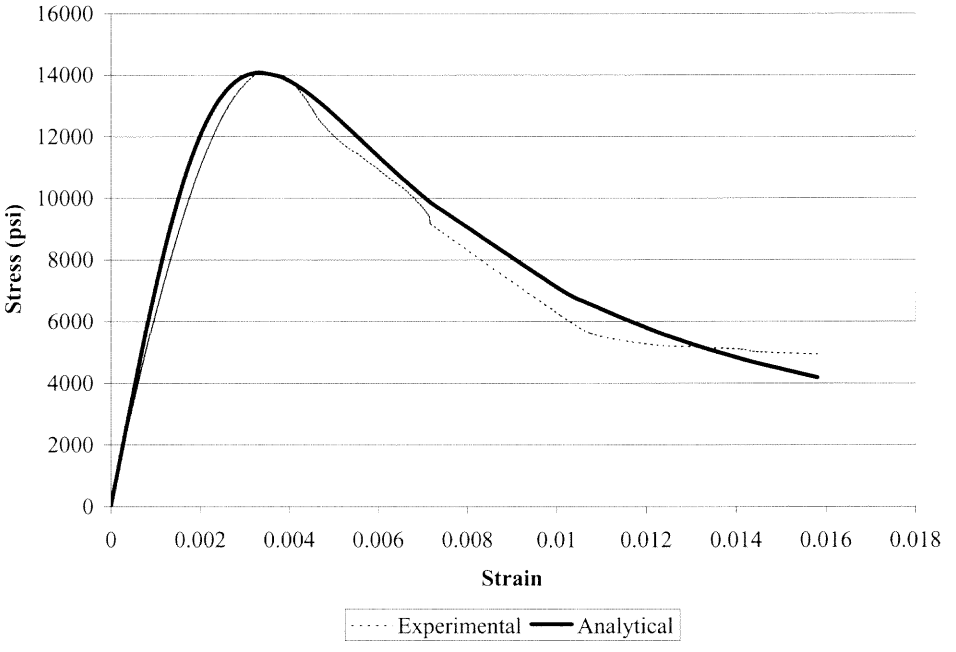

Figure A.19 Comparison of Proposed Equation and Experimental Data (Steel Fiber 2%, HP2S3)

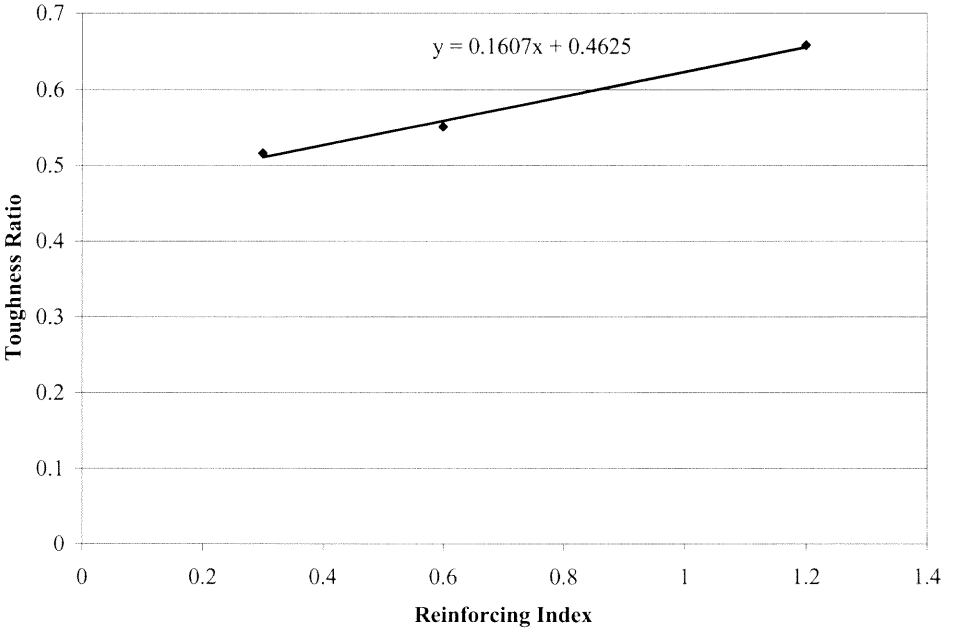

Figure A.20 Variation of Toughness Ratio with Reinforcing Index

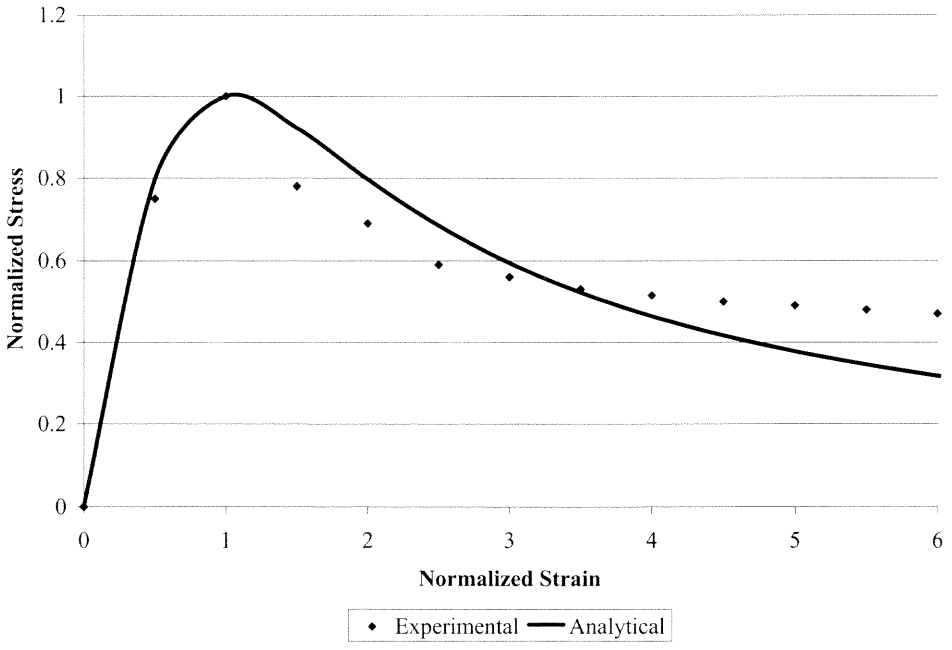

Figure A.21 Comparison of Proposed Equation and Experimental Data for Hoop S=50mm

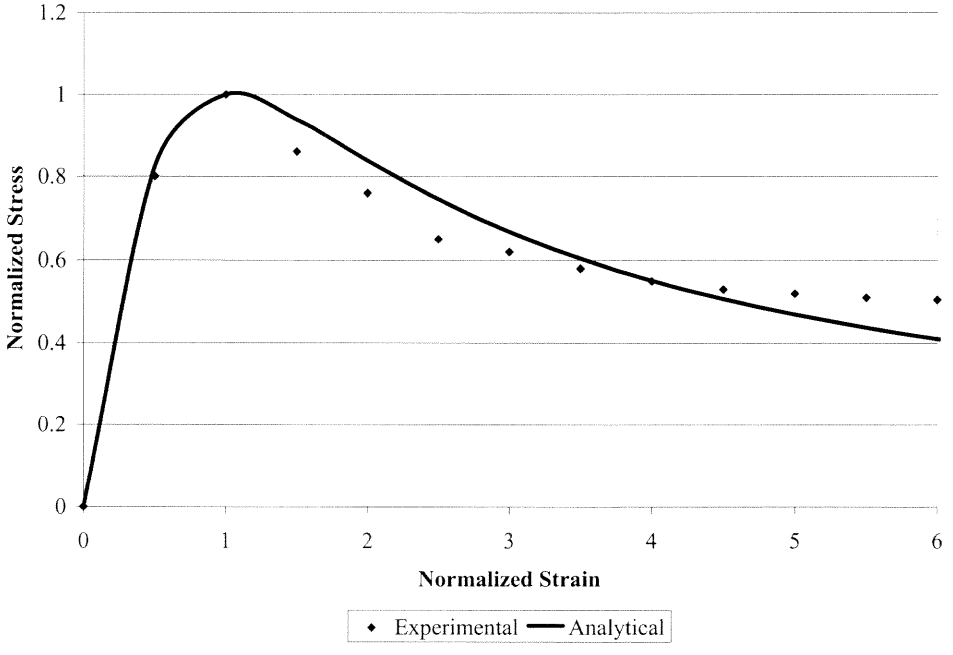

Figure A.22 Comparison of Proposed Equation and Experimental Data for Hoop S=40mm

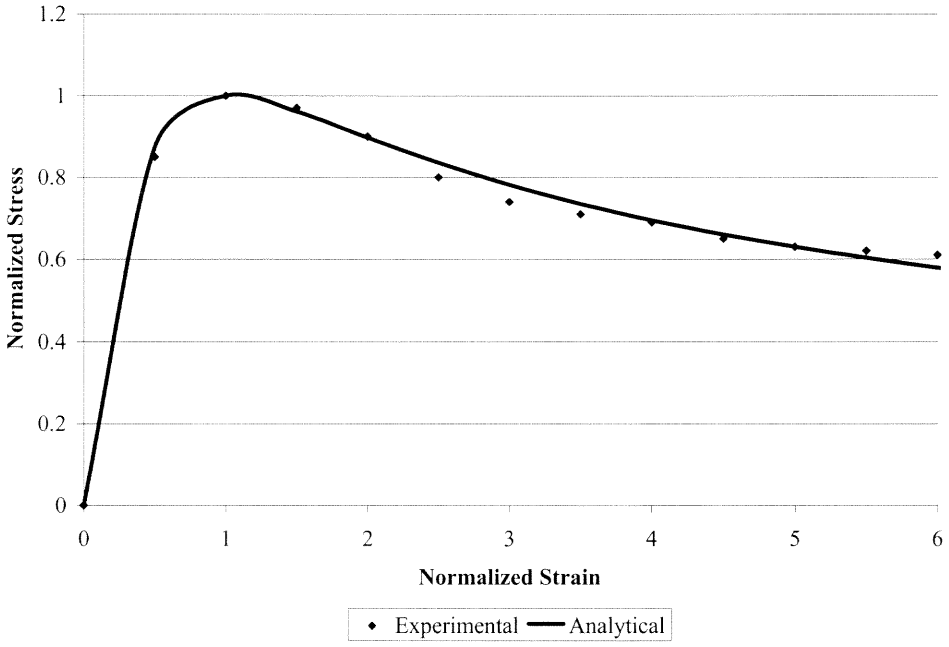

Figure A.23 Comparison of Proposed Equation and Experimental Data for Hoop S=30mm

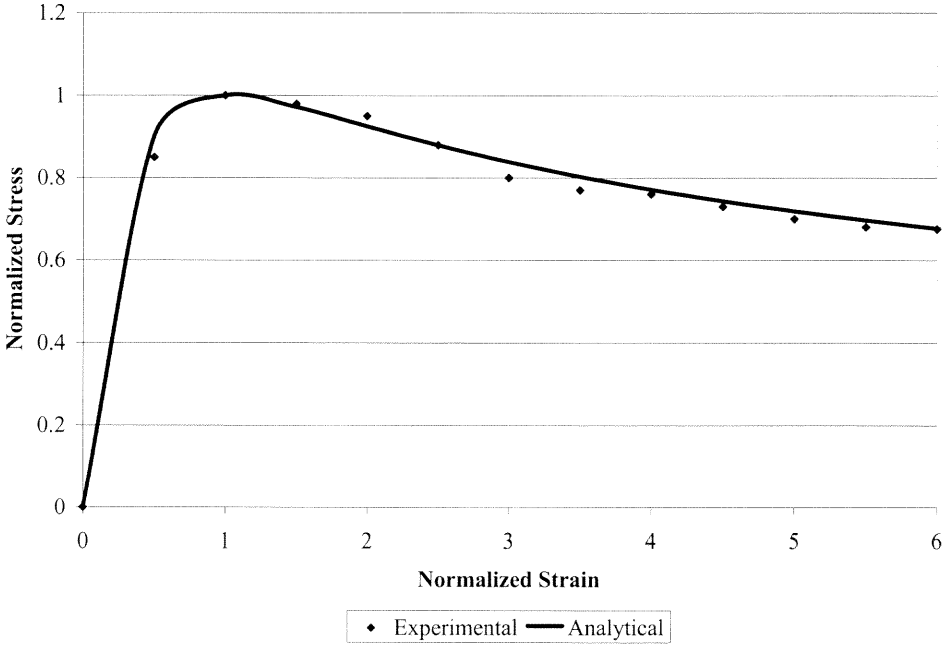

Figure A.24 Comparison of Proposed Equation and Experimental Data for Hoop S=20mm

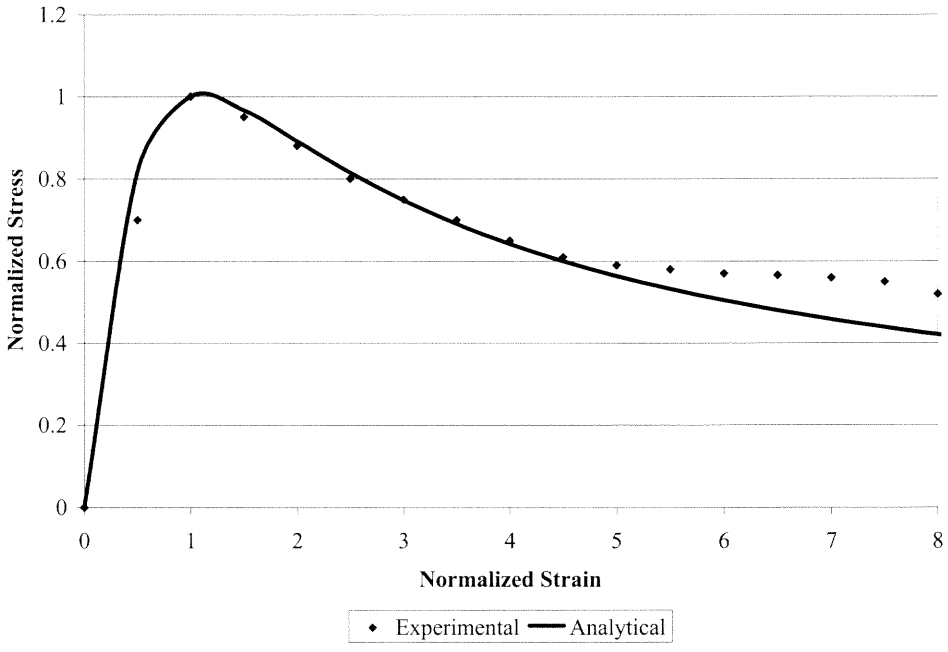

Figure A.25 Comparison of Proposed Equation and Experimental Data for 1% Steel Fiber + Hoop S=50mm

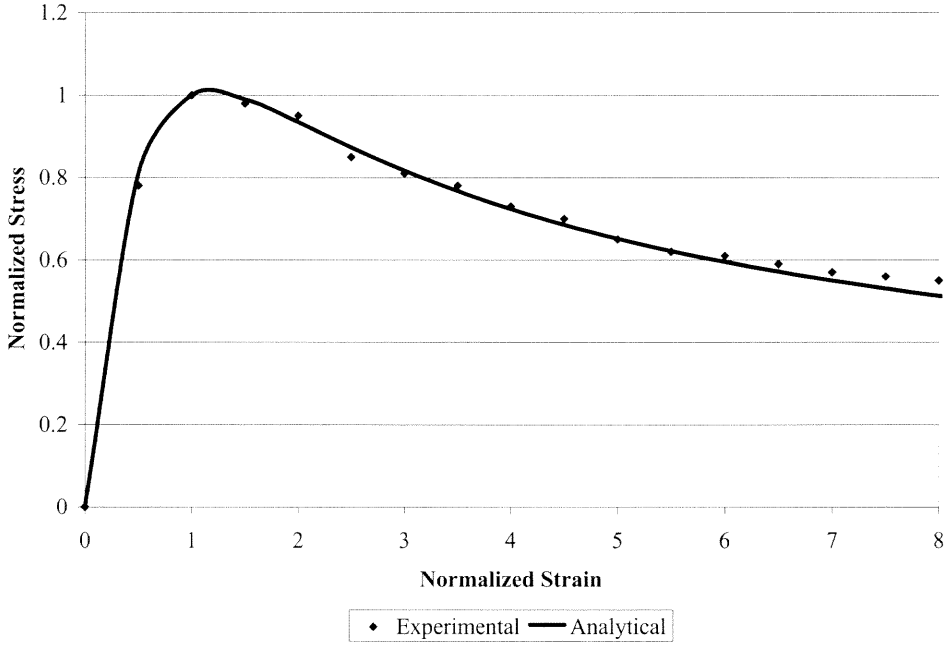

Figure A.26 Comparison of Proposed Equation and Experimental Data for 1% Steel Fiber + Hoop S=40mm

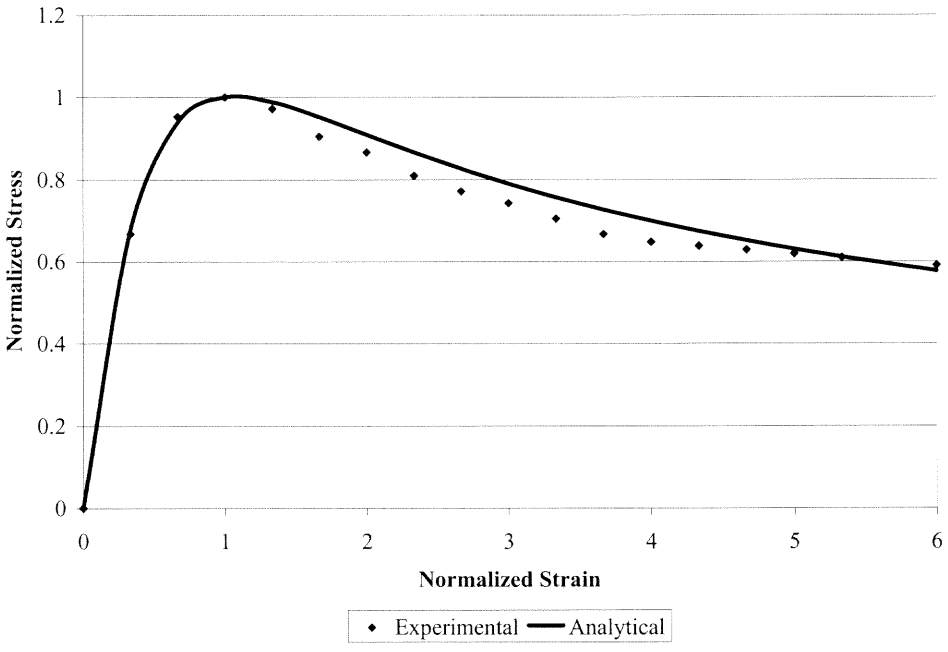

Figure A.27 Comparison of Proposed Equation and Experimental Data for 1% Steel Fiber + Hoop S=20mm

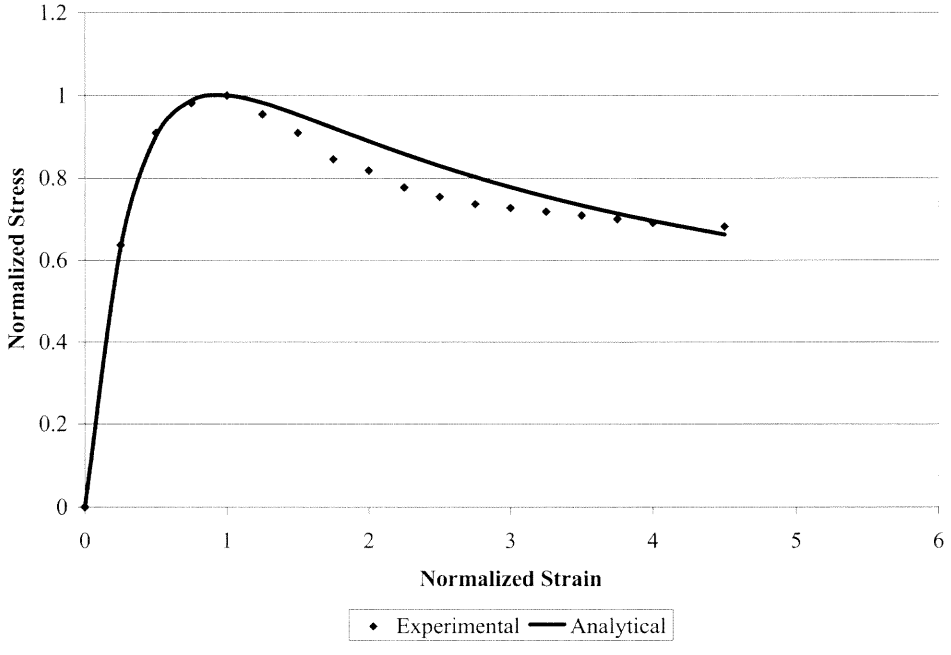

Figure A.28 Comparison of Proposed Equation and Experimental Data for 1% Steel Fiber + Hoop S=10mm

APPENDIX B

EXPERIMENTAL DATA OF HIGH PERFORMANCE FLY ASH CONCRETE

In this appendix, experimental results of high performance fly ash concrete are shown.

Table B.1 Compression Test Results of Control Cylinder

Specimen Number	Compressive Strength (psi)	Strain at Peak Stress	Modulus of Elasticity (ksi)
FC-01	5127	0.001729	4186
FC-02	5207	0.001714	4277
FC-03	5080	0.001685	4685
FC-04	5105	0.001653	4660
FC-05	5089	0.001666	4232
FC-06	5223	0.001710	4565
FC-07	5173	0.001690	4369
FC-08	5150	0.001685	4678
FC-09	5190	0.001686	4625
FC-10	5243	0.001723	4856
Average	5158	0.001694	4513

Table B.2 Compression Test Results of 10% Fly Ash Replacement Mix

Specimen Number	Compressive Strength (psi)	Strain at Peak Stress	Modulus of Elasticity (ksi)
F10-01	5210	0.001666	4701
F10-02	5232	0.001646	4930
F10-03	5127	0.001691	4304
F10-04	5151	0.001616	4581
F10-05	5312	0.001725	4320
F10-06	5120	0.001592	4785
F10-07	5222	0.001623	4210
F10-08	5230	0.001648	4110
F10-09	5236	0.001658	4865
F10-10	5252	0.001711	4555
Average	5209	0.001657	4536

Table B.3 Compression Test Results of 20% Fly Ash Replacement Mix

Specimen Number	Compressive Strength (psi)	Strain at Peak Stress	Modulus of Elasticity (ksi)
F20-01	5252	0.001706	4984
F20-02	4955	0.001766	4137
F20-03	5246	0.001695	4648
F20-04	5260	0.001710	4486
F20-05	4970	0.001653	4636
F20-06	5120	0.001666	4734
F20-07	5135	0.001694	4748
F20-08	5222	0.001625	5002
F20-09	5030	0.001599	4844
F20-10	5150	0.001650	4263
Average	5134	0.001676	4648

Table B.4 Compression Test Results of 30% Fly Ash Replacement Mix

Specimen Number	Compressive Strength (psi)	Strain at Peak Stress	Modulus of Elasticity (ksi)
F30-01	5013	0.001569	4728
F30-02	4774	0.001547	4689
F30-03	4775	0.001601	4243
F30-04	4690	0.001651	4555
F30-05	4812	0.001653	4589
F30-06	4770	0.001623	4855
F30-07	4866	0.001645	4956
F30-08	4712	0.001644	4702
F30-09	4655	0.001529	4825
F30-10	4612	0.001599	4312
Average	4767	0.001606	4645

Table B.5 Compression Test Results of Steel Fiber 0.5% Mix

Specimen Number	Compressive Strength (psi)	Strain at Peak Stress	Modulus of Elasticity (ksi)	Toughness	Toughness Ratio
FS05-01	5380	0.001962	4587	31.3	0.387
FS05-02	5249	0.001917	4739	29.1	0.368
FS05-03	5231	0.001915	4156	30.2	0.383
FS05-04	5213	0.001875	3900	29.4	0.376
FS05-05	5320	0.001942	4210	26.5	0.326
FS05-06	5256	0.001902	4320	25.3	0.353
FS05-07	5366	0.001899	4026	27.5	0.299
FS05-08	5278	0.001986	4385	25.7	0.345
Average	5286	0.001924	4290	28.1	0.354

Table B.6 Compression Test Results of Steel Fiber 1% Mix

Specimen Number	Compressive Strength (psi)	Strain at Peak Stress	Modulus of Elasticity (ksi)	Toughness	Toughness Ratio
FS1-01	5890	0.002063	5558	43.1	0.493
FS1-02	5810	0.002055	4497	47.5	0.555
FS1-03	5709	0.002043	4385	46.8	0.554
FS1-04	5621	0.002126	4245	42.8	0.484
FS1-05	5678	0.002078	4578	41.2	0.511
FS1-06	5689	0.002111	4521	46.5	0.523
FS1-07	5712	0.002212	4755	43.2	0.503
FS1-08	5788	0.002180	4650	42.3	0.533
Average	5737	0.002108	4648	44.1	0.519

Table B.7 Compression Test Results of Steel Fiber 2% Mix

Specimen Number	Compressive Strength (psi)	Strain at Peak Stress	Modulus of Elasticity (ksi)	Toughness	Toughness Ratio
FS2-01	6048	0.002595	4099	70.1	0.772
FS2-02	5888	0.002515	4313	69.9	0.791
FS2-03	6127	0.002638	4663	76.0	0.826
FS2-04	5968	0.002516	4763	69.4	0.775
FS2-05	5875	0.002803	4114	77.2	0.829
FS2-06	5912	0.002612	4652	72.2	0.723
FS2-07	6023	0.002578	4324	73.3	0.755
FS2-08	5988	0.002645	4253	72.9	0.765
Average	5978	0.002612	4397	72.6	0.779

Table B.8 Compression Test Results of Hoop S=4in. Mix

Specimen Number	Compressive Strength (psi)	Strain at Peak Stress	Modulus of Elasticity (ksi)
FH4-01	5176	0.002371	4889
FH4-02	5097	0.002197	5034
FH4-03	5217	0.002298	4259
FH4-04	5203	0.002245	4555
FH4-05	5146	0.002281	4592
FH4-06	5187	0.002253	4678
FH4-07	5153	0.002308	4474
FH4-08	5210	0.002258	4437
Average	5173	0.002276	4614

Table B.9 Compression Test Results of Hoop S=2in. Mix

Specimen Number	Compressive Strength (psi)	Strain at Peak Stress	Modulus of Elasticity (ksi)
FH2-01	5230	0.002514	4997
FH2-02	5300	0.002620	5209
FH2-03	5245	0.002560	5124
FH2-04	5278	0.002564	4423
FH2-05	5298	0.002523	4689
FH2-06	5214	0.002579	4764
FH2-07	5278	0.002614	4682
FH2-08	5188	0.002456	4726
Average	5253	0.002553	4826

Table B.10 Compression Test Results of Hoop S=1in. Mix

Specimen Number	Compressive Strength (psi)	Strain at Peak Stress	Modulus of Elasticity (ksi)
FH1-01	5310	0.002910	4408
FH1-02	5454	0.003320	4875
FH1-03	5400	0.003145	5577
FH1-04	5385	0.002985	5423
FH1-05	5438	0.002967	5212
FH1-06	5422	0.003034	5312
FH1-07	5503	0.003075	5245
FH1-08	5487	0.003145	4965
Average	5424	0.003072	5127

Table B.11 Compression Test Results of Steel Fiber with Hoop S=4in. Mix

Specimen Number	Compressive Strength (psi)	Strain at Peak Stress	Modulus of Elasticity (ksi)
FSH4-01	5310	0.002480	5093
FSH4-02	5380	0.002610	4351
FSH4-03	5230	0.002432	4451
FSH4-04	5395	0.002573	4141
FSH4-05	5239	0.002566	4549
FSH4-06	5289	0.002578	4537
FSH4-07	5301	0.002586	4386
FSH4-08	5245	0.002475	4852
Average	5298	0.002537	4545

Steel Fiber content=0.5%

Table B.12 Compression Test Results of Steel Fiber with Hoop S=2in. Mix

Specimen Number	Compressive Strength (psi)	Strain at Peak Stress	Modulus of Elasticity (ksi)
FSH2-01	5570	0.002701	5545
FSH2-02	5585	0.002703	4582
FSH2-03	5635	0.002786	4252
FSH2-04	5600	0.002740	4802
FSH2-05	5512	0.002713	4567
FSH2-06	5532	0.002723	4852
FSH2-07	5456	0.002697	4531
FSH2-08	5486	0.002689	4751
Average	5547	0.002719	4735

Steel Fiber content=0.5%

Table B.13 Compression Test Results of Steel Fiber with Hoop S=1in. Mix

Specimen Number	Compressive Strength (psi)	Strain at Peak Stress	Modulus of Elasticity (ksi)
FSH1-01	6040	0.003420	3766
FSH1-02	5825	0.003248	3909
FSH1-03	5868	0.003256	4173
FSH1-04	5910	0.003313	3167
FSH1-05	5875	0.003245	4213
FSH1-06	5736	0.003264	3943
FSH1-07	5846	0.003341	3845
FSH1-08	5756	0.003371	3988
Average	5857	0.003307	3875

Steel Fiber content=0.5%

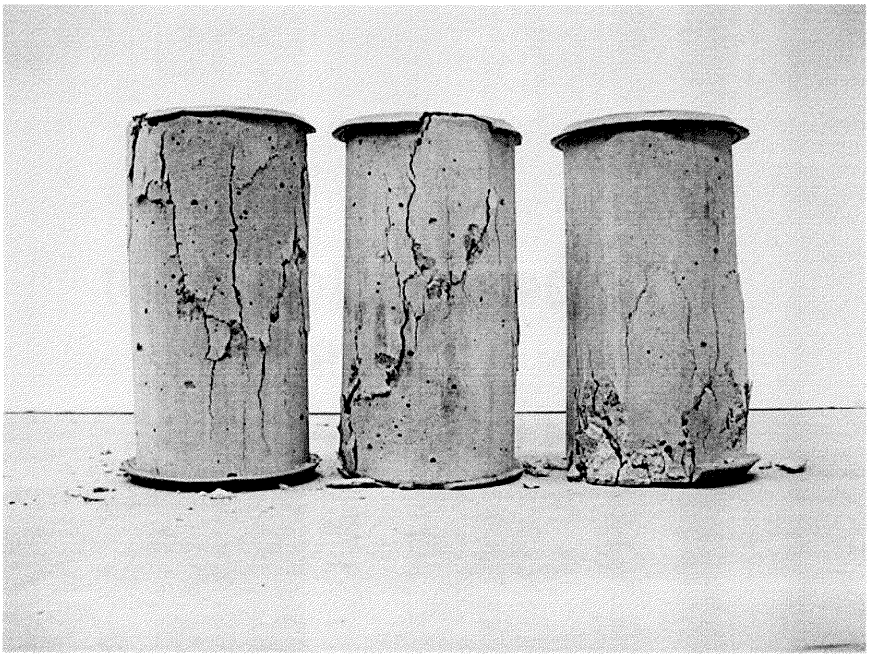

Figure B.1 Cylinder after Compression Test (Plain Fly Ash)

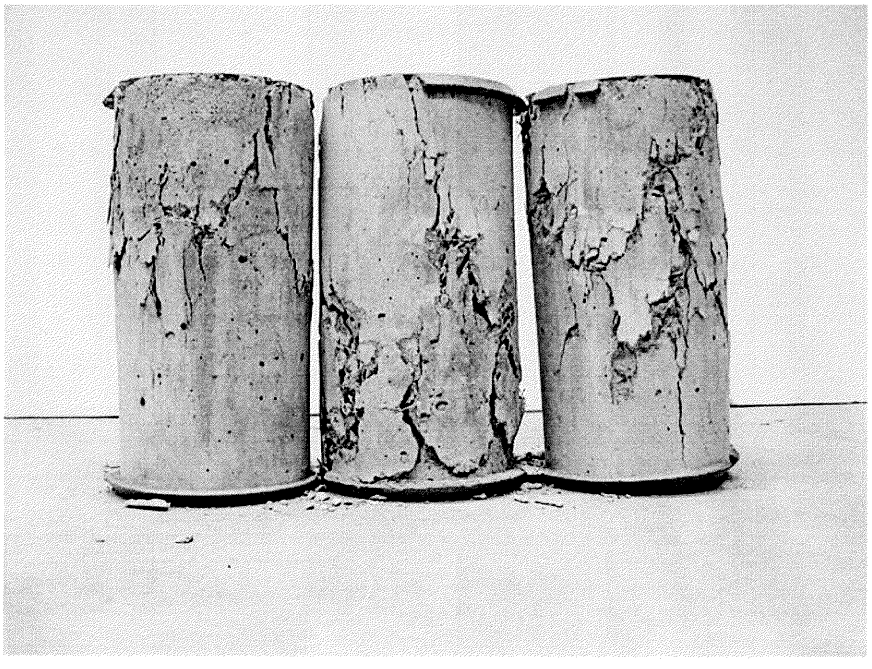

Figure B.2 Cylinder after Compression Test (Steel Fiber 0.5%)

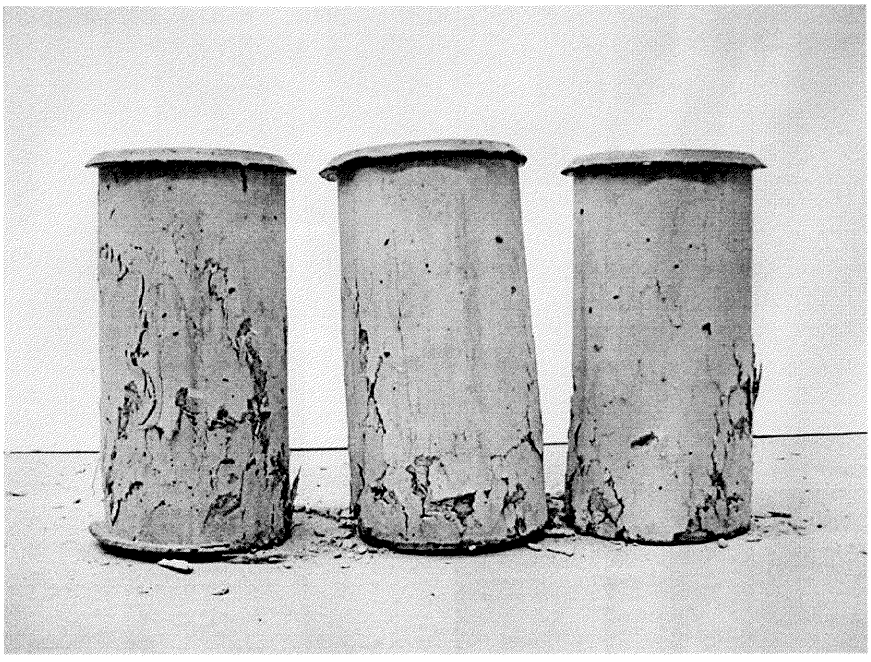

Figure B.3 Cylinder after Compression Test (Steel Fiber 1%)

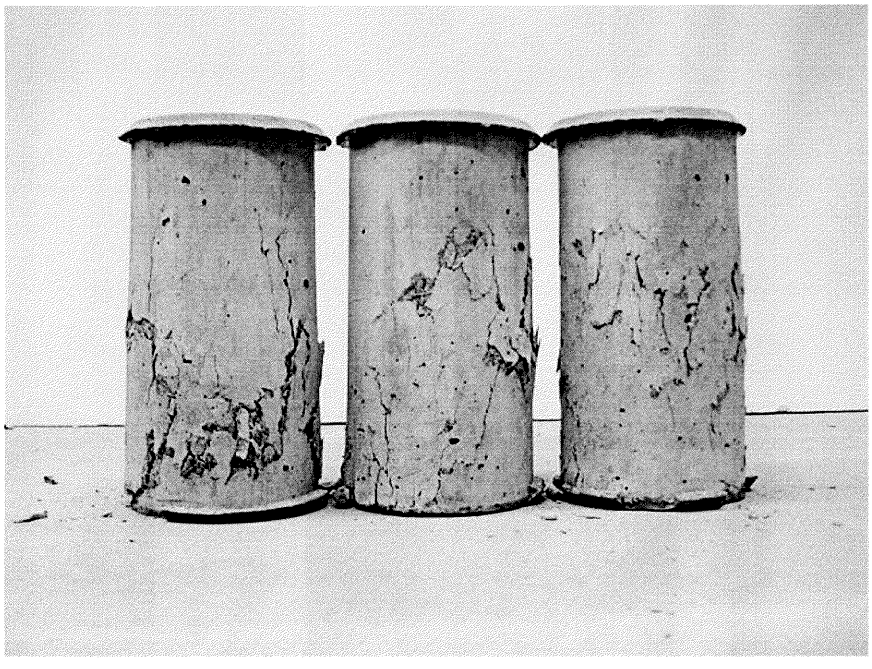

Figure B.4 Cylinder after Compression Test (Steel Fiber 2%)

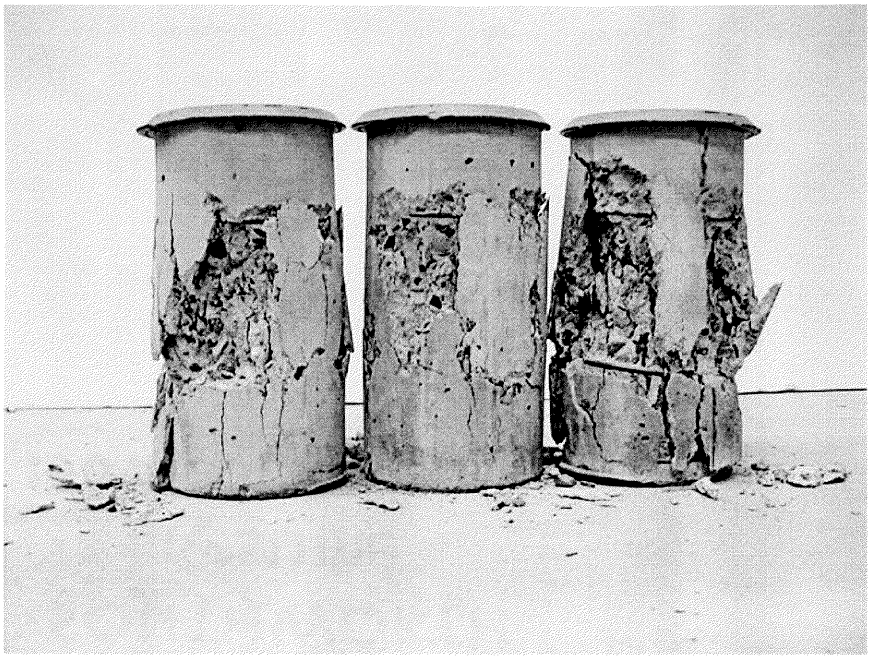

Figure B.5 Cylinder after Compression Test (Hoop S=4 in.)

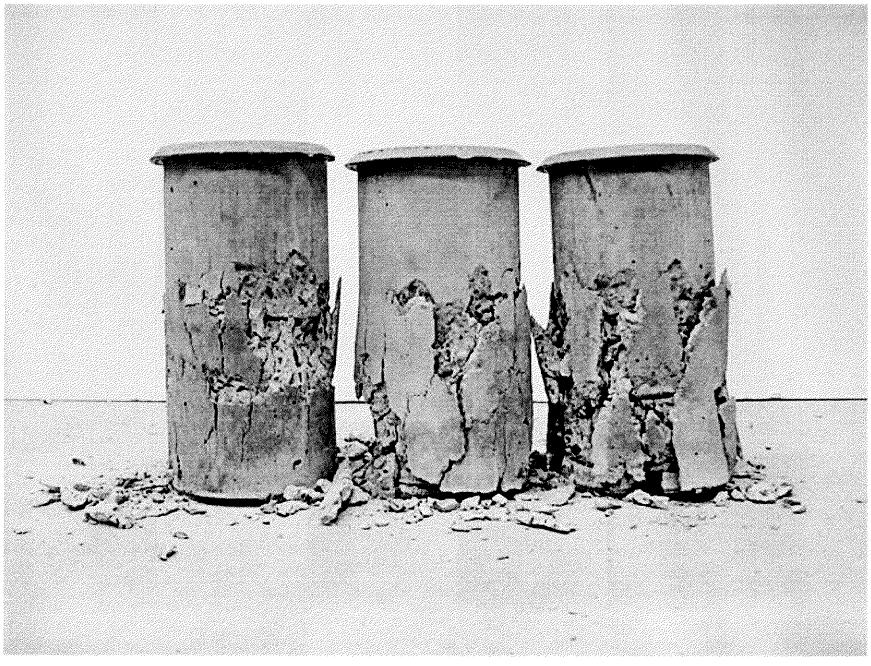

Figure B.6 Cylinder after Compression Test (Hoop S=2 in.)

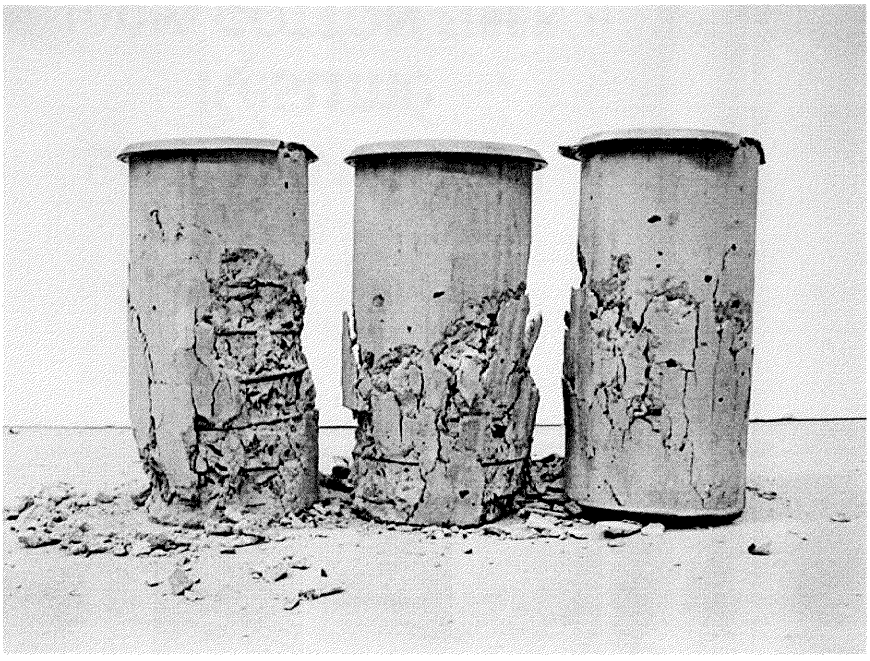

Figure B.7 Cylinder after Compression Test (Hoop S=1 in.)

Figure B.8 Cylinder after Compression Test (Hoop + Steel Fiber)

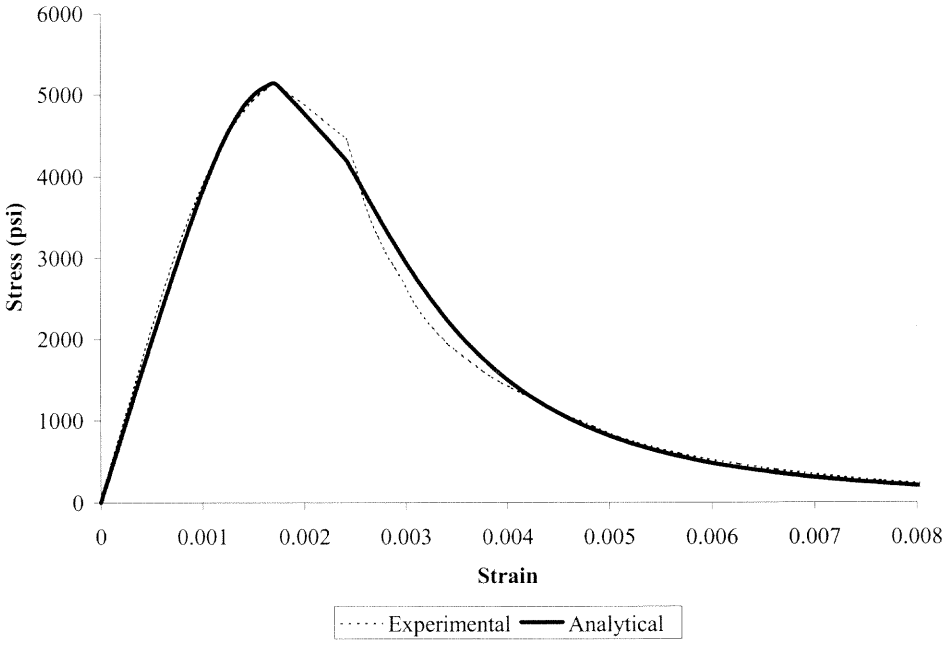

Figure B.9 Comparison of Proposed Equation and Experimental Data for Control Concrete (FC-1)

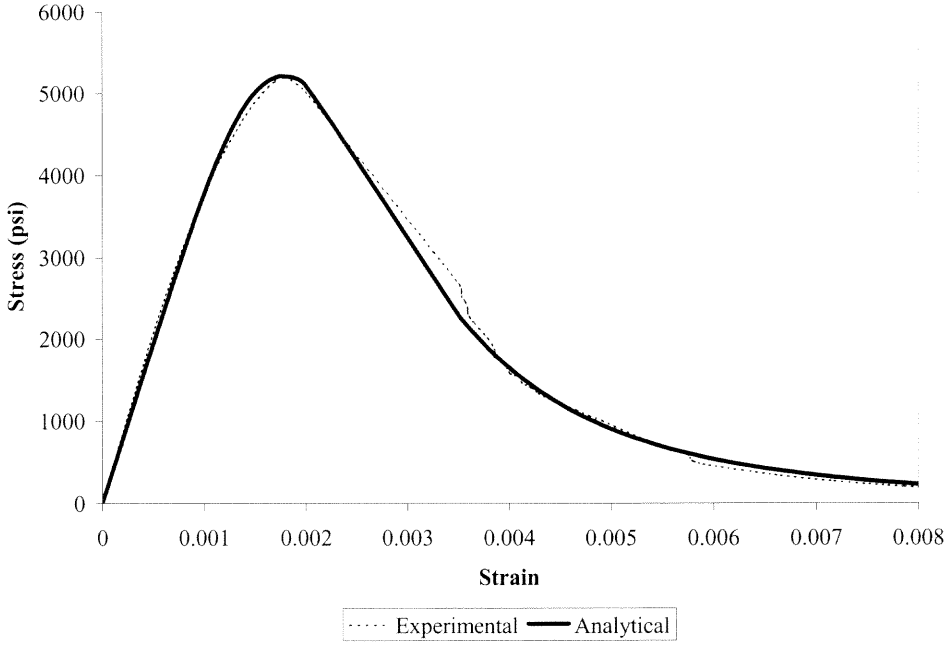

Figure B.10 Comparison of Proposed Equation and Experimental Data for Control Concrete (FC-2)

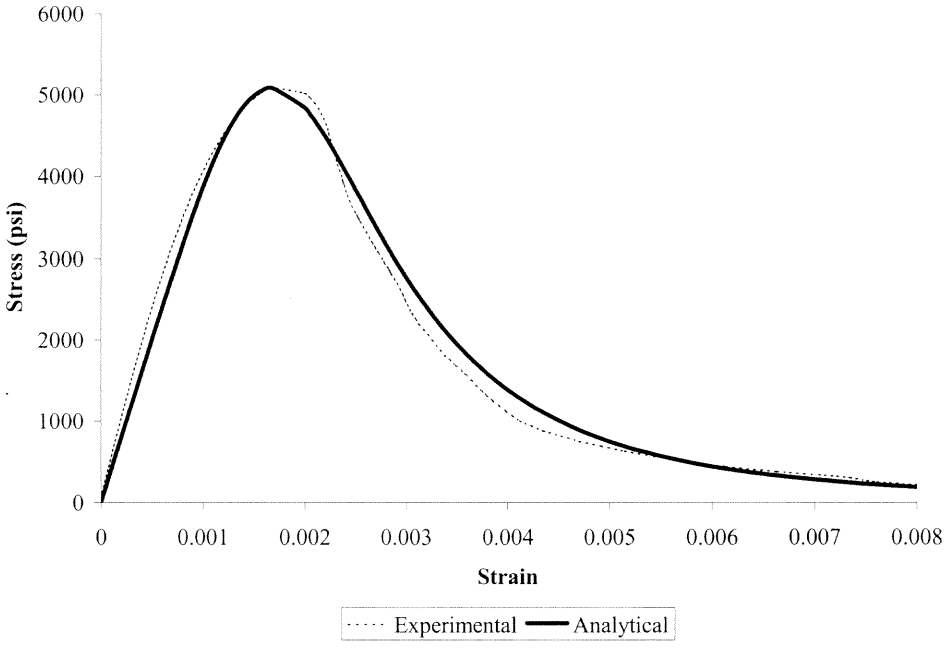

Figure B.11 Comparison of Proposed Equation and Experimental Data for Control Concrete (FC-3)

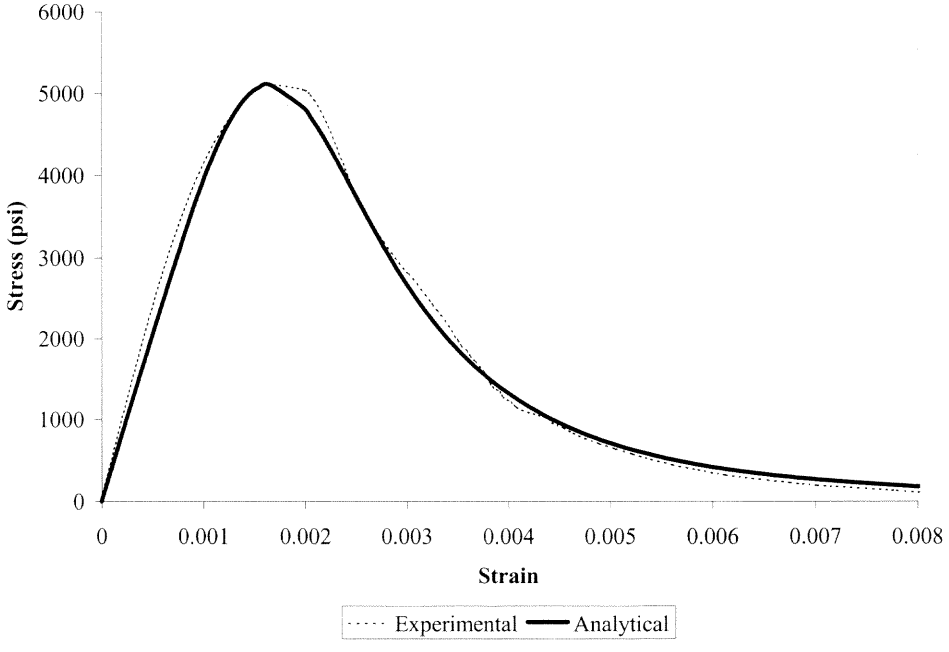

Figure B.12 Comparison of Proposed Equation and Experimental Data for Control Concrete (FC-4)

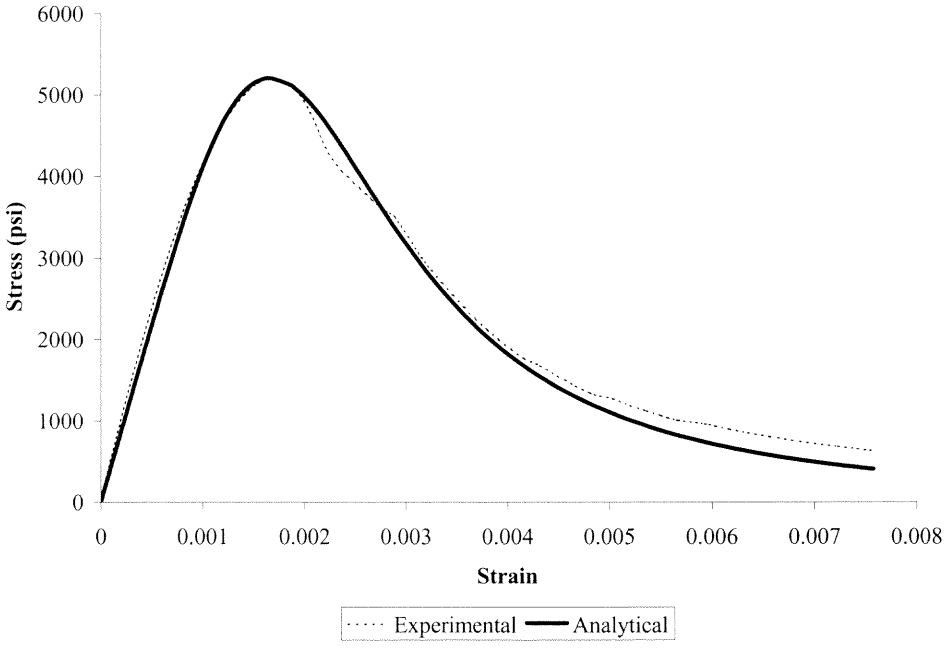

Figure B.13 Comparison of Proposed Equation and Experimental Data for 10% Fly Ash Replacement Concrete (F10-01)

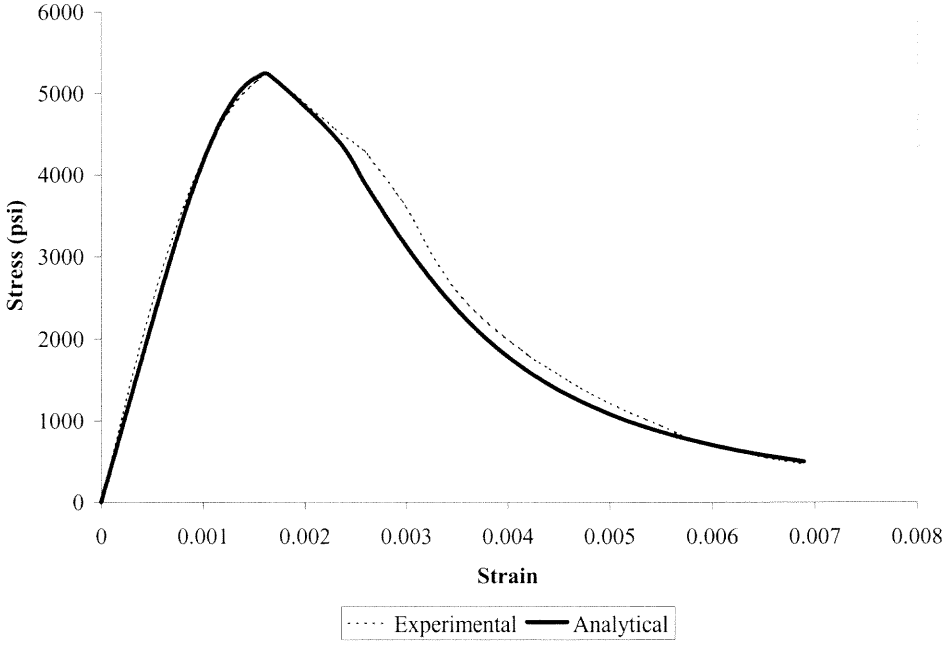

Figure B.14 Comparison of Proposed Equation and Experimental Data for 10% Fly Ash Replacement Concrete (F10-02)

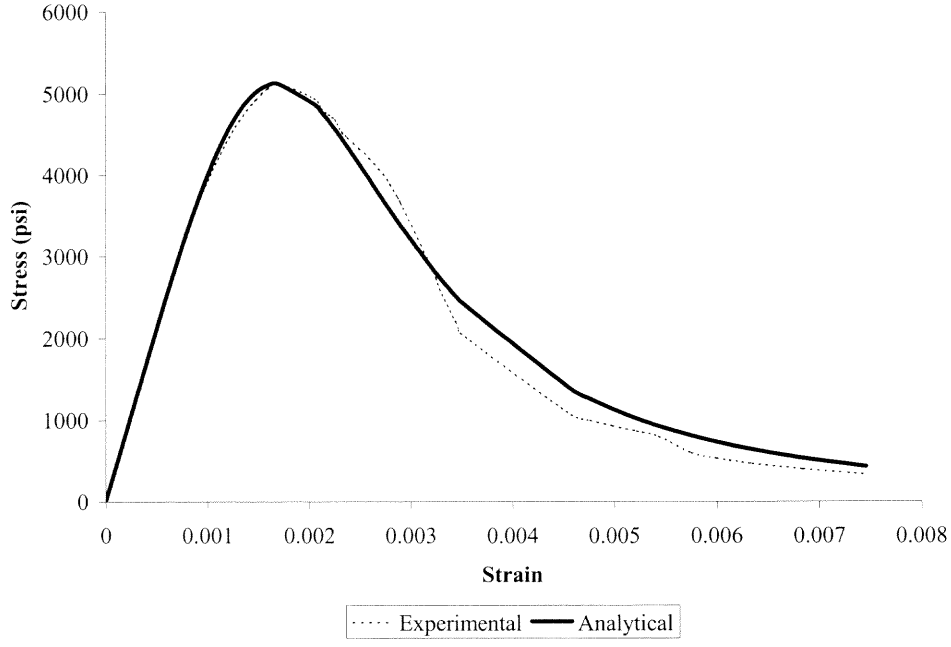

Figure B.15 Comparison of Proposed Equation and Experimental Data for 10% Fly Ash Replacement Concrete (F10-03)

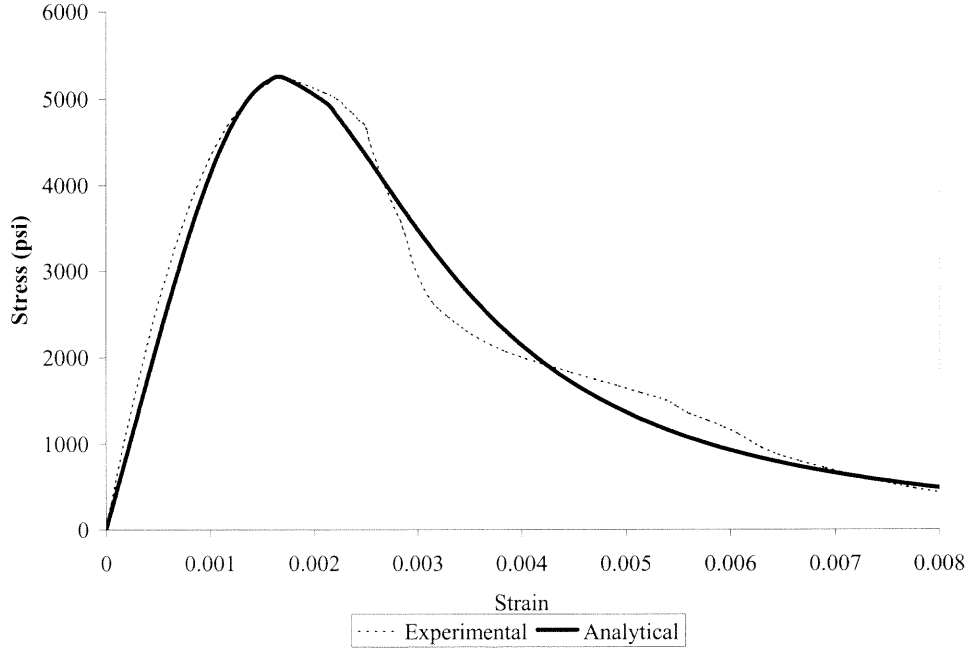

Figure B.16 Comparison of Proposed Equation and Experimental Data for 20% Fly Ash Replacement Concrete (F20-01)

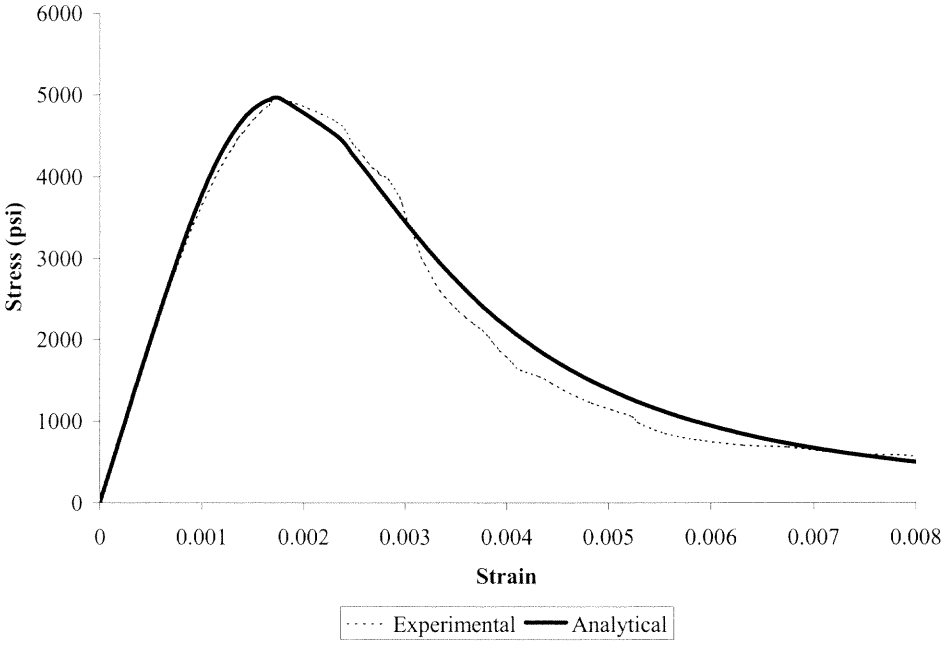

Figure B.17 Comparison of Proposed Equation and Experimental Data for 20% Fly Ash Replacement Concrete (F20-02)

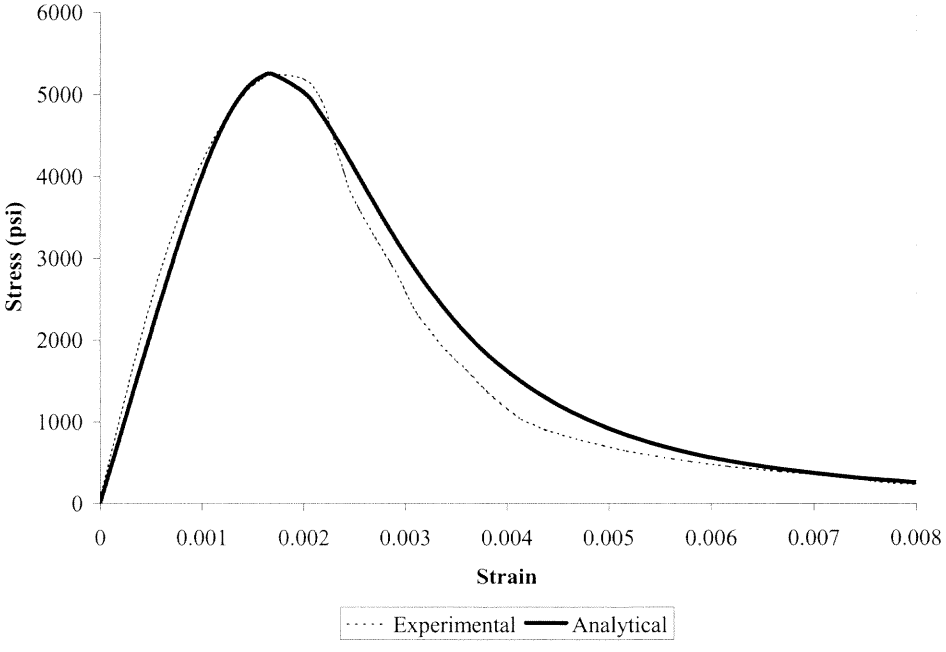

Figure B.18 Comparison of Proposed Equation and Experimental Data for 20% Fly Ash Replacement Concrete (F20-03)

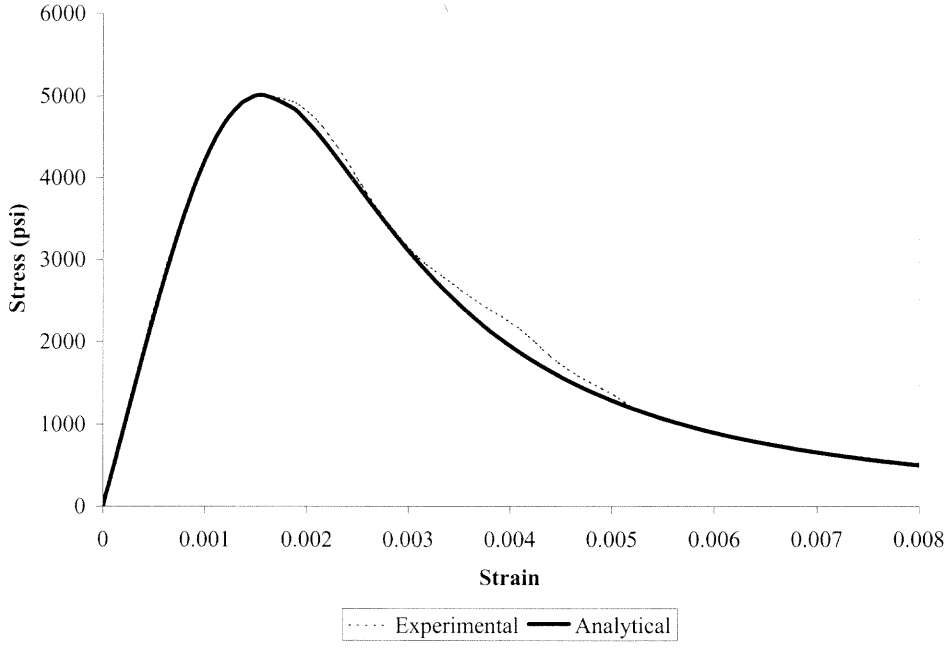

Figure B.19 Comparison of Proposed Equation and Experimental Data for 30% Fly Ash Replacement Concrete (F30-01)

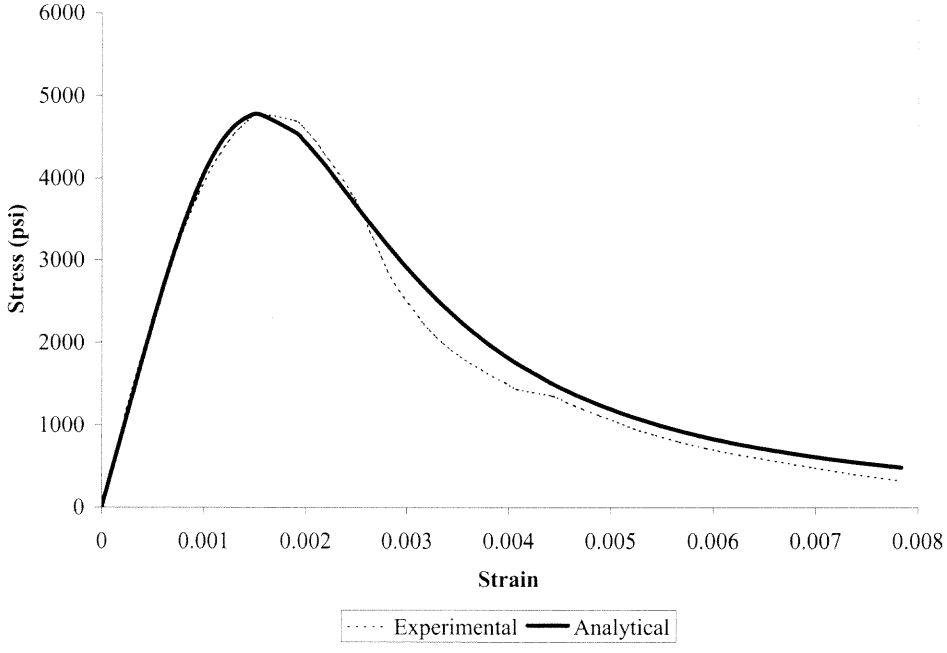

Figure B.20 Comparison of Proposed Equation and Experimental Data for 30% Fly Ash Replacement Concrete (F30-02)

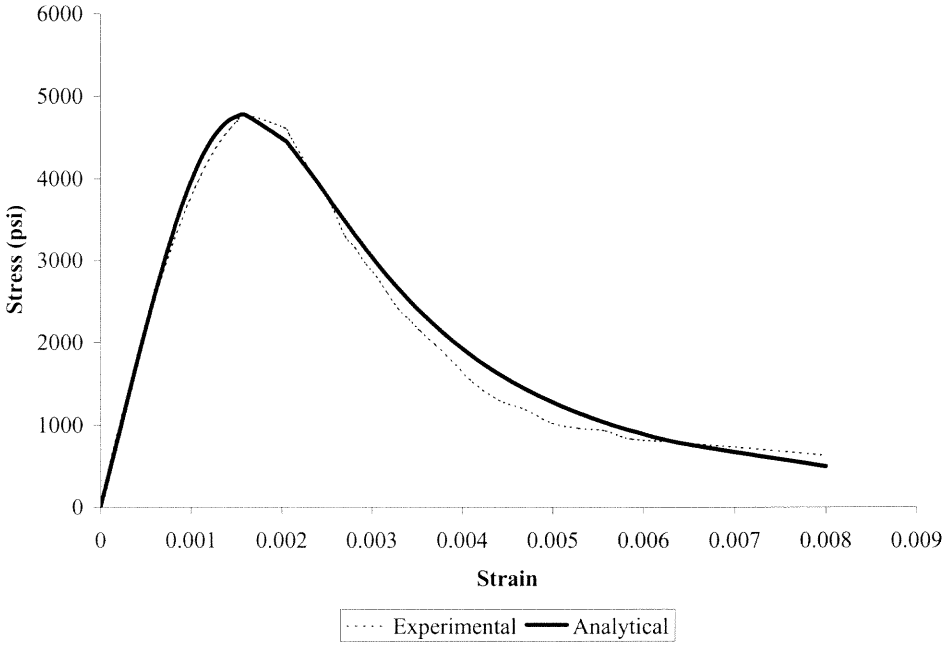

Figure B.21 Comparison of Proposed Equation and Experimental Data for 30% Fly Ash Replacement Concrete (F30-03)

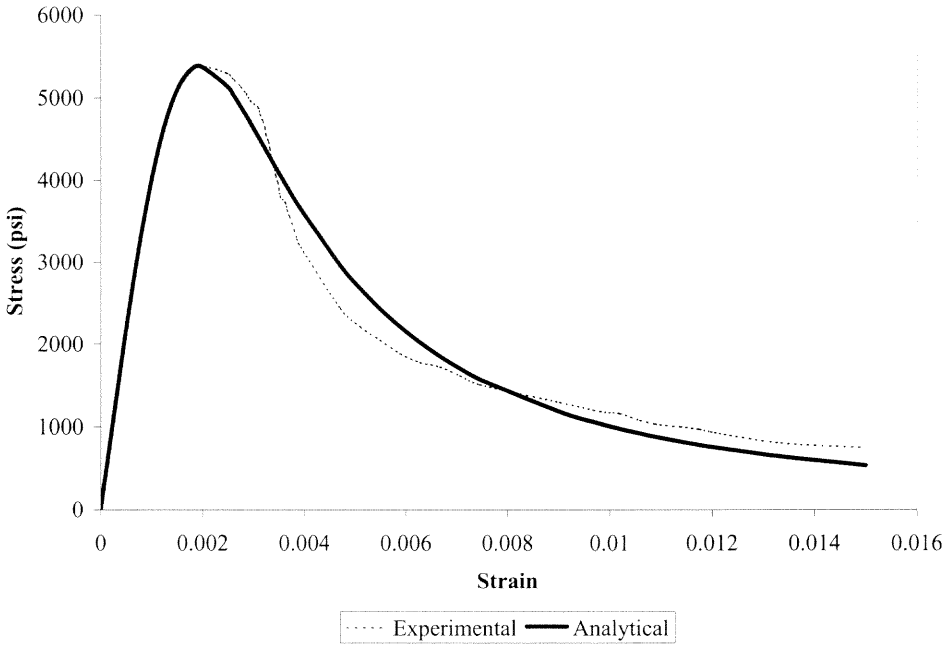

Figure B.22 Comparison of Proposed Equation and Experimental Data for concrete with 0.5% Steel Fiber (FS05-01)

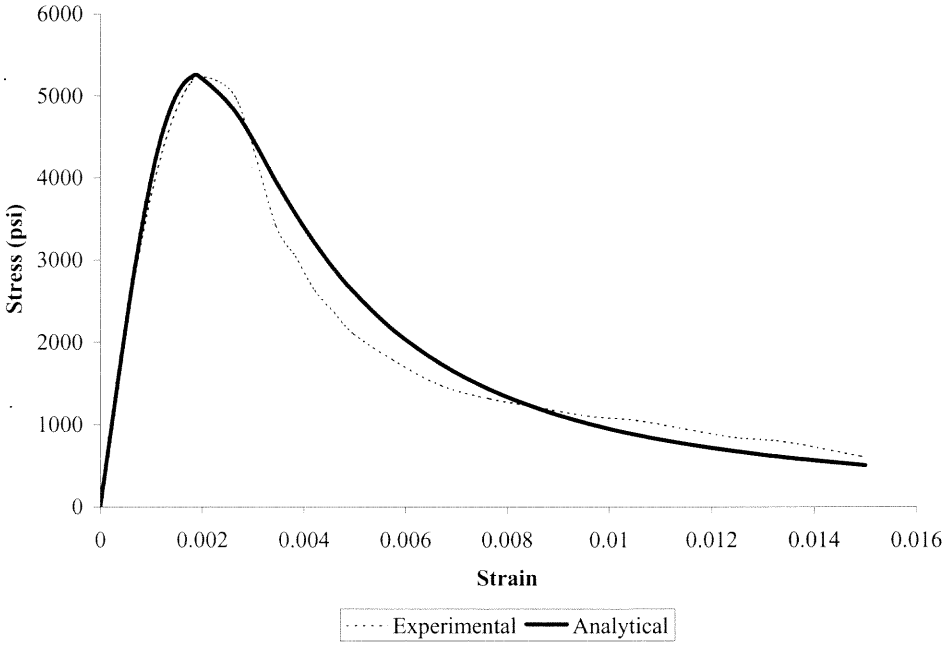

Figure B.23 Comparison of Proposed Equation and Experimental Data for concrete with 0.5% Steel Fiber (FS05-02)

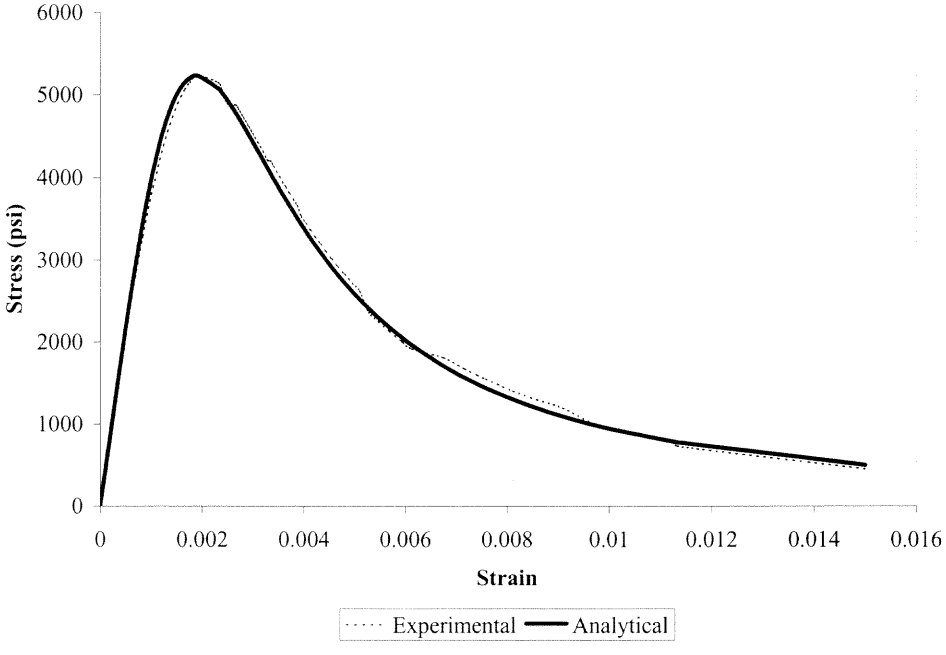

Figure B.24 Comparison of Proposed Equation and Experimental Data for concrete with 0.5% Steel Fiber (FS05-03)

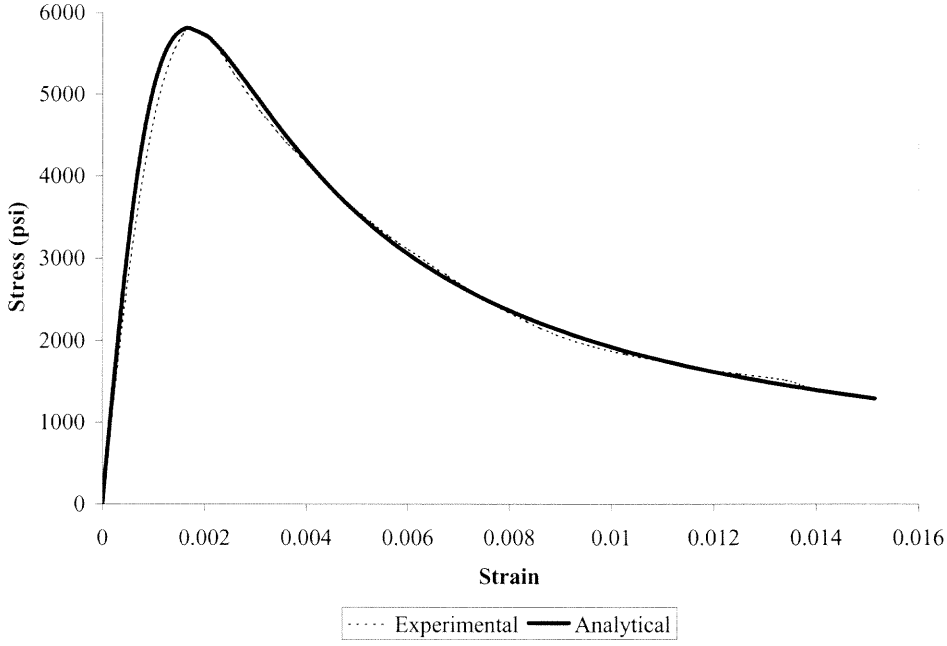

Figure B.25 Comparison of Proposed Equation and Experimental Data for concrete with 1% Steel Fiber (FS1-01)

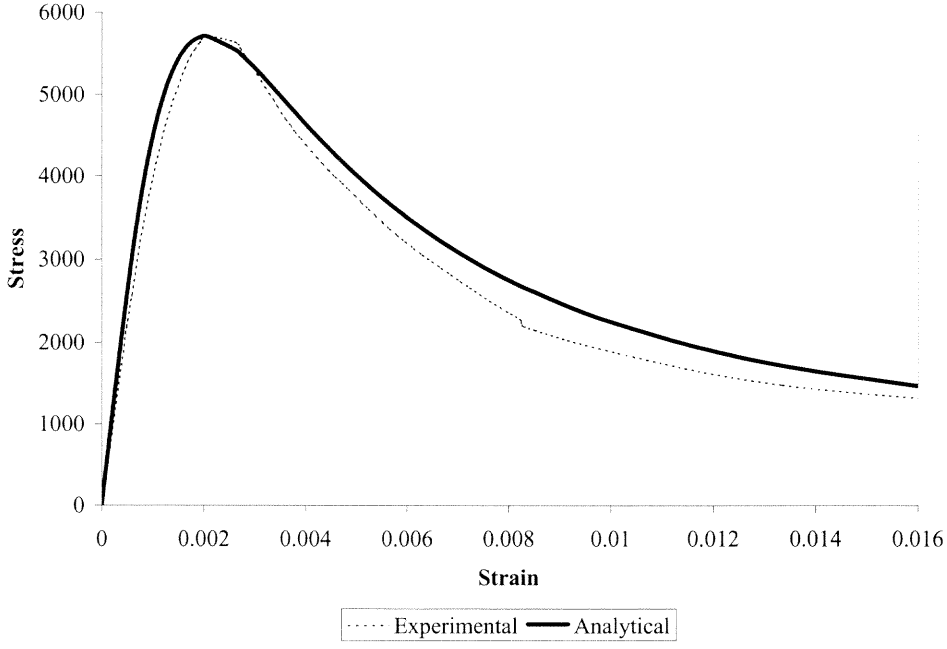

Figure B.26 Comparison of Proposed Equation and Experimental Data for concrete with 1% Steel Fiber (FS1-02)

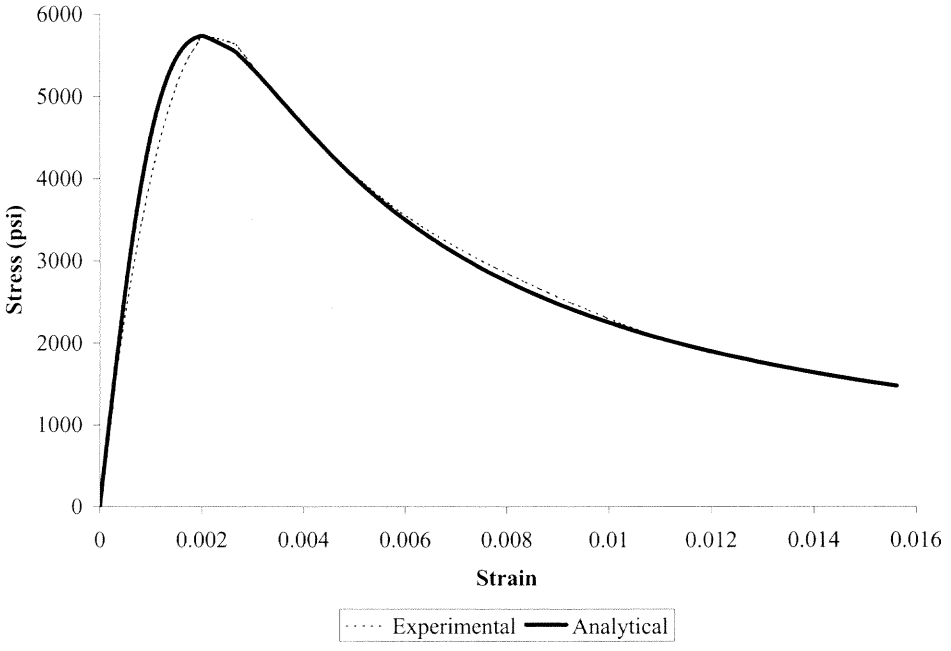

Figure B.27 Comparison of Proposed Equation and Experimental Data for concrete with 1% Steel Fiber (FS1-03)

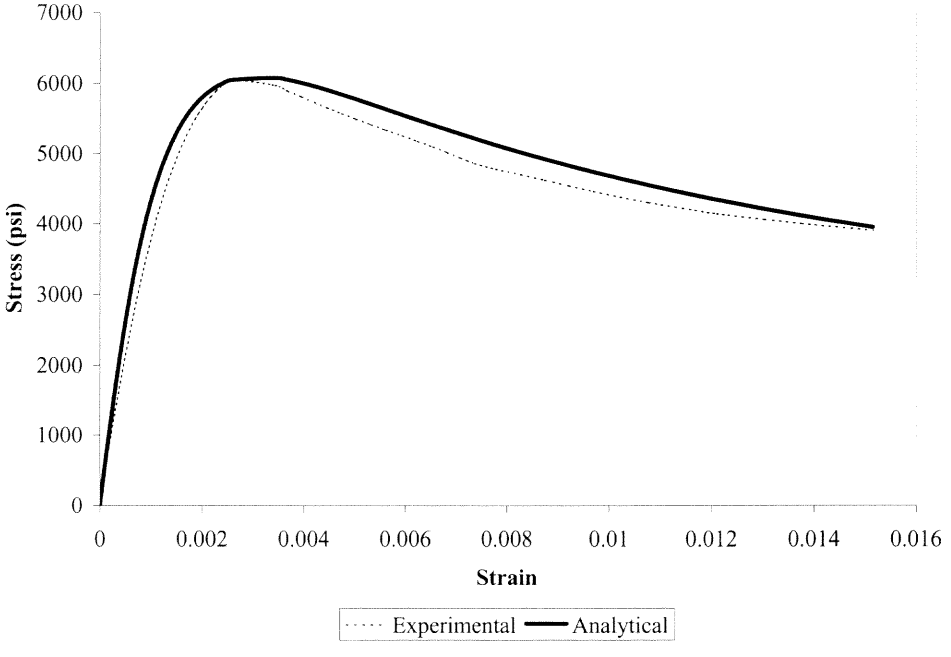

Figure B.28 Comparison of Proposed Equation and Experimental Data for concrete with 2% Steel Fiber (FS2-01)

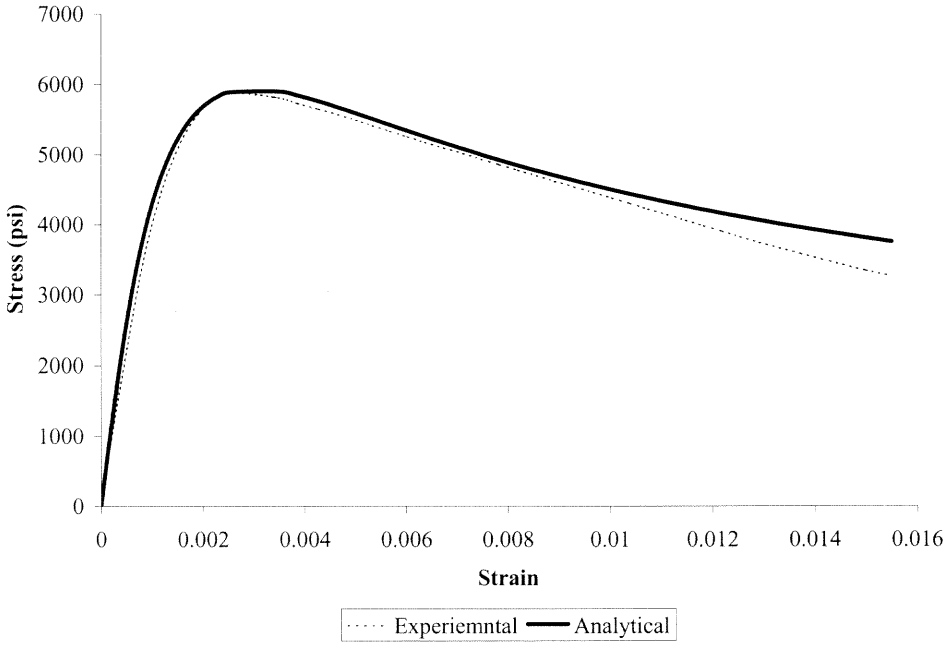

Figure B.29 Comparison of Proposed Equation and Experimental Data for concrete with 2% Steel Fiber (FS2-02)

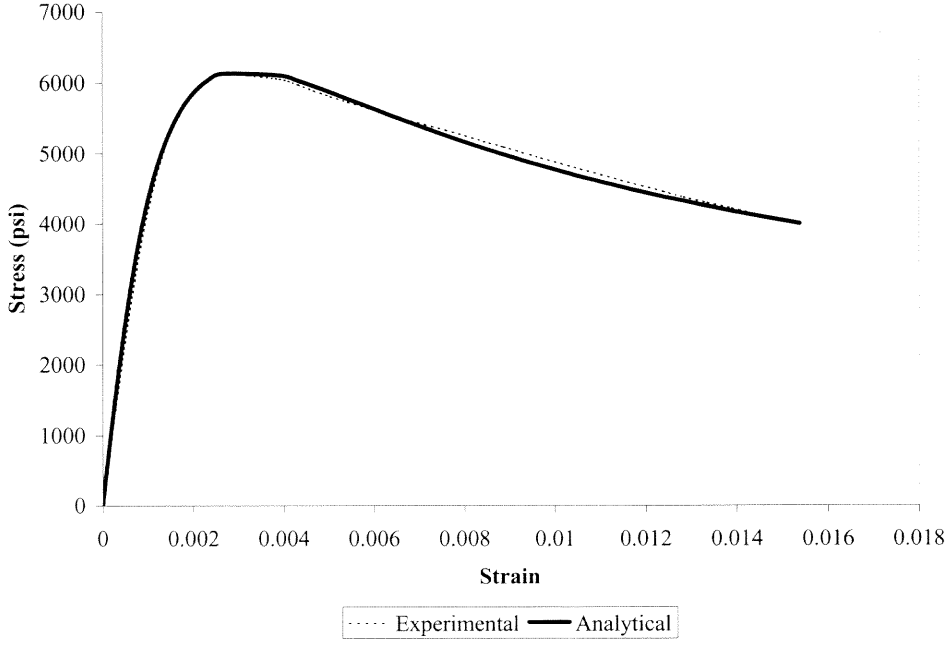

Figure B.30 Comparison of Proposed Equation and Experimental Data for concrete with 2% Steel Fiber (FS2-03)

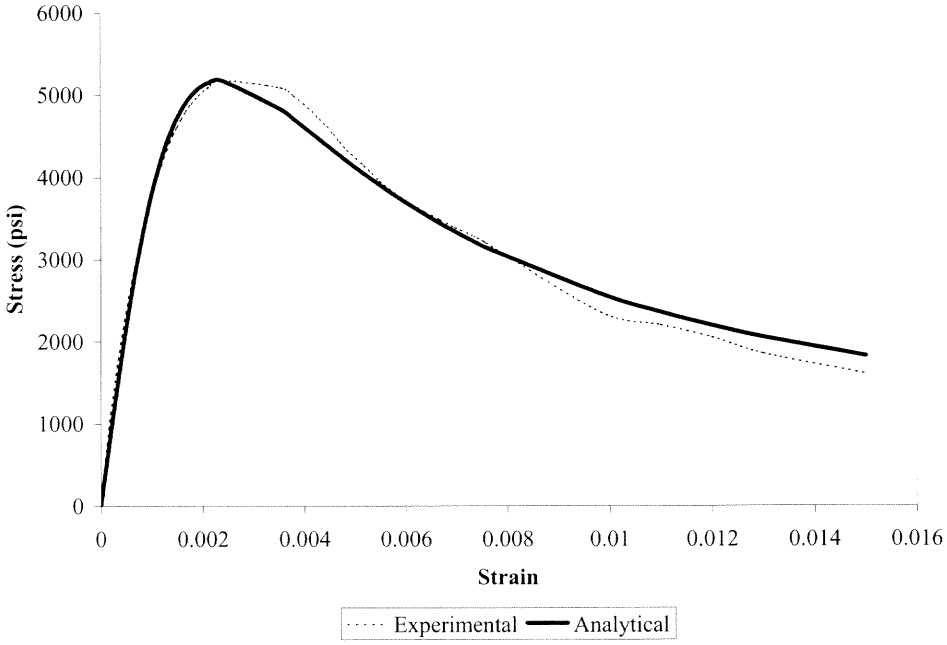

Figure B.31 Comparison of Proposed Equation and Experimental Data for concrete with 4 in Tie Spacing (FH4-01)

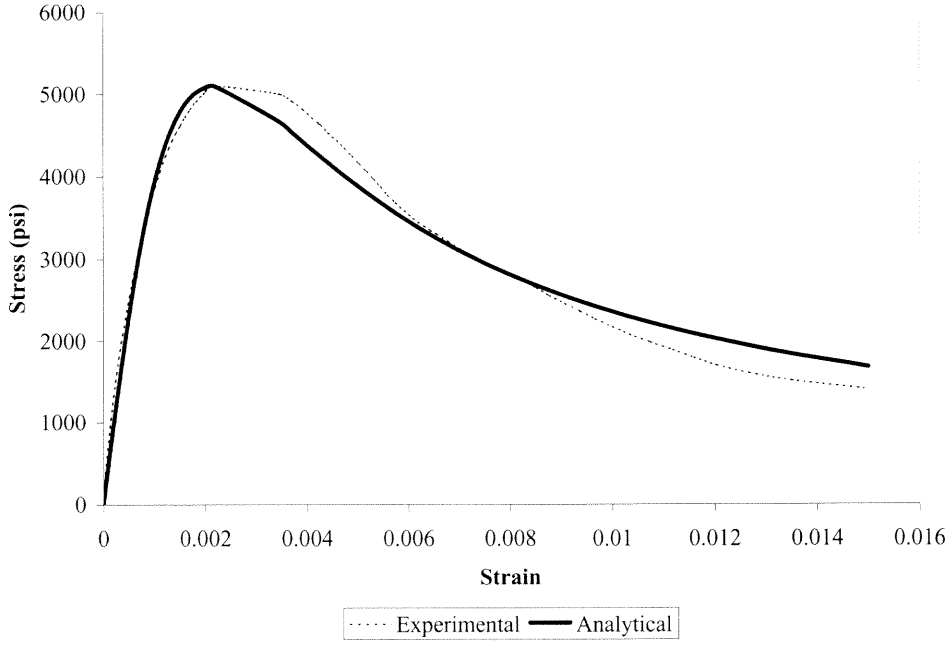

Figure B.32 Comparison of Proposed Equation and Experimental Data for concrete with 4 in Tie Spacing (FH4-02)

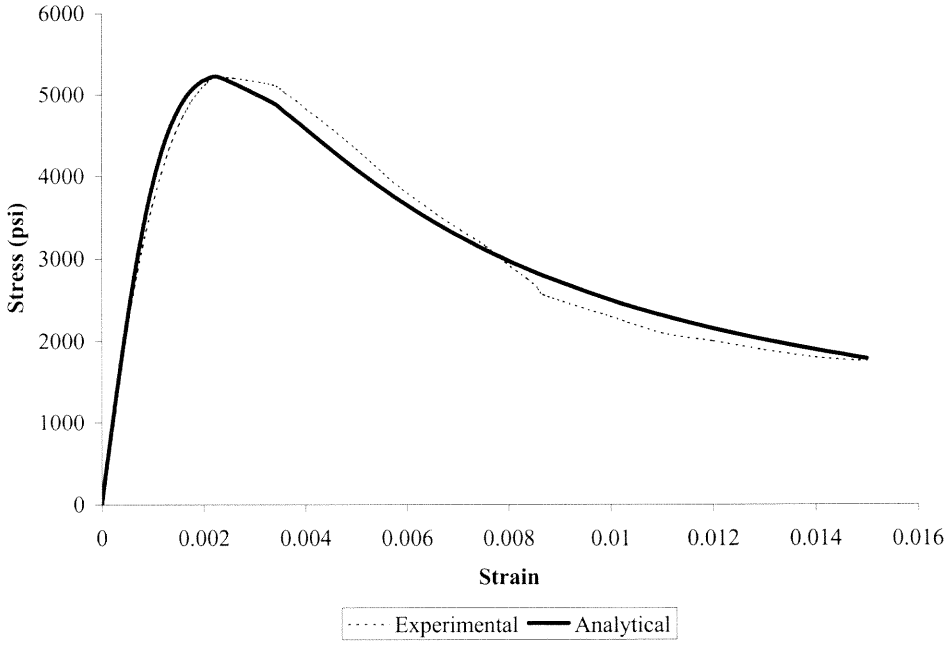

Figure B.33 Comparison of Proposed Equation and Experimental Data for concrete with 4 in Tie Spacing (FH4-03)

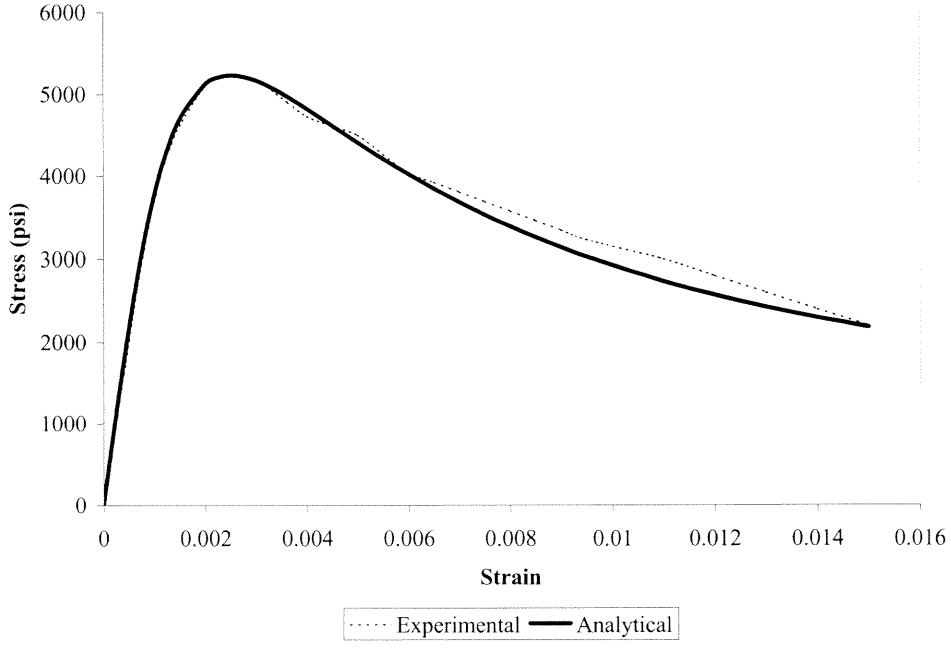

Figure B.34 Comparison of Proposed Equation and Experimental Data for concrete with 2 in Tie Spacing (FH2-01)

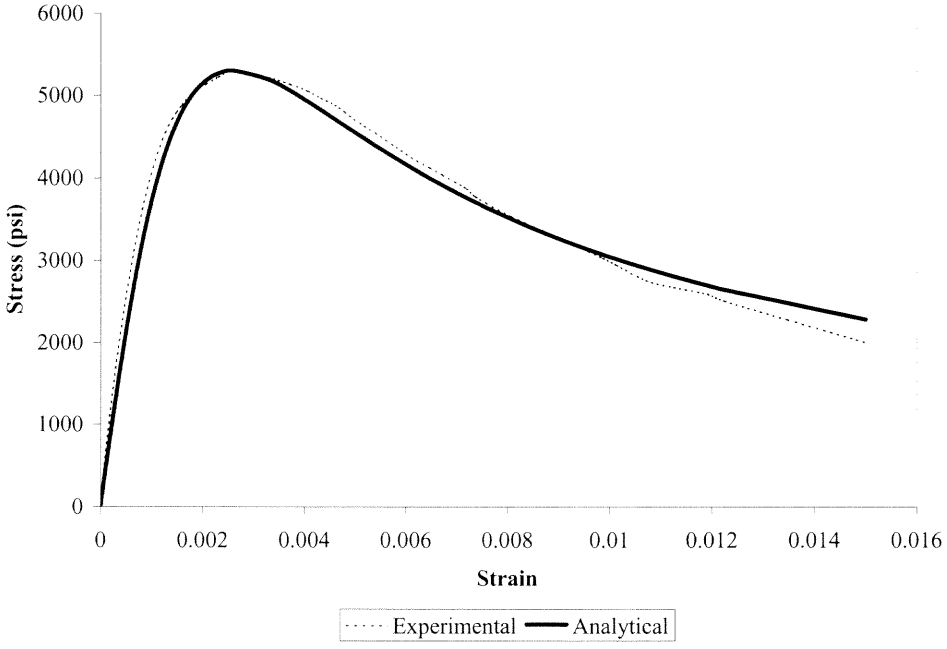

Figure B.35 Comparison of Proposed Equation and Experimental Data for concrete with 2 in Tie Spacing (FH2-02)

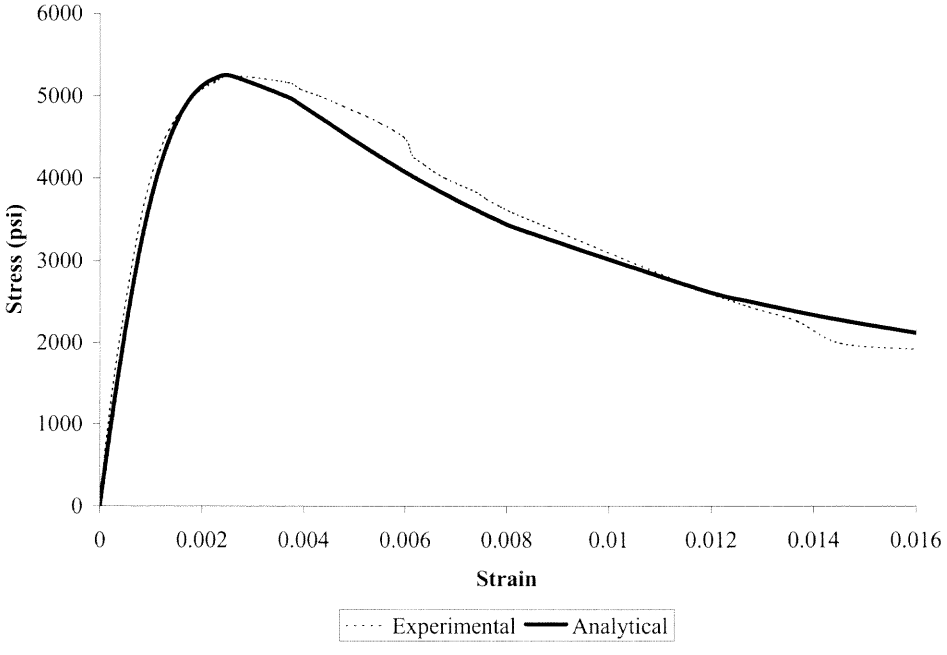

Figure B.36 Comparison of Proposed Equation and Experimental Data for concrete with 2 in Tie Spacing (FH2-03)

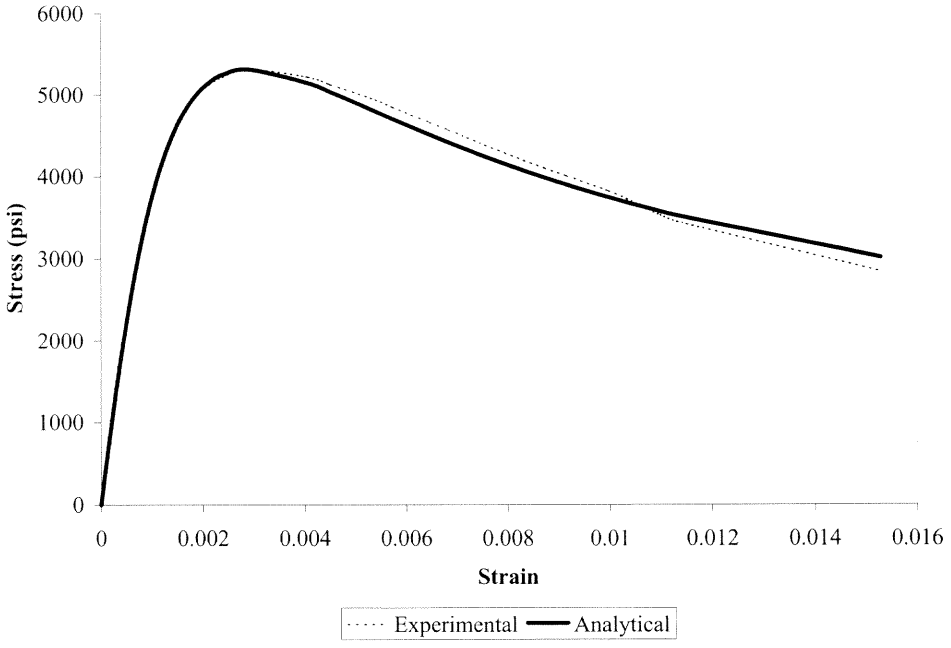

Figure B.37 Comparison of Proposed Equation and Experimental Data for concrete with 1 in Tie Spacing (FH1-01)

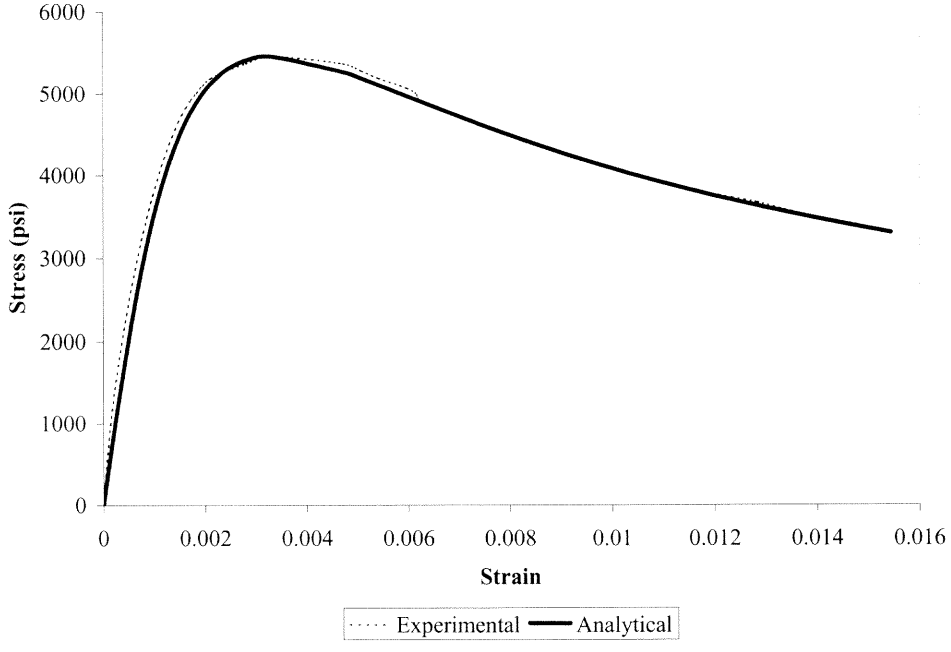

Figure B.38 Comparison of Proposed Equation and Experimental Data for concrete with 1 in Tie Spacing (FH1-02)

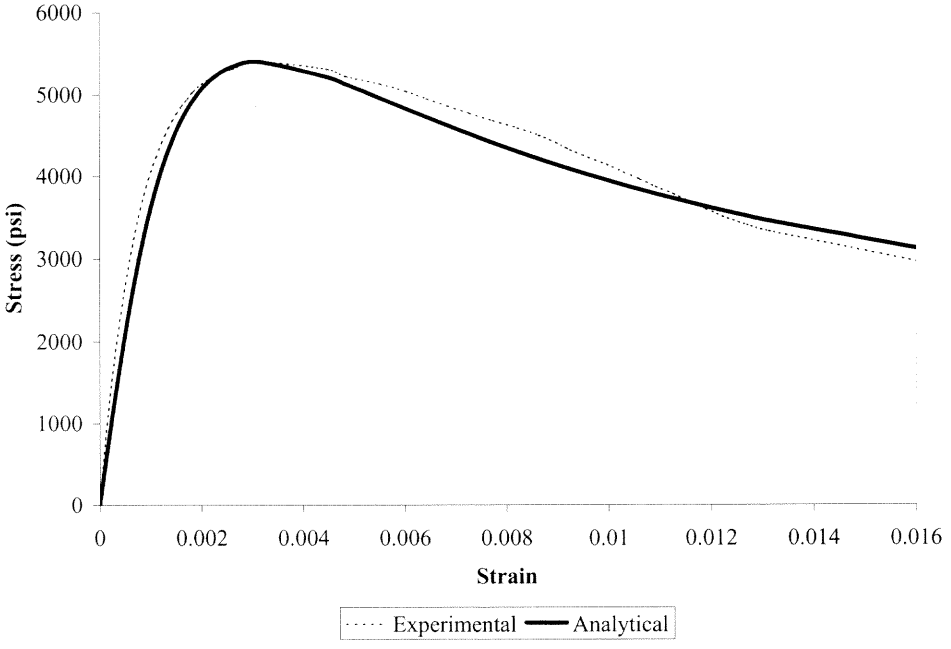

Figure B.39 Comparison of Proposed Equation and Experimental Data for Concrete with 1 in Tie Spacing (FH1-03)

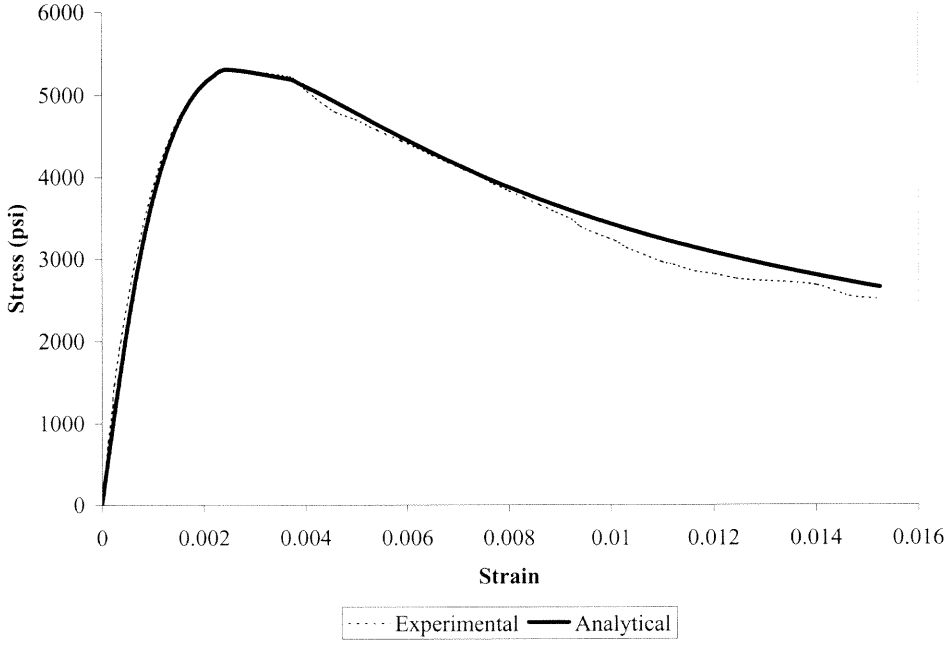

Figure B.40 Comparison of Proposed Equation and Experimental Data for Fibrous Concrete with 4 in Tie Spacing (FSH4-01)

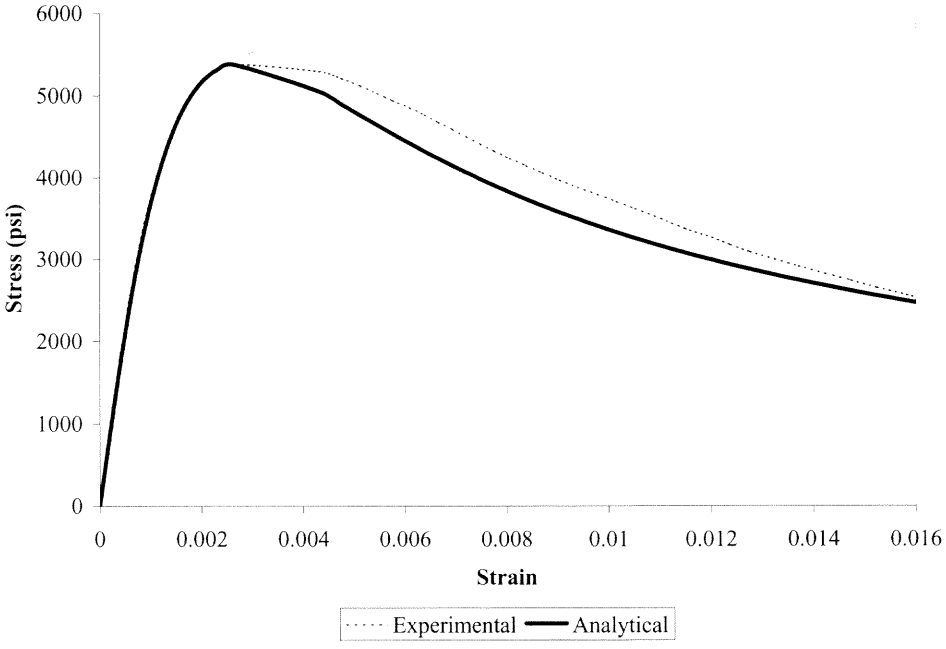

Figure B.41 Comparison of Proposed Equation and Experimental Data for Fibrous Concrete with 4 in Tie Spacing (FSH4-02)

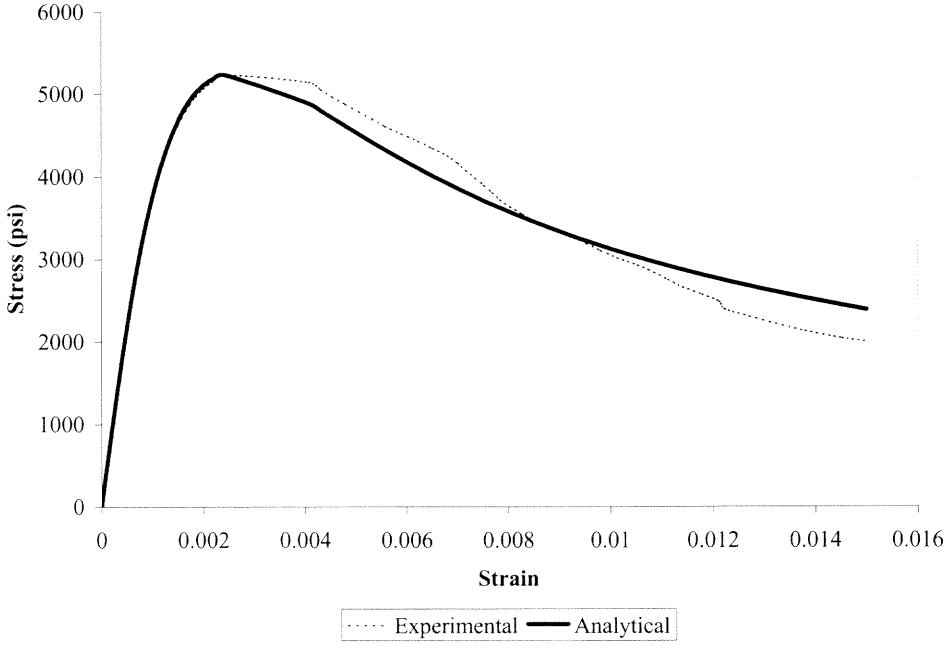

Figure B.42 Comparison of Proposed Equation and Experimental Data for Fibrous Concrete with 4 in Tie Spacing (FSH4-03)

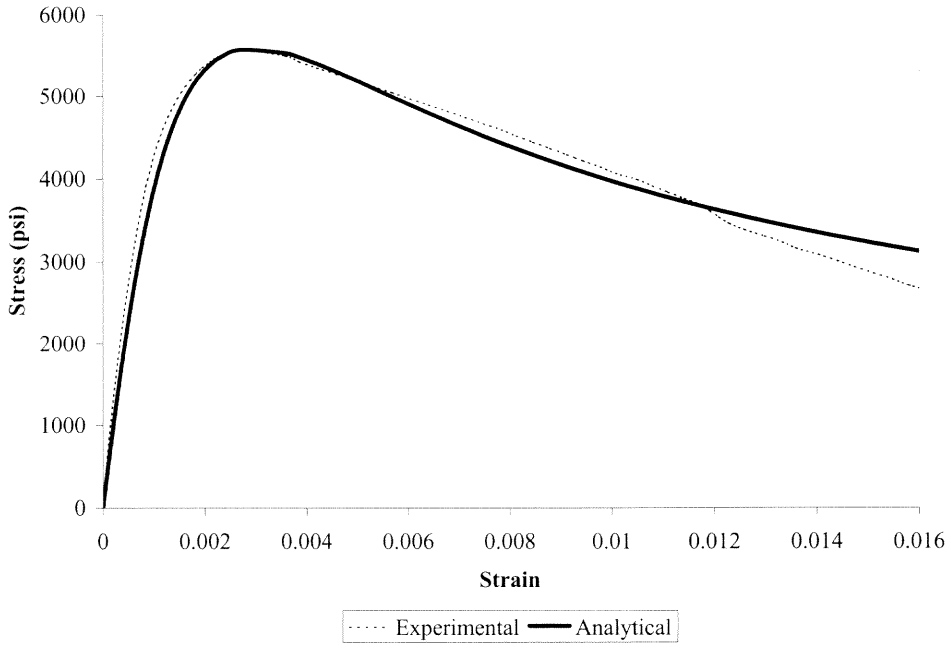

Figure B.43 Comparison of Proposed Equation and Experimental Data for Fibrous Concrete with 2 in Tie Spacing (FSH2-01)

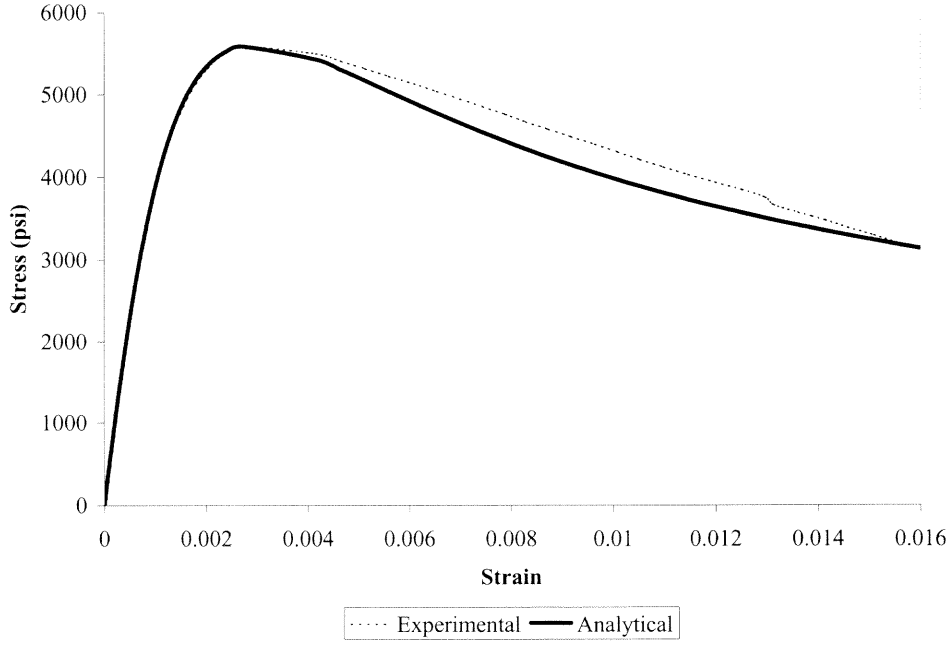

Figure B.44 Comparison of Proposed Equation and Experimental Data for Fibrous Concrete with 2 in Tie Spacing (FSH2-02)

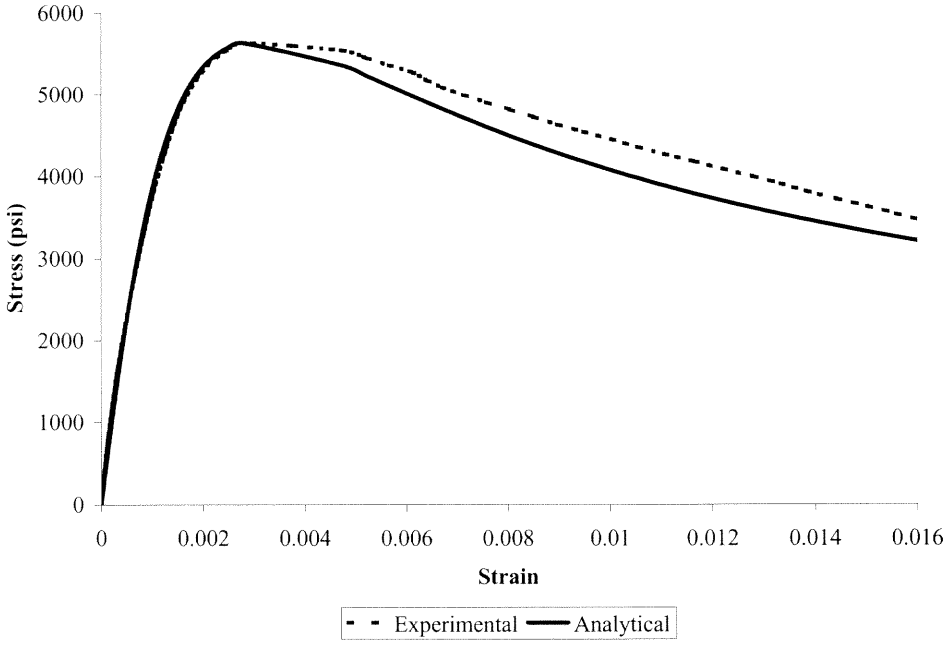

Figure B.45 Comparison of Proposed Equation and Experimental Data for Fibrous Concrete with 2 in Tie Spacing (FSH2-03)

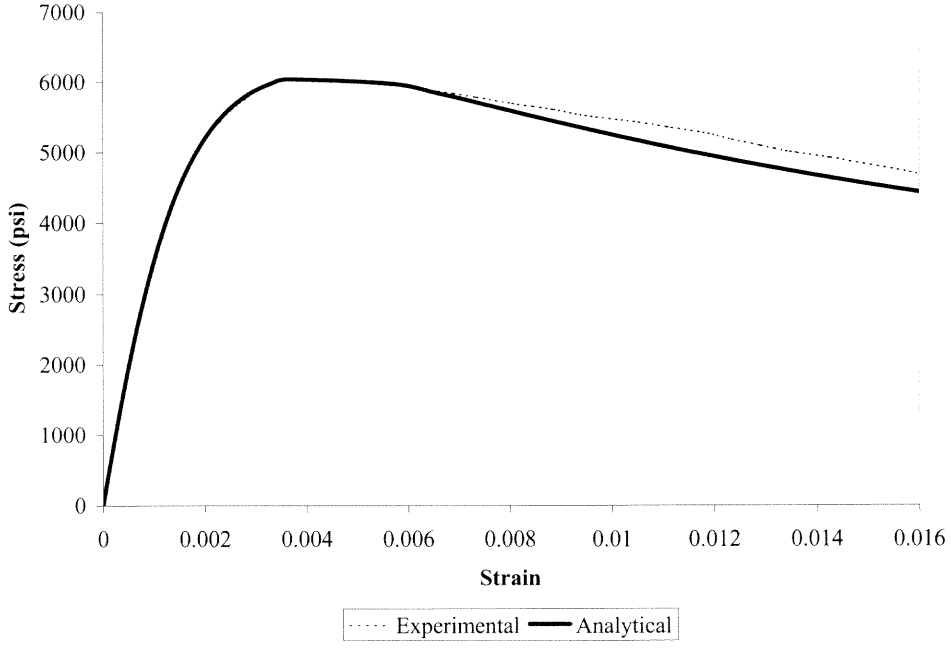

Figure B.46 Comparison of Proposed Equation and Experimental Data for Fibrous Concrete with 1 in Tie Spacing (FSH1-01)

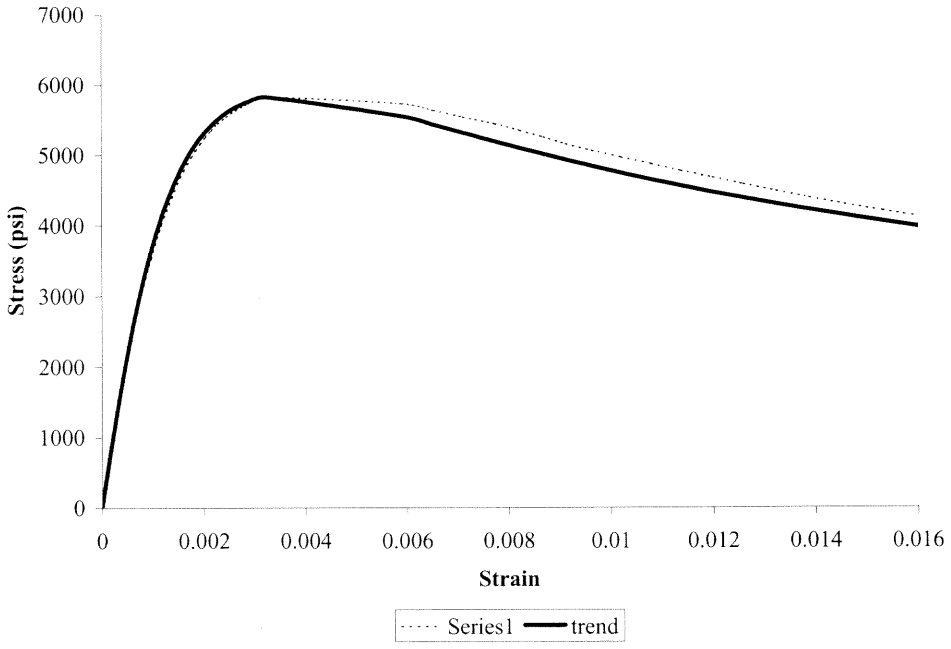

Figure B.47 Comparison of Proposed Equation and Experimental Data for Fibrous Concrete with 1 in Tie Spacing (FSH1-02)

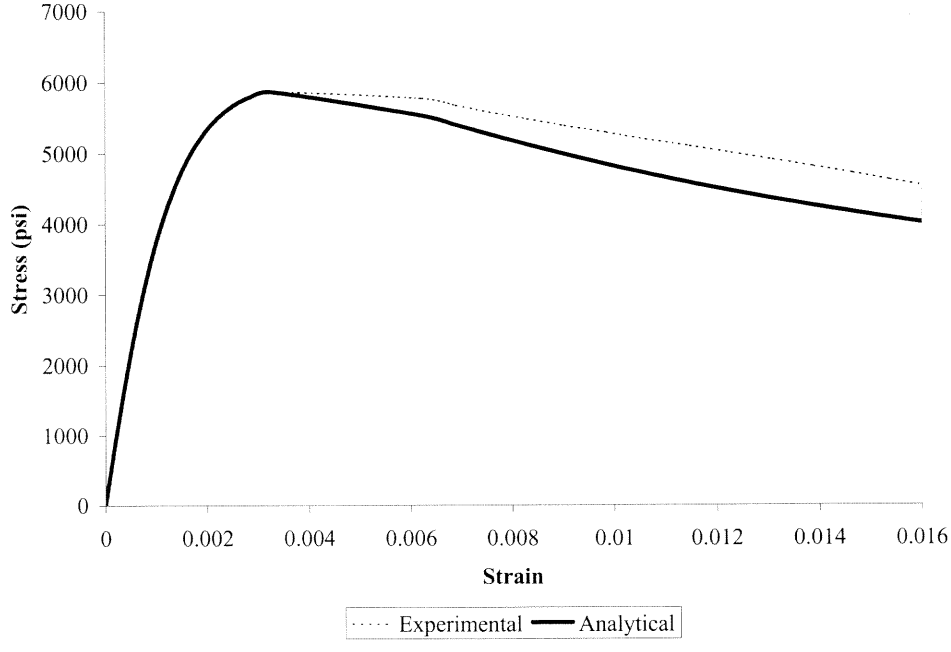

Figure B.48 Comparison of Proposed Equation and Experimental Data for Fibrous Concrete with 1 in Tie Spacing (FSH1-03)

REFERENCES

Abdun-Nur, E., "Fly Ash in concrete, an Evaluation," Bulletin No. 284, Highway Research Board, Washington, DC, 1961, 138 pp.

ACI, Manual of Concrete Practice, 1999.

Ahmad, S. H. and Shah S. P., "Stress-Strain Curves of Concrete Confined by Spiral Reinforcement," ACI Journal, V. 79, No. 6, Nov-Dec 1982, pp. 484-490.

Attard M. M. and Setunge S., "Stress-Strain Relationship of confined and Unconfined Concrete," ACI Materials Journal, V. 93, No. 5, Sep-Oct 1996, pp. 432-442.

Berry, E. E., and Malhotra V. M., "Fly Ash for Use in concrete-A Critical Review," ACI Journal, V. 77, No. 2, March-April 1980, pp. 59-73.

Breitenbücher, I. R., "Development and applications of high-performance concrete," Materials and Structures, V. 31, April 1998, pp. 209-215.

Cain, C. J., "Fly Ash in Concrete Pipe," Concrete Pipe News, V. 31, No. 6, Dec. 1979, pp. 114-116.

Cannon, R. W., "Proportioning Fly Ash Concrete Mixes for Strength and Economy," ACI journal, V. 65, No. 11, Nov. 1968, pp. 969-979.

Carreira, D. and Chu, K-H, "Stress-Strain Relationship for plain Concrete in compression," ACI Journal, V. 82, No. 6, Nov-Dec 1985, pp. 797-804.

CEB-FIP Model Code 1990, May 1993.

Chen, R., "Pozzolanic Admixtures in concrete Mix," Master Thesis, Department of Civil and Environmental Engineering, New Jersey Institute of Technology, Newark, NJ, 1986, 72 pp.

Chin, M. S., Mansur M. A., and Wee, T. H., "Effect of shape, size, and Casting Direction of Specimens on Stress-Strain curves of High-Strength Concrete," ACI Materials Journal, V. 94, No. 3, May-June 1997, pp. 209-219.

Cook, J. E., "Fly Ash in Concrete-Technical Considerations," Concrete International, September 1983, pp. 51-59.

Desayi, P., and Krishnan, S., "Equation for the Stress-Strain Curve of Concrete," ACI Journal, V. 61, No. 3, Mar 1964, pp. 345-350.

Desayi, P., et al., "Equation for stress-strain curve of concrete confined in circular steel spiral," Materials and Structures, V. 11, No. 65, 1978, pp. 339-345.

Ezeldin, A. S., and Balaguru, P. N., "Normal- and High-Strength Fiber-Reinforced Concrete under Compression," Journal of Materials in Civil Engineering, V. 4, No. 4, Nov 1992, pp. 415-429.

Fanella, D. A. and Naaman A. E., "Stress-Strain Properties of Fiber Reinforced Mortar in Compression," V. 82, No. 4, July-August 1985, pp. 475-483.

Forster, S. W., "High-Performance Concrete-Stretching the Paradigm," Concrete International, V. 16, No. 10, 1994, pp. 33-34.

Goodspeed, C. H., et al., "High-Performance Concrete Defined for Highway Structures," Concrete International, V. 18, No. 2, 1996, pp. 62-67.

Gopalan M. K., and Haque, M. N., "Mix Design for Optimal Strength Development of Fly Ash Concrete," Cement and concrete Research, V. 19 1989, pp. 634-641.

Hsu, L. S., "Behavior of High Strength Concrete and Slender Reinforced Concrete columns With and Without Steel Fibers," Ph.D. Dissertation, Department of Civil and Environmental Engineering, New Jersey Institute of Technology, Newark, NJ, 1992, 265 pp.

Hsu, L. S. and Hsu, C.-T. T., "Stress-Strain Behavior of Steel-Fiber High-Strength Concrete," ACI Structural Journal, V. 91, No. 4, July-August 1994.

Hsu, L. S. and Hsu, C.-T. T., "Complete stress-strain behavior of high-strength concrete under compression," Magazine of Concrete Research, V. 46, No. 169, Dec 1994, pp. 301-312.

Idorn, G. M., and Henriksen, K. R., "State of the Art for Fly Ash Uses in concrete," Cement and concrete Research, V. 14, No. 4 July 1984, pp. 463-470

Issa, M. A. and Tobaa, H., "Strength and ductility enhancement in high-strength confined concrete," Magazine of concrete Research, V.46, No. 168, 1994, pp. 177-189.

Jansen, D. C., et al., "Stress-Strain Results of Concrete from Circumferential Strain Feedback Control Testing," ACI Materials Journal, V. 92, No. 4, July-August 1995, pp. 419-428.

Lam, I., Wong, Y. L., and Poon, C. S., "Effect of Fly Ash and Silica Fume on compressive and Fracture Behaviors of Concrete," Cement and concrete Research, V. 28, No. 2, 1998, pp. 271-283.

Lane, R. O., and Best, J. F., "Properties and Use of Fly Ash in Portland Cement Concrete," Concrete International, V. 4, No. 7, July 1982, pp. 81-92.

Lessard, M., and et al., "Testing High-Strength concrete compressive Strength," ACI Materials Journal, V. 90, No. 4, July-August 1993, pp. 303-308.

Lovewell, C. E., and Washa, G. W., "Proportioning concrete Mixtures Using Fly Ash," ACI Proceedings, V. 29, No. 12, June 1958, pp. 1093-1101.

Mansur, M. A., Chin, M. S., and Wee T. H., "Stress-Strain Relationship of Confined High-Strength Plain and Fiber concrete," Journal of Materials in civil engineering, V. 9, No. 4, Nov 1997, pp. 171-179.

Mansur, M. A., Chin, M. S., and Wee T. H., "Stress-Strain Relationship of High-Strength Fiber Concrete in compression," Journal of Materials in civil engineering, V.11, No. 1, Beb 1999, pp. 21-29.

Mansur, M. A., et al., "Deviation of the complete stress-strain curves for concrete in compression," Magazine of Concrete Research, V. 47, No. 173, Dec 1995, pp. 285-290.

Mehta P. K. and Monteiro P. J. M., *Concrete*, 2nd Edition, 1993.

Mehta, P. K. and Aïtcin. P. C., "Principles underlying production of High_performance Concrete," Cement, concrete, and Aggregate, V. 12, No. 2 Winter 1990, pp. 70-78.

Mehta, P. K. and Monteiro, P. J. M., *Concrete*, Prentice Hall, 1993.

Mier, J. G. M., et al., "Strain-softening of concrete in uniaxial compression," Materials and Structures, V. 30, May 1997.

Nataraja, M. C., et al., "Stress-strain curves for steel-fiber reinforced concrete under compression," Cement & Concrete Composites, V. 21, 1999, pp. 383-390.

Nawy, E. G., High-Performance Concrete, John Wiley & Sons, Inc, 2001.

Nicolo, B. D., and Pozzo, M., "The increase in peak strength and strain in confined concrete for a wide range of strengths and degrees of confinement," Materials and Structures, V. 30, March 1997, pp. 87-95.

Okubo, S. and Nishimatsu, Y., "Uniaxial Compression Testing Using a Linear Combination of Stress and Strain as the Control Variable," Int. J. Rock Mech., Min. Sci. and Geomech. Abstr., V. 22, No. 5, 1985, pp. 323-330.

Owens, P., "pulverized Fuel Ash-Part 1 and Part 2," Concrete, V. 14, July and Oct. 1980, pp. 35-36, 33-34.

Papworth, F. and Ratcliffe, R., "High-Performance Concrete-The concrete Future," Concrete International, V. 16, No. 10, 1994, pp. 39-44.

Popovics, S., "A Numerical Approach to the Complete Stress-Strain curve of concrete," Cement and Concrete Research, V. 3, No. 5, May 1973, pp. 583-599.

Ravina, D., "Slump Loss of Fly Ash Concrete," Concrete International, V. 6, No. 4, 1984, pp. 35-39.

RILEM TC 148-SSC, "Strain-softening of concrete in uniaxial compression," Materials and Structures, V. 30, May 1997, pp. 195-209.

Russel, H. G., "ACI Defines High-Performance concrete," Concrete International, V. 21, No. 2, 1999, pp. 56-57.

Sargin, M., et al., "Effects on Lateral Reinforcement Upon the Strength and Deformation Properties of concrete," Magazine of Concrete Research, V. 23, No. 75-76, June-Sept 1971, pp. 99-108.

Shah, S. P., and G. Batson, Fiber Reinforced Concrete Properties and applications ACI SP-105, 1987.

Shin, S. W., Ghosh, S. K., and Moreno, J., "Flexural Ductility of Ultra-High-Strength concrete Members," ACI Structural Journal, V. 86, No. 4, July-August 1989, pp. 394-400

Smith, G. M., and Young, L. E., "Ultimate Flexural analysis Based on Stress-Strain Curves of Cylinders," ACI Journal, V. 53, No. 6, Dec 1956, pp. 597-610.

Taerwe, L. R., "Influence of Steel Fibers on Strain-Softening of High-Strength Concrete," ACI materials Journal, V. 88, No. 6, Jan-Feb 1992.

Wang, P. T., et al., "Stress-Strain Curves of Normal and Lightweight Concrete in Compression," ACI Journal, V. 75, No. 11, Nov 1978, pp. 603-611.

Wang, P-T, et al., "High-Strength concrete in Ultimate Strength Design," Journal of Structural Engineering, ASCE, V. 104, No. 11, Nov 1978, pp. 1761-1773.

Wee, T. H., Chin, M. S., and Mansur M. A., "Stress-Strain Relationship of High – Strength Concrete in Compression," Journal of Materials in Civil Engineering, V. 8, No. 2, May 1996, pp. 70-76.

Young, J. F., and et al., The Science and Technology of Civil Engineering Materials, Prentice Hall, 1998.